2016-03-01

Conjugate Heat Transfer and Average Versus Variable Heat Transfer Coefficients

Tyler James Macbeth
Brigham Young University - Provo

Conjugate Heat Transfer and Average Versus

Variable Heat Transfer Coefficients

Tyler James Macbeth

A thesis submitted to the faculty of
Brigham Young University
in partial fulfillment of the requirements for the degree of

Master of Science

Matthew R. Jones, Chair
Brian D. Iverson
S. Andrew Ning

Department of Mechanical Engineering

Brigham Young University

March 2016

ABSTRACT

Conjugate Heat Transfer and Average Versus
Variable Heat Transfer Coefficients

Tyler James Macbeth
Department of Mechanical Engineering, BYU
Master of Science

An average heat transfer coefficient, $\bar{h}$, is often used to solve heat transfer problems. It should be understood that this is an approximation and may provide inaccurate results, especially when the temperature field is of interest. The proper method to solve heat transfer problems is with a conjugate approach. However, there seems to be a lack of clear explanations of conjugate heat transfer in literature. The objective of this work is to provide a clear explanation of conjugate heat transfer and to determine the discrepancy in the temperature field when the interface boundary condition is approximated using $\bar{h}$ compared to a local, or variable, heat transfer coefficient, $h(x)$.

Simple one-dimensional problems are presented and solved analytically using both $h(x)$ and $\bar{h}$. Due to the one-dimensional assumption, $h(x)$ appears in the governing equation for which the common methods to solve the differential equations with an average coefficient are no longer valid. Two methods, the integral equation and generalized Bessel methods are presented to handle the variable coefficient. The generalized Bessel method has previously only been used with homogeneous governing equations. This work extends the use of the generalized Bessel method to non-homogeneous problems by developing a relation for the Wronskian of the general solution to the generalized Bessel equation.

The solution methods are applied to three problems: an external flow past a flat plate, a conjugate interface between two solids and a conjugate interface between a fluid and a solid. The main parameter that is varied is a combination of the Biot number and a geometric aspect ratio, $A_1^2 = Bi\frac{L^2}{d_1^2}$. The Biot number is assumed small since the problems are one-dimensional and thus variation in A_1^2 is mostly due to a change in the aspect ratio. A large A_1^2 represents a long and thin solid whereas a small A_1^2 represents a short and thick solid. It is found that a larger A_1^2 leads to less problem conjugation. This means that use of $\bar{h}$ has a lesser effect on the temperature field for a long and thin solid. Also, use of $\bar{h}$ over $h(x)$ tends to generally under predict the solid temperature. In addition is was found that A_2^2, the A^2 value for the second subdomain, tends to have more effect on the shape of the temperature profile of solid 1 and A_1^2 has a greater effect on the magnitude of the difference in temperature profiles between the use of $h(x)$ and $\bar{h}$. In general increasing the A^2 values reduced conjugation.

Keywords: conjugate heat transfer, coupled heat transfer, variable heat transfer coefficient, local heat transfer coefficient, generalized Bessel equation, Wronskian, variable coefficient differential equations, average heat transfer coefficient

ACKNOWLEDGMENTS

I would like to thank my advisor, Dr. Matthew Jones, for giving me the opportunity to work on this research and for his continual support and encouragement. As he exhorts all his students in each of his classes, he taught me to always go back to the fundamental concepts and laws of mathematics and heat transfer. I also want to thank the other professors on my committee for the time they took to quickly provide me with their comments and suggestions to improve my thesis. I would like to thank and recognize Edwards Lifesciences and BYU Capstone for their funding and support.

Lastly, I must also express gratitude for my wife, Kaeli, and my two daughters, Keira and Emmilyn, for their support and much sacrifice for allowing me to complete this work.

TABLE OF CONTENTS

LIST OF TABLES

LIST OF FIGURES

NOMENCLATURE

α	Thermal Diffusivity
β	Generalized Bessel equation parameter
δ	Hydrodynamic boundary layer
δ_t	Thermal boundary layer
η	Non-dimensional y
θ	Non-dimensional T
γ	Parameter defining the degree of relaxation
κ	Thermal diffusivity ratio
λ	Separation constant
ξ	Non-dimensional x
ρ	Density
Σ	Summation
τ	Non-dimensional t
ϕ	Spacial eigenfunction
ψ	Integral transformation
a	Temporal eigenfunction
b	Generalized Bessel equation parameter
c	Constant used in general solution of differential equations
c_p	Specific Heat
d	Thickness
g	Source term
h	Convective heat transfer coefficient
k	Thermal Conductivity
m	Generalized Bessel equation parameter
$\dot{m}$	Mass flow rate
n	Summation index value
p	Generalized Bessel equation parameter
$\dot{q}$	Volumetric heat generation
q''	Heat flux
t	Temporal variable
u	Velocity in x direction
v	Velocity in y direction
w	Width into the page
x	Horizontal spacial variable
y	Vertical spacial variable
A_c	Cross-sectional area
A_s	Surface area
A	Non-dimensional constant
B	Non-dimensional constant
C	Constant
$\dot{E}_{in}$	Energy rate in
$\dot{E}_{out}$	Energy rate out
$\dot{E}_{gen}$	Energy generation rate

$\dot{E}_{st}$	Energy storage rate
L	Length
L_c	Characteristic length
R	Generalized Bessel equation parameter
T	Temperature
T_0	Temperature at $x = 0$ also $t = 0$
T_L	Temperature at $x = L$
U	Conductance heat transfer coefficient
W	Wronskian
Br	Brun number
Bi	Biot number
Nu	Nusselt number
Pe	Pectlet number
Pr	Prandtl number
Re	Reynolds number
J_ν	Bessel function of the first kind of order ν
Y_ν	Bessel function of the second kind of order ν
I_ν	Modified Bessel function of the first kind of order ν
K_ν	Modified Bessel function of the second kind of order ν

Subscripts, superscripts, and other indicators

$[\,](t)$	indicates [ ] is a function of t
$[\,](x)$	indicates [ ] is a function of x
$[\,](y)$	indicates [ ] is a function of y
$[\,]_1$	Parameter is associated with subdomain 1
$[\,]_2$	Parameter is associated with subdomain 2
$[\,]_s$	Parameter is associated with the solid
$[\,]_f$	Parameter is associated with the fluid
$[\,]_i$	Parameter is associated with the interface
$[\,]_\infty$	Parameter is associated with the free-stream fluid
$[\,]_0$	Magnitude of the parameter
$\bar{[\,]}$	Parameter is averaged
$\tilde{[\,]}$	Unitless function of the variation of the parameter
$\Delta[\,]$	Difference between two values of the given parameter

CHAPTER 1. INTRODUCTION

1.1 Motivation

Radiofrequency cardiac ablation (RFCA) is a medical procedure used to correct certain arrhythmic heart conditions. The procedure involves placing a catheter electrode inside the heart to locate the site of the origin of the arrhythmia. The electrode then emits an alternating current at radio frequencies heating and permanently damaging – ablating – a small region of the cardiac tissue. The lesion formed in this manner has reduced electrical conductivity, which prevents transmission of aberrant electrical impulses and cures the arrhythmia. Formation of the lesion requires that the tissue be heated above a critical temperature for a specified amount of time. Therefore, successful implementation of an RFCA procedure requires an accurate model of the time-dependent temperature field in the tissue in order to ensure that the pathway for the aberrant electrical impulses is completely blocked while minimizing the amount of cardiac tissue that is damaged. [1]

There are many applications besides RFCA that require accurate modeling of the temperature field between a fluid and a solid. Due to the rapid and continual increase in performance and compactness of electronics, designing methods to remove the increased heat from electronic devices has become an area of great interest [2]. In nuclear reactor cooling, highly non-uniform heat transfer from fuel elements to coolants requires accurate modeling of temperature fields to ensure sufficient reactor cooling [3]. In fact, accurate modeling of temperature fields can be of benefit to nearly any application that has thermal considerations and especially those where a critical temperature can result in damage or failure.

1.2 Modeling Temperature Fields

In order to understand how to accurately model temperature fields, some fundamentals of heat transfer will first be reviewed. Temperature is a relative measure of the amount of thermal energy in a system. A higher temperature is equal to a greater amount of energy. The movement of thermal energy is called heat transfer, or just heat, and occurs due to a temperature difference. Heat flows from higher to lower temperatures until the entire system has reached equilibrium. Now consider a typical heat transfer scenario shown in Figure 1.1 where a fluid with uniform temperature and velocity profiles flows over a solid with a temperature greater than the fluid free-stream temperature, $T_s(x,y) > T_\infty$.

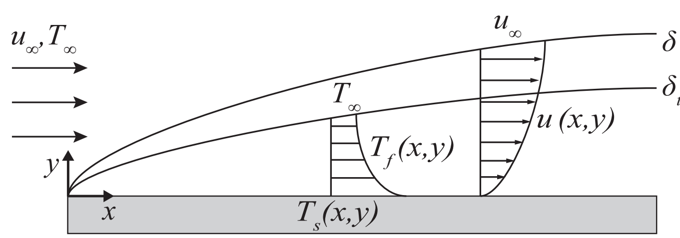

Figure 1.1: Typical temperature and velocity profiles for flow past a flat plate

The variation of temperature in the solid, $T_s(x,y)$, is due to the non-uniform heat transfer from the higher temperature solid to the lower temperature fluid. The heat transfer is non-uniform due to the development of a boundary layer that begins at the leading edge of the solid and grows with x, as shown by δ in Figure 1.1. The boundary layer is the distance in the y-direction from the solid surface, $y = 0$, to where the fluid is no longer affected by the solid. Thus, outside the boundary layer the fluid effectively cannot "see" the solid and it continues to flow as if there were no solid. Solving for the fluid temperature field is essentially solving the boundary layer equations. There are two types of boundary layers. The hydrodynamic boundary layer, δ, is the area where the fluid velocity is changing from zero at the solid surface up the the free-stream velocity, u_∞. The thermal boundary layer, δ_t, is the area in the fluid where the temperature is changing from matching the solid surface at the interface, $T_f(x,0) = T_s(x,0)$, up to the free-stream temperature of the fluid, T_∞. The thicker the boundary layer, the more resistance there is to heat transfer. Clearly, the greatest amount of heat transfer occurs at the leading edge of the solid where the boundary layer is thinnest and decreases with x. This often leads to significant temperature variation in the solid.

Since a temperature difference drives heat transfer, the heat transfer between the solid and the fluid is determined by the temperature gradient at the solid-fluid interface. The interface gradient is influenced by both the solid and the fluid temperature fields and thus they are coupled. This means that the fluid or the solid cannot be solved independently from the other, but they must be solved simultaneously.

The correct and most accurate approach to solve for the temperature field in a coupled system is to solve the governing equations in both the fluid and the solid with matching interface boundary conditions. This is called a conjugate approach or conjugate heat transfer. Technically, all heat transfer problems are conjugate problems, however, conjugate solutions are difficult and time-consuming to develop and thus simpler methods are generally used. The most common method is to use an average convective heat transfer coefficient, $\bar{h}$, at the interface boundary which decouples the fluid and the solid. The decoupling occurs since $\bar{h}$ approximates the boundary layer and thus all the variation in the fluid as a constant removing the need to solve the fluid governing equations. Also, textbooks often present classical solutions to heat transfer problems that generally assume constant temperatures or heat fluxes. The next sections will discuss all these methods further.

1.2.1 Conjugate Heat Transfer

Conjugate heat transfer (CHT) is frequently described as heat transfer between a fluid, and a solid in which the interface condition is initially unknown and is found from the heat transfer solution [4]. Perelman [5], the first to coin the term ”conjugate”, defined a conjugate problem as the common solution of heat conduction equations for a body and a liquid. Dorfman [6], defines CHT as problems which contain two or more subdomains with phenomena described by different differential equations and after solving the problem in each subdomain, these solutions should be conjugated. Neither of these definitions fully define CHT nor are clear to the common reader.

To formulate a better a definition for CHT, first explore the meaning of the word conjugate. Conjugate is defined as ”joined together” or ”coupled” and comes from the Latin *conjugātus* which means to ”yoke together” [7]. Just as a yoke connects two oxen, CHT involves multiple subdomains that are yoked together; one cannot move or change without affecting the other.

Most heat transfer problems consider thermal interactions between a fluid and a solid and because of this many believe and define CHT as heat transfer between a fluid and a solid. However, Dorfman’s definition makes the point that CHT is not restricted to just between a fluid and a solid. This will also be demonstrated in Chapter 3. However, since the most important CHT phenomena are thermal interactions between a fluid and a solid, CHT is widely considered to be modeling convection without using a convective heat transfer coefficient.

When modeling heat transfer in some domain of interest, the thermal behavior is described using partial differential equations with specified boundary conditions. Conjugate heat transfer refers to the modeling of thermal interactions between multiple unique subdomains with varying and unknown interface boundary conditions. The term unique refers to differences between the subdomains’ differential equations, material properties or boundary conditions. Each subdomain cannot be solved independently because its temperature distribution is dependent on the other subdomain’s temperature distribution. More specifically, the interface boundary condition is unknown and the governing equations cannot be solved without fully specified boundary conditions.

The procedure to solve CHT problems, or the conjugation of the subdomains, is to satisfy the First Law of Thermodynamics by matching the temperature and heat flux at the interface between the subdomains. This results in two equations for the interface boundary condition which may also be referred to as a conjugate boundary condition or boundary condition of the fourth kind

$$T_s(x,0) = T_f(x,0) \tag{1.1}$$

$$-k_s \frac{dT_s}{dy}\bigg|_{y=0} = -k_f \frac{dT_f}{dy}\bigg|_{y=0} \tag{1.2}$$

where k is the thermal conductivity and $y = 0$ is at the interface. One boundary condition is used for one subdomain and the other boundary condition is used for the other subdomain to ensure both are satisfied. Since the interface boundary condition involves the temperature distributions for both subdomains, the subdomains must be solved simultaneously. It should be noted that the interface temperature is the key to conjugate problems and once it is known the problem no longer needs to be solved conjugately, but each subdomain can be solved independently since all boundary conditions are fully specified.

Except for extremely simplified heat transfer problems, developing analytical solutions cannot generally be done. With the development of computers, it is now practical to solve conjugate problems using numerical methods. The most common method for solving CHT problems is with high-fidelity computational fluid dynamics (CFD) software. Modeling realistic scenarios often requires many CPUs, large amounts of memory and data storage and can take hours or days to solve. The time constraint restricts the use of conjugate models for time-sensitive applications, such as RFCA, with currently available solution methods.

1.2.2 Convective Heat Transfer Coefficient

Conjugate heat transfer, as discussed previously, is the analysis of the fluid boundary layer and solid by solving the governing equations with specified boundary conditions. The local convective heat transfer coefficient, $h(x)$, decouples the conjugate problem by approximating the boundary layer as a single node in the y-direction (the direction perpendicular to the surface). A single node approximation means all the variation of the temperature in the boundary layer is average in the y-direction. It should be noted that this assumption would be correct if the velocity and temperature profile in the boundary layer are linear. However, if they are not linear, the use of h can lead to significant error. [8]

To illustrate, consider a typical CHT problem shown in Figure 1.2. A fluid with uniform temperature and velocity profiles flows over a thin flat plate with a surface temperature greater than the free-stream temperature, $T_s(x,y) > T_\infty$.

To correctly model and obtain an exact solution, a conjugate approach should be used. The two-dimensional, steady, laminar, incompressible boundary layer equations with constant fluid properties and no pressure gradient, Eqns. 1.3-1.5, would need to be solved for $T_f(x,y)$ while simultaneously solving the energy equation, Eqn. 1.6, for the solid $T_s(x,y)$.

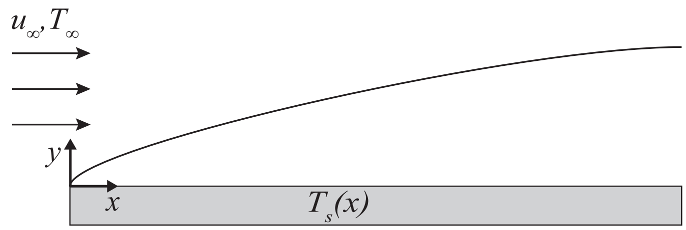

Figure 1.2: Typical flow past a flat plate where the fluid is represented by the two-dimensional, steady, laminar, incompressible boundary layer equations with constant fluid properties and no pressure gradient

Fluid

$$\frac{\partial u}{\partial x}+\frac{\partial v}{\partial y}=0 \qquad \textit{Mass} \tag{1.3}$$

$$u\frac{\partial u}{\partial x}+v\frac{\partial u}{\partial y}=\nu\frac{\partial^2 u}{\partial y^2} \qquad \textit{Momentum} \tag{1.4}$$

$$u\frac{\partial T_f}{\partial x}+v\frac{\partial T_f}{\partial y}=\alpha\frac{\partial^2 T_f}{\partial y^2} \qquad \textit{Energy} \tag{1.5}$$

Solid

$$\frac{\partial^2 T_s}{\partial x^2}+\frac{\partial^2 T_s}{\partial y^2}=0 \qquad \textit{Energy} \tag{1.6}$$

Once the solid temperature profile, $T_s(x,y)$, has been found the heat flux, $q_s''(x)$, can be computed using Fourier's Law

$$q_s''(x) = -k_s\frac{dT_s}{dy}\bigg|_{y=0}. \tag{1.7}$$

In general, this is no simple task. The use of $h(x)$ would reduce this conjugate problem to the following decoupled problem. The solid energy equation is the same as for the conjugate problem above

$$\frac{\partial^2 T_s}{\partial x^2}+\frac{\partial^2 T_s}{\partial y^2}=0.$$

All boundary conditions would remain the same except for the interface boundary ($y = 0$) which changes from a conjugate to a convective boundary condition, also called boundary condition of the third kind which is essentially an energy balance at the surface equating the heat rate in the solid (Fourier's Law) to the heat rate in the fluid (Newton's Law of Cooling)

$$-k_s \frac{dT_s}{dy}\bigg|_{y=0} = h(x)(T_s(x,0) - T_\infty). \tag{1.8}$$

Note that use of h removes the need for matching the temperatures at the interface as is done in the conjugate boundary condition. The convective boundary condition above is very difficult to solve because $h(x)$, is a function of x. The problems encountered when using $h(x)$ are discussed further in Chapter 2 and Appendix B. Thus in practice, $h(x)$, is generally not used but is averaged in the x-direction (along the surface) and called the average, or global, convective heat transfer coefficient,

$$\bar{h} = \frac{1}{L}\int_0^L h(x)dx. \tag{1.9}$$

Now $\bar{h}$ is a single node analysis of the boundary layer in both the x and y directions. This means all the temperature variation in the boundary layer is averaged and distributed evenly across the interface. The boundary condition using $\bar{h}$ becomes

$$-k\frac{dT_s}{dy}\bigg|_{y=0} = \bar{h}(T_s(x,0) - T_\infty) \tag{1.10}$$

which results in a typical problem solved in heat transfer courses.

If only the heat rate from a surface is needed Newton's Law of Cooling can be used

$$h(x) = \frac{q_s''(x)}{T_s(x) - T_{ref}(x)} \tag{1.11}$$

where $q_s''(x)$ is the heat flux from the surface and $T_{ref}(x)$ is some reference temperature. The heat transfer from the surface to the fluid is calculated by rearranging Eqn. 1.11 to solve for $q_s''(x)$ and integrating over the area of the interface. Neglecting variations in the direction normal to the page, the total heat rate is

$$q_s = \int_A q_s''(A)dA \tag{1.12}$$

$$q_s = \int_0^L h(x)(T_s(x) - T_{ref}(x))wdx \tag{1.13}$$

where w is the width of the plate and L is the length of the plate in the direction of the flow. In general, $T_s(x) - T_{ref}(x)$ is unknown and is commonly replaced by the difference between the average surface temperature and the free stream temperature, $T_{avg} - T_\infty$, for external flow problems or by the log-mean temperature difference, ΔT_{lm}, for internal flow problems. With these approximations, $(T_{avg} - T_\infty) \simeq \Delta T_{ref}$ is constant with respect to x, and Eqn. 1.13 is written as

$$q_s = \Delta T_{ref} wL \frac{1}{L} \int_0^L h(x)dx. \tag{1.14}$$

Letting the surface area, $A_s = wL$ and substituting in $\bar{h}$ results in

$$q_s = \bar{h} A_s \Delta T_{ref}. \tag{1.15}$$

This is the commonly used form of Newton's Law of Cooling which is a function of only constants. Note the major assumptions made to develop this commonly used equation for the heat flux are the averaging of the heat transfer coefficient, surface temperature, and the reference temperature. The problem now centers on how to find an appropriate value for $\bar{h}$.

As discussed in introductory heat transfer textbooks [9], the Nusselt number — a non-dimensional representation of $\bar{h}$ — may be correlated with the Reynolds number and the Prandtl number for a particular flow geometry. The Reynolds and Prandtl numbers are dimensionless parameters that characterize the flow and the fluid. Methods for developing Nusselt number correlations are referred to as the central problem of convective heat transfer [9]. Empirical correlations may be obtained by measuring the total heat rate convected from the surface of a particularly shaped object and the average surface temperature under varying flow conditions.

Although this engineering approach is widely used, it is important to note that values of $\bar{h}$ obtained using this approach represent an approximate total heat rate. The use of $\bar{h}$ in a convective boundary condition to solve the decoupled heat diffusion equation for the temperature profile in the solid will lead to distortions in the time-dependent temperature field. In applications that only require accurate modeling of the heat rate from the solid, distortions in the temperature field may be unimportant. However, in applications such as thermal modeling of the temperature field in cardiac tissue that is undergoing radiofrequency ablation, an accurate representation of the time-dependent temperature field is essential, and use of a convective heat transfer coefficient is likely to lead to significant error. In electronics cooling, the use of $\bar{h}$ could lead to the under predicting of peak chip temperatures and lead to damaged components.

To illustrate why $\bar{h}$ results in distortions in the temperature field, consider the plot of the local heat transfer coefficient, $h(x)$, in Figure 1.3, which is typical for flow over a flat plate. The average heat transfer coefficient for these conditions is represented by the horizontal dashed line. At point x_p, $\bar{h}$ is considerably larger than $h(x)$. If Newton's Law of Cooling with $\bar{h}$ is used as the boundary condition the calculated surface temperature will be less than the actual surface temperature at this location. These distortions in the calculated surface temperatures propagate throughout the solid and result in an inaccurate representation of the time-dependent temperature field. The magnitude of the inaccuracies depend on the flow conditions and properties of the solid and the fluid for each specific problem. There are some cases when the error is negligible and $\bar{h}$ may be confidently used, and there are some cases in which the errors are significant. The problem is knowing the magnitude of the error when $\bar{h}$ is used without needing to solve the conjugate problem.

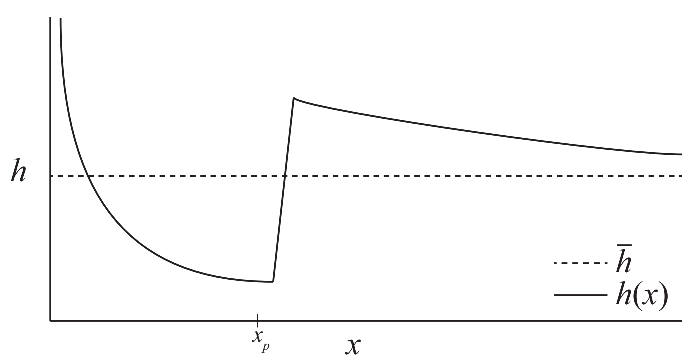

Figure 1.3: Typical plots for $\bar{h}$ and $h(x)$ for flow over a flat plate

1.2.3 Classical Solutions

Many textbooks provide solutions for typical heat transfer cases, such as external flow past a plate or internal flow through a pipe. However, it should be noted that these solutions decouple the conjugate problem by only being valid for certain assumptions. For example, for external flow over a plate the Blasius solution for the flow can be used to solve the energy equation for the fluid. However, to make this problem tractable, the plate must be assumed to be a uniform temperature. For an internal Poiseuille flow, the walls must be assumed one-dimensional and must either be a uniform temperature or a uniform heat flux. Although these solutions can be useful in certain situations, the assumptions used restrict their use for many other necessary problems.

1.3 When is a Conjugate Approach Necessary

A conjugate approach to heat transfer problems is most accurate but can take many resources to solve. The use of the average convective heat transfer coefficient, $\bar{h}$, decouples the problem and makes it is easier to solve but leads to less accurate results. It would be beneficial to have a parameter to help determine when a problem can be solved using $\bar{h}$ and still provide adequate results for the given problem. This section will explore prior efforts to define such a method.

Often non-dimensional numbers can indicate when certain assumptions can reasonably be made for a particular problem. The Biot number, Bi, is a ratio of the resistance to heat transfer in the solid to the resistance to heat transfer in the fluid boundary layer. If Bi is much less than 1, $Bi << 1$, the solid can be considered isothermal and the governing equation doesn't need to be solved for the solid. If Bi is much greater than 1, $Bi >> 1$, the solid resistance dominates and a sufficiently accurate solution can be found without needing to solve the fluid equations.

Development of a parameter that measures the degree of conjugation and thus whether a problem can accurately be solved using h was first attempted for an external flow fluid-solid interface by Luikov [10] and named the Brun number, Br. Luikov derived the Brun number from the matching heat flux conjugate boundary condition,

$$-k_s \frac{dT_s}{dy}\bigg|_{y=0} = -k_f \frac{dT_f}{dy}\bigg|_{y=0}. \tag{1.16}$$

Rearranging Eqn. 1.16 results in

$$\frac{dT_s}{dT_f} = \frac{k_f}{k_s}\frac{dy_s}{dy_f}. \tag{1.17}$$

If it is assumed that the temperature profiles in the solid, as well as the fluid boundary layer are linear, then

$$\frac{\Delta T_s}{\Delta T_f} = \frac{k_f}{k_s}\frac{d_s}{\delta_t(x)} \tag{1.18}$$

where d_s is the thickness of the solid, $\delta_t(x)$ is the thermal boundary layer thickness in the fluid and k is the thermal conductivity. From analysis of the fluid x-momentum and energy equations using the boundary layer approximations,

$$\delta_t(x) = \frac{x}{Nu_x} \tag{1.19}$$

where

$$Nu_x = CPr^m Re_x^n \tag{1.20}$$

is a common form of Nu for correlations based on the Prandtl number, Pr, and the Reynolds number, Re. Substituting these into Eqn. 1.18 results in

$$\frac{\Delta T_s}{\Delta T_f} = \frac{k_f}{k_s}\frac{d_s}{x}CPr^m Re_x^n. \tag{1.21}$$

Dropping the constant, C, defines the local Brun number

$$\frac{\Delta T_s}{\Delta T_f} \sim Br_x = \frac{k_f}{k_s}\frac{d_s}{x}Pr^m Re_x^n. \tag{1.22}$$

Luikov found that for a laminar incompressible flow over a flat plate with a constant surface temperature at the base, a $Br > .1$ leads to an error greater than 5 percent.

Slightly different parameters were developed by Cole [4] and Li [11] and called conjugate Peclet numbers. Dorfman [12] argues that each of the different parameters are essentially Biot numbers. Compare the definition of the Brun number with the Biot number, Bi

$$\frac{\Delta T_s}{\Delta T_f} = Bi = \frac{hL_c}{k_s} \tag{1.23}$$

where L_c is a characteristic length, often represented by the volume divided by the surface area. Since $\frac{\Delta T_s}{\Delta T_f} \sim Br_x$ and $\frac{\Delta T_s}{\Delta T_f} = Bi$ then $Br_x \sim Bi$. Substituting Eqn. 1.20 into the Brun number, Eqn.

1.22, results in

$$Br_x = \frac{k_f}{k_s}\frac{d_s}{x}\frac{Nu_x}{C} \tag{1.24}$$

Recall that $Nu_x = \frac{hx}{k_f}$ and substituting in

$$Br_x = \frac{k_f}{k_s}\frac{d_s}{x}\frac{hx}{Ck_f} \tag{1.25}$$

and after canceling terms

$$Br = \frac{1}{C}\frac{hd_s}{k_s}.$$

Thus

$$Br = \frac{Bi}{C}$$

where $L_c = d_s$. The Brun number is in fact proportional to the Biot number and Dorfman's claim that they are essentially the same is correct. Therefore, the governing parameter to determine conjugation will vary depending on the specific problem.

Petrikevich [13] showed that the Brun number may not reflect all subtleties of the heat transfer processes and in some cases can lead to conflicting conclusions. Thus, a universally applicable conjugation parameter is not available, and criteria need to be developed for geometries of interest. At the beginning if this research, preliminary simulations using STAR-CCM+ were performed on internal flow past a flat surface with a cylindrical electrode perpendicular to the surface to simulate the heating in RFCA. These simulations also appeared to show results that did not agree with the Brun number. Since there was no way to validate the simulations to know if the results were correct, an attempt was made to develop analytical solutions to simpler conjugate problems.

The answer to the question of "when is a conjugate approach necessary?" depends on the specific problem and how precise of a solution is needed. Dorfman [12] defines two general conclusions to answer this question. First, for turbulent problems with high Prandtl numbers, greater than 100, the traditional approach with a convective boundary condition is sufficient. Second, if the temperature head, the difference between the surface and free-stream temperature, is decreasing in the flow direction or in time, then conjugation is usually significant. For all other problems, conjugation depends on the specific problem but Dorfman has suggested some general guidelines which have been compiled into Table 1.1.

Table 1.1: Factors that contribute to the degree of conjugation for a given problem. [12]

Greater Conjugation	Lesser Conjugation
Decreasing temperature head	Increasing temperature head
Comparable resistances, $Bi \simeq 1$	$Bi << 1$ or $Bi >> 1$
Unfavorable pressure gradient	Favorable pressure gradient
Fluids in counterflow	Fluids in parallel flow
Laminar	Turbulent
Unsteady	Steady-state
Low Prandlt numbers	High Prandlt numbers
Low Reynolds numbers	High Reynolds numbers
Non-Newtonian fluid with $n > 1$	Non-Newtonian fluid with $n < 1$
Small surface curvature	Large surface curvature

1.4 Overview of Thesis

This work attempts to provide a clear, fundamental explanation of conjugate heat transfer, which seems to be lacking in literature. Insight to the question of when does the use of $\bar{h}$ provide an adequate solution for the temperature field in a solid will also be addressed. This will be done by solving various problems for two cases, using $\bar{h}$ and $h(x)$, and comparing the resulting temperature fields. It was anticipated to solve each problem using commercial CFD software and validating the results with an analytical solution, however, obtaining one-dimensional results was unsuccessful. Therefore, each problem will be solved using two separate analytical methods to validate the results. The following chapters will develop several analytical methods and apply them to 3 different problems: a decoupled flat plate problem in Chapter 2, a solid-solid conjugate problem in Chapter 3 and a fluid-solid conjugate problem in Chapter 4.

CHAPTER 2. VARIABLE HEAT TRANSFER COEFFICIENT

2.1 Problem Introduction

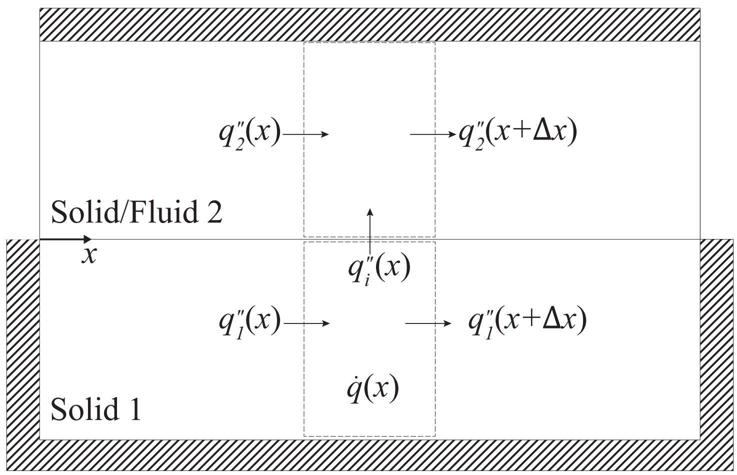

Figure 2.1: Conjugate heat transfer between an insulated solid 1 and either a solid or fluid on top

The remainder of this work will focus on the scenario shown in Figure 2.1. Solid 1, the lower subdomain, is unchanged from Chapter 1 and is surrounded on all sides with an adiabatic, or insulated, boundary condition except for the top interface boundary which is in direct contact with another subdomain and will have an interface heat flux boundary condition, q_i''. There is also a volumetric heat generation, $\dot{q}$ in solid 1. The second subdomain will either be a solid, considered in Chapter 3, or a fluid, considered in Chapter 4. The top boundary condition is adiabatic and the remaining boundary conditions will be dependent on the specific case and will be determined later. The temperature field of solid 1 is of most interest and will be the focus of this work.

The purpose of the problem in Figure 2.1 is to model an internal flow past a solid that has a sufficient thickness to result in a significant variation in the solid temperature field. This scenario can be related to physical applications such as radiofrequency cardiac ablation where blood flows through the heart and the heart tissue is being heated by an electrode. It can also relate to electronics cooling where chips are cooled by forced convection inside electronic devices.

Two-dimensional conjugate problems are difficult to solve with analytical methods. One difficulty that arises is due to having a variable coefficient in the boundary condition which complicates the use of separation of variables to solve partial differential equations. More on this can be found in Appendix B. The problem shown in Figure 2.1 will be reduced to one-dimension in both subdomains. This leads to the interface boundary condition not being able to be represented by the full conjugate condition. The temperature cannot match at the interface otherwise both subdomains would be identical since the temperature is being assumed constant in the vertical direction and thus there must be a temperature jump at the interface. The interface heat flux will be defined as

$$q_i''(x) = h(x)\big(T_1(x) - T_2(x)\big). \tag{2.1}$$

The intent of solving this problem is to gain insight to the error that arises from averaging the convective heat transfer coefficient. The problem will be solved both using an average heat transfer coefficient, $\bar{h}$, and a local heat transfer coefficient, $h(x)$. The solutions will be compared to determine the range in which $\bar{h}$ can adequately be used.

In the next section an energy balance will be performed on solid 1. Then a simple flat plate problem will be introduced and analytical solution methods will be demonstrated using a flat plate example.

2.2 Energy Balance

Performing an energy balance on solid 1 of Figure 2.1 by using the law of conservation of energy

$$\dot{E}_{in} - \dot{E}_{out} + \dot{E}_{gen} = \dot{E}_{st} \tag{2.2}$$

results in

$$q_1''(x,t)wd_1 - q_1''(x+\Delta x,t)wd_1 - q_i''(x+\frac{\Delta x}{2},t)w\Delta x + \dot{q}(x+\frac{\Delta x}{2},t)wd_1\Delta x = \rho_1 c_{p1} wd_1 \Delta x \frac{\partial T_1(x,t)}{\partial t} \tag{2.3}$$

where d_1 and w are the thickness and width respectively. The width cancels on all terms. Taking the limit as Δx approaches zero

$$\lim_{\Delta x \to 0} \left[\frac{-(q_1''(x+\Delta x,t) - q_1''(x,t))}{\Delta x} d_1 - q_i''(x+\frac{\Delta x}{2},t) - T_2(x+\frac{\Delta x}{2},t)) + \dot{q}(x+\frac{\Delta x}{2},t)d_1 \right.$$
$$\left. = \rho_1 c_{p1} d_1 \frac{\partial T_1(x,t)}{\partial t} \right] \tag{2.4}$$

results in

$$-\frac{\partial q_1''(x,t)}{\partial x} d_1 - q_i''(x,t) + \dot{q}(x,t)d_1 = \rho_1 c_{p1} d_1 \frac{\partial T_1(x,t)}{\partial t}. \tag{2.5}$$

Fourier's Law, $q_1'' = -k_1 \frac{\partial T_1(x,t)}{\partial x}$, can be substituted in for the heat flux, and after rearranging

$$\frac{\partial^2 T_1(x,t)}{\partial x^2} = \frac{1}{\alpha_1}\frac{\partial T_1(x,t)}{\partial t} + \frac{q_i''(x,t)}{k_1 d_1} - \frac{\dot{q}(x,t)}{k_1}. \tag{2.6}$$

Let $\dot{q}(x,t) = \dot{q}_0 \tilde{q}(x,t)$ where $\dot{q}_0$ is the magnitude of the volumetric generation and $\tilde{q}(x,t)$ is the variation represented by some unitless function of position and time

$$\frac{\partial^2 T_1(x,t)}{\partial x^2} = \frac{1}{\alpha_1}\frac{\partial T_1(x,t)}{\partial t} + \frac{q_i''(x,t)}{k_1 d_1} - \frac{\dot{q}_0 \tilde{q}(x,t)}{k_1}. \tag{2.7}$$

The boundary conditions are

$$\left.\frac{\partial T_1}{dx}\right|_{x=0} = 0 \tag{2.8}$$

$$\left.\frac{\partial T_1}{dx}\right|_{x=L} = 0 \tag{2.9}$$

$$T_1(x,0) = T_0 \tag{2.10}$$

where T_0 is the initial temperature at $t = 0$ and L is the length of the interface. For utility and ease of solving, the problem can be non-dimensionalized with the following

$$\xi = \frac{x}{L} \tag{2.11}$$

$$\theta_1 = \frac{k_1}{\dot{q}_0 L^2}(T_1 - T_\infty) \tag{2.12}$$

$$\tau = \frac{\alpha_1 t}{L^2} \tag{2.13}$$

which results in

$$
\begin{aligned}
\frac{\partial^2 \theta_1(\xi,\tau)}{\partial \xi^2} =& \frac{\partial \theta_1(\xi,\tau)}{\partial \tau} + \frac{q_i''(\xi,\tau)}{\dot{q}_0 d_1} - \tilde{q}(\xi,\tau) && (2.14)\\
\frac{\partial \theta_1}{d\xi}\Big|_{\xi=0} =& 0 && (2.15)\\
\frac{\partial \theta_1}{d\xi}\Big|_{\xi=1} =& 0 && (2.16)\\
\theta_1(\xi,0) =& \theta_0 && (2.17)
\end{aligned}
$$

This work will only consider steady-state problems. The steady-state problem is

$$
\begin{aligned}
\frac{d^2 \theta_1(\xi)}{d\xi^2} =& \frac{q_i''(\xi)}{\dot{q}_0 d_1} - \tilde{q}(\xi) && (2.18)\\
\frac{d\theta_1}{d\xi}\Big|_{\xi=0} =& 0 && (2.19)\\
\frac{d\theta_1}{d\xi}\Big|_{\xi=1} =& 0 && (2.20)
\end{aligned}
$$

2.3 Solution Methods

This section will introduce a simple problem for flow past a one-dimensional flat plate that will be used to demonstrate the analytical methods that will be used in this work. Consider flow past an insulated flat plate with heat generation as in Figure 2.2. Only the governing equation for the plate will be solved and the fluid will be approximated using the convective heat transfer coefficient, *h*.

The heat flux leaving the surface will be expressed using Newton's Law of Cooling with a variable heat transfer coefficient

$$
q_i''(x) = h(x)\big(T_1(x) - T_\infty\big). \tag{2.21}
$$

Using the results from the energy balance performed previously and assuming steady-state, the governing equation becomes an ordinary differential equation

$$
\frac{d^2 \theta_1(\xi)}{d\xi^2} = \frac{q_i''(\xi)}{\dot{q}_0 d_1} - \tilde{q}(\xi). \tag{2.22}
$$

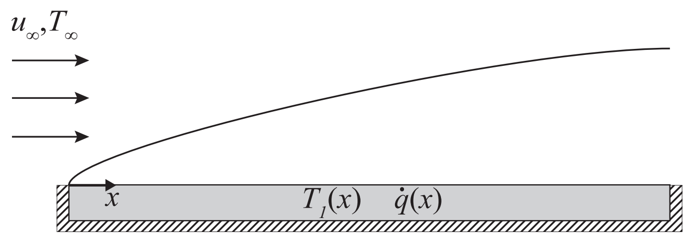

Figure 2.2: Flow past a flat plate with generation

Substituting the non-dimensionalizatons into Eqn. 2.21 results in

$$q_i''(\xi) = \frac{\dot{q}_0 L^2}{k_1} h(\xi)\theta_1(\xi) \tag{2.23}$$

and substituting in to the governing equation

$$\frac{d^2\theta_1(\xi)}{d\xi^2} = \frac{h(\xi)L^2}{k_1 d_1}\theta_1(\xi) - \tilde{q}(\xi). \tag{2.24}$$

As was done for the volumetric heat generation, let $h(\xi) = h_0\tilde{h}(\xi)$ where h_0 is the magnitude of h and $\tilde{h}(\xi)$ is the dimensionless variation represented by some unitless function of position. Also, define a new constant coefficient as

$$A_1^2 = \frac{h_0 L^2}{k_1 d_1} \tag{2.25}$$

and the equation becomes

$$\frac{d^2\theta_1(\xi)}{d\xi^2} - A_1^2\tilde{h}(\xi)\theta_1(\xi) = -\tilde{q}(\xi) \tag{2.26}$$

with boundary conditions

$$\left.\frac{d\theta_1}{d\xi}\right|_{\xi=0} = 0 \tag{2.27}$$

$$\left.\frac{d\theta_1}{d\xi}\right|_{\xi=1} = 0. \tag{2.28}$$

Note, from Eqn. 2.25 , that when A_1^2 is multiplied by $\frac{d_1}{d_1}$ the result is the Biot number and a geometric ratio,

$$A_1^2 = \frac{h_0 d_1}{k_1}\frac{L^2}{d_1^2} = Bi\frac{L^2}{d_1^2}. \tag{2.29}$$

Since the plate is assumed to be one-dimensional it is required that $Bi << 1$ for the posed problem to be valid. For simplicity, the remainder of this work will assume that $Bi = 0.1$. This effectively makes A_1^2 an aspect ratio and any change will be due to variation in the length to thickness ratio.

Several analytical methods will now be demonstrated by using the flat plate problem just introduced. Solutions will be developed for both laminar and turbulent flow by using different $\tilde{h}(\xi)$. Note that $\tilde{h}(\xi)$ is in the governing equation which makes solving the differential equation much more difficult since since it is a variable coefficient.

First the problem will be solved using an average heat transfer coefficient. Three methods will be explored to solve the accompanying differential equation with a variable coefficient. The three methods will be identified as the power series, integral equation and generalized Bessel methods. The power series method is the most general approach but difficulties are encountered for the given problem. The last two methods will be fully developed and be used to solve the flat plate problem with a variable coefficient.

2.3.1 Average Heat Transfer Coefficient

The following is the solution to the flat plate problem formulated above when an average heat transfer coefficient, $\bar{h}$, is used. The governing equation as found in Eqn. 2.26 is

$$\frac{d^2\theta_1(\xi)}{d\xi^2} - A_1^2\tilde{h}(\xi)\theta_1(\xi) = -\tilde{q}(\xi) \tag{2.30}$$

Recall that the average heat transfer coefficient is found by integrating the local heat transfer coefficient over the length of the boundary

$$\bar{h} = \int_0^1 \tilde{h}(\xi)d\xi \tag{2.31}$$

where $\tilde{h}(\xi) = \xi^{-\frac{1}{2}}$ for laminar and $\tilde{h}(\xi) = \xi^{-\frac{1}{5}}$ for turbulent flow. Integrating, $\bar{h}$ leads to

$$\bar{h} = \int_0^1 \xi^{-\frac{1}{2}} d\xi = 2 \qquad \text{Laminar} \tag{2.32}$$

$$\bar{h} = \int_0^1 \xi^{-\frac{1}{5}} d\xi = \frac{5}{4} \qquad \text{Turbulent} \tag{2.33}$$

The problem to be solved is

$$\frac{d^2\theta_1(\xi)}{d\xi^2} - A_1^2 \bar{h} \theta_1(\xi) = -\tilde{q}(\xi) \tag{2.34}$$

$$\left.\frac{d\theta_1}{d\xi}\right|_{\xi=0} = 0 \tag{2.35}$$

$$\left.\frac{d\theta_1}{d\xi}\right|_{\xi=1} = 0. \tag{2.36}$$

Since the governing equation contains a heat generation term the problem is non-homogeneous and the solution is the sum of the homogeneous, θ_{1h}, and particular, θ_{1p}, solutions

$$\theta_1(\xi) = \theta_{1h}(\xi) + \theta_{1p}(\xi). \tag{2.37}$$

The homogeneous solution comes from the general solution commonly used for the given second order differential equation and can be found in most differential equations textbooks

$$\theta_{1h}(\xi) = c_1 \cosh(\sqrt{\bar{h}} A_1 \xi) + c_2 \sinh(\sqrt{\bar{h}} A_1 \xi). \tag{2.38}$$

The particular solution is found by using variation of parameters

$$\theta_{1p}(\xi) = -y_1(\xi) \int_0^{\xi} \frac{y_2(\xi')g(\xi')}{W(\xi')} d\xi' + y_2(\xi) \int_0^{\xi} \frac{y_1(\xi')g(\xi')}{W(\xi')} d\xi' \tag{2.39}$$

where g is the non-homogeneous term, y_1 and y_2 are linearly independent solutions to the homogeneous differential equation, from the homogeneous solution, and W is the Wronskian of y_1 and y_2

$$W(y_1, y_2) = \begin{vmatrix} y_1 & y_2 \\ \frac{dy_1}{d\xi} & \frac{dy_2}{d\xi} \end{vmatrix} = y_1 \frac{dy_2}{d\xi} - y_2 \frac{dy_1}{d\xi} \tag{2.40}$$

$$W = \sqrt{\bar{h}} A_1 [\cosh^2(\sqrt{\bar{h}} A_1 \xi) - \sinh^2(\sqrt{\bar{h}} A_1 \xi)] \tag{2.41}$$

$$W = \sqrt{\bar{h}} A_1. \tag{2.42}$$

The particular solution is

$$\begin{aligned} \theta_{1p}(\xi) =& -\cosh(\sqrt{\bar{h}} A_1 \xi) \int_0^\xi \frac{\sinh(\sqrt{\bar{h}} A_1 \xi')(-\tilde{q}(\xi))}{\sqrt{\bar{h}} A_1} d\xi' \\ &+ \sinh(\sqrt{\bar{h}} A_1 \xi) \int_0^\xi \frac{\cosh(\sqrt{\bar{h}} A_1 \xi')(-\tilde{q}(\xi))}{\sqrt{\bar{h}} A_1} d\xi' \end{aligned} \tag{2.43}$$

and rearranging

$$\theta_{1p}(\xi) = \frac{\cosh(\sqrt{\bar{h}} A_1 \xi)}{\sqrt{\bar{h}} A_1} \int_0^\xi \sinh(\sqrt{\bar{h}} A_1 \xi') \tilde{q}(\xi) d\xi' - \frac{\sinh(\sqrt{\bar{h}} A_1 \xi)}{\sqrt{\bar{h}} A_1} \int_0^\xi \cosh(\sqrt{\bar{h}} A_1 \xi') \tilde{q}(\xi) d\xi'. \tag{2.44}$$

Combining the homogeneous and particular solutions results in

$$\begin{aligned} \theta_1(\xi) =& c_1 \cosh(\sqrt{\bar{h}} A_1 \xi) + c_2 \sinh(\sqrt{\bar{h}} A_1 \xi) + \frac{\cosh(\sqrt{\bar{h}} A_1 \xi)}{\sqrt{\bar{h}} A_1} \int_0^\xi \sinh(\sqrt{\bar{h}} A_1 \xi') \tilde{q}(\xi) d\xi' \\ &- \frac{\sinh(\sqrt{\bar{h}} A_1 \xi)}{\sqrt{\bar{h}} A_1} \int_0^\xi \cosh(\sqrt{\bar{h}} A_1 \xi') \tilde{q}(\xi) d\xi'. \end{aligned} \tag{2.45}$$

Since both boundary conditions contain derivatives, the derivative of the solution must be performed and is

$$\begin{aligned} \frac{d\theta_1}{d\xi} =& c_1 \sqrt{\bar{h}} A_1 \sinh(\sqrt{\bar{h}} A_1 \xi) + c_2 \sqrt{\bar{h}} A_1 \cosh(\sqrt{\bar{h}} A_1 \xi) + \sinh(\sqrt{\bar{h}} A_1 \xi) \int_0^\xi \sinh(\sqrt{\bar{h}} A_1 \xi') \tilde{q}(\xi) d\xi' \\ &- \cosh(\sqrt{\bar{h}} A_1 \xi) \int_0^\xi \cosh(\sqrt{\bar{h}} A_1 \xi') \tilde{q}(\xi) d\xi'. \end{aligned} \tag{2.46}$$

Applying the boundary condition at $\xi = 0$, Eqn. 2.35, results in

$$c_2 = 0 \tag{2.47}$$

and the boundary condition at $\xi = 1$, Eqn. 2.36, results in

$$c_1 = -\frac{1}{\sqrt{\bar{h}}A_1}\int_0^1 \sinh(\sqrt{\bar{h}}A_1\xi')\tilde{q}(\xi)d\xi' + \frac{1}{\sqrt{\bar{h}}A_1\tanh(\sqrt{\bar{h}}A_1)}\int_0^1 \cosh(\sqrt{\bar{h}}A_1\xi')\tilde{q}(\xi)d\xi'. \quad (2.48)$$

At first thought, this same method may be attempted for $h(\xi)$. However, the general solution used above is not a solution if h is not a constant. To see an example of why this method doesn't work for a variable coefficient, see Appendix A.1.

2.3.2 Power Series Method

The power series method is one of the most general and powerful methods to solve differential equations with variable coefficients. In fact, the general solution used from the previous method was developed using this method for a constant coefficient differential equation. To use the power series method consider Eqn. 2.26

$$\frac{d^2\theta_1(\xi)}{d\xi^2} - A_1^2\tilde{h}(\xi)\theta_1(\xi) = -\tilde{q}(\xi)$$

The power series cannot be used with an arbitrary function of ξ so let $\tilde{h}(\xi) = \xi^{-\frac{1}{2}}$ since this is the variation of $h(\xi)$ for laminar flow past a flat plate. First a solution is assumed to be of the form

$$\theta_1(\xi) = \sum_{n=0}^{\infty} c_n\xi^n \quad (2.49)$$

with derivatives

$$\frac{d\theta_1(\xi)}{d\xi} = \sum_{n=1}^{\infty} nc_n\xi^{n-1} \quad (2.50)$$

$$\frac{d^2\theta_1(\xi)}{d\xi^2} = \sum_{n=2}^{\infty} n(n-1)c_n\xi^{n-2}. \quad (2.51)$$

The homogeneous case will first need to be solved

$$\frac{d^2\theta_1(\xi)}{d\xi^2} - A_1^2\xi^{-\frac{1}{2}}\theta_1(\xi) = 0. \quad (2.52)$$

Substituting the assumed form of the solution into the differential equation

$$\sum_{n=2}^{\infty} n(n-1)c_n\xi^{n-2} - A_1^2\xi^{-\frac{1}{2}}\sum_{n=0}^{\infty} c_n\xi^n = 0 \tag{2.53}$$

and combining the ξ terms results in

$$\sum_{n=2}^{\infty} n(n-1)c_n\xi^{n-2} - A_1^2\sum_{n=0}^{\infty} c_n\xi^{n-\frac{1}{2}} = 0. \tag{2.54}$$

The power of ξ needs to match in both terms so both terms can be combined into a single summation. It is required for the indices, n, to be an integer, and it appears impossible to match $n-2$ and $n-\frac{1}{2}$ without creating a fractional index. Thus the power series cannot be used for the given variable coefficient. It could have been noticed that $\xi^{-\frac{1}{2}}$ is not analytic at $\xi = 0$ which also prevents the power series from being used.

2.3.3 Integral Equation Method

The integral equation (IE) method is an approach to solve a differential equation with variable coefficients by transforming the differential equation to an integral equation. The variable coefficient term is simply lumped with the source term and the equation is then integrated until the derivatives are gone and the solution is in terms of integrals. The dependent variable that is being solved for is also contained inside the integral which requires the iterative method of successive approximations to be used to find the solution. This method has been used by [14] when dealing with the integro-differential radiative heat transfer equation and [15] when solving nonlinear differential equations. Consider Eqn. 2.26

$$\frac{d^2\theta_1(\xi)}{d\xi^2} - A_1^2\tilde{h}(\xi)\theta_1(\xi) = -\tilde{q}(\xi)$$

with boundary conditions

$$\left.\frac{d\theta_1}{d\xi}\right|_{\xi=0} = 0 \tag{2.55}$$

$$\left.\frac{d\theta_1}{d\xi}\right|_{\xi=1} = 0. \tag{2.56}$$

To apply the IE method, simply move the term with the variable coefficient to the right hand side of the equal sign

$$\frac{d^2\theta_1(\xi)}{d\xi^2} = A^2\tilde{h}(\xi)\theta_1(\xi) - \tilde{q}(\xi)$$

then treat everything on the right hand side as some function of x

$$\frac{d^2\theta_1(\xi)}{d\xi^2} = g(x). \tag{2.57}$$

The general solution can be found by simply integrating twice

$$T_1(x) = c_2 + c_1 x + \int_0^x \int_0^{x'} g(x'')dx''dx'. \tag{2.58}$$

Integrate the differential equation once

$$\frac{d\theta_1(\xi)}{d\xi} = c_1 + \int_0^{\xi} A_1^2\tilde{h}\xi'\theta_1(\xi') - \tilde{q}(\xi')d\xi' \tag{2.59}$$

and integrate again

$$\theta_1(\xi) = c_2 + c_1\xi + \int_0^{\xi}\int_0^{\xi'} A_1^2\tilde{h}(\xi'')\theta_1(\xi'') - \tilde{q}(\xi'')d\xi''d\xi'. \tag{2.60}$$

Apply the boundary condition at $\xi = 0$.

$$c_1 = 0 \tag{2.61}$$

Apply the boundary condition at $\xi = 1$.

$$0 = \int_0^1 A_1^2\tilde{h}(\xi')\theta_1(\xi') - \tilde{q}(\xi')d\xi' \tag{2.62}$$

At first it may seem that this boundary condition is of no use and c_2 cannot be found. However, c_2 is buried in the θ_1 term and if θ_1 is substituted in it is possible to solve for c_2

$$c_2 = -\frac{1}{\int_0^1 \tilde{h}(\xi)}d\xi \int_0^1 \tilde{h}(\xi')\int_0^{\xi'}\int_0^{\xi''} A_1^2\tilde{h}(\xi''')\theta_1(\xi''') - \tilde{q}(\xi''')d\xi'''d\xi'' - \tilde{q}(\xi')d\xi'. \tag{2.63}$$

Normally this approach would not be desirable since it introduces the need to iterate to obtain a solution. However, since two regions are being coupled, each region depends on the others' temperature distribution and the solution already requires an iterative solution.

The IE method often requires implementing a technique used in numerical analysis called relaxation when evaluating the solution to obtain specific values. Relaxation reduces the amount the solution changes between each iteration and is implemented by

$$\theta_{\text{new}} = (1-\gamma)\theta_{\text{last iteration}} + \gamma\theta_{\text{current iteration}} \tag{2.64}$$

where γ is some value between 0 to 1. When using relaxation, each iteration's solution is the sum of the previous iteration's solution and the current iterations solution. The weight of each iteration's solution that contributes to the new solution is determined by γ. If $\gamma = 1$ the results is the same as not using relaxation and the new solution is the same as the current solution. As γ decreases, the new solution is more heavily influenced by the previous iterations solution. A smaller γ results in a more stable solution, however, it also slows convergence.

It should be noted that use of relaxation increases the number of terms in the solution every iteration which slows down the computation. It can be beneficial to curve fit the solution each iteration to keep the solution to a set number of terms. This increases the number of iterations required to converge but each iteration takes less time.

2.3.4 Generalized Bessel Method

The generalized Bessel (GB) method is another approach to solve differential equations with variable coefficients which makes use of the generalized Bessel equation. This method is not commonly used for this application and the only place in literature that it was similarly used is in [16] for heat transfer in extended surfaces. However, generation terms were not considered and the differential equations used were homogeneous. This method will now be extended to non-homogeneous equations. Reconsider Eqn. 2.26

$$\frac{d^2\theta_1(\xi)}{d\xi^2} - A_1^2\tilde{h}(\xi)\theta_1(\xi) = -\tilde{q}(\xi) \tag{2.65}$$

with boundary conditions

$$\left.\frac{d\theta_1}{d\xi}\right|_{\xi=0} = 0 \tag{2.66}$$

$$\left.\frac{d\theta_1}{d\xi}\right|_{\xi=1} = 0. \tag{2.67}$$

The solution to a non-homogeneous ordinary differential equation is the sum of the homogeneous and the particular solutions

$$\theta_1(\xi) = \theta_{1h}(\xi) + \theta_{1p}(\xi). \tag{2.68}$$

2.3.4.1 Homogeneous Solution

First, consider the homogeneous problem of Eqn. 2.26 which needs to be transformed to the form of the generalized Bessel equation

$$\frac{d^2\theta_{1h}(\xi)}{d\xi^2} - A_1^2\tilde{h}(\xi)\theta_{1h}(\xi) = 0. \tag{2.69}$$

The generalized Bessel equation adapted from [17] is

$$\frac{d^2R}{d\xi^2} + \left[\frac{1-2m}{x} - 2\beta\right]\frac{dR}{d\xi} + \left[p^2b^2\xi^{2p-2} + \beta^2 + \frac{\beta(2m-1)}{\xi} + \frac{m^2 - p^2\nu^2}{\xi^2}\right]R = 0 \tag{2.70}$$

with the general solution

$$R = \xi^m e^{\beta\xi}\left[c_1 J_\nu(b\xi^p) + c_2 Y_\nu(b\xi^p)\right] \tag{2.71}$$

or if ν is not an integer

$$R = \xi^m e^{\beta\xi}\left[c_1 J_\nu(b\xi^p) + c_2 J_{-\nu}(b\xi^p)\right] \tag{2.72}$$

where J_ν and Y_ν are the Bessel function of the first kind and second kind respectively, of order ν. To transform Eqn. 2.69 into the form of Eqn. 2.70, the coefficients for each term are equated. The second order term coefficient is already the same so no change is needed. There is no first order term so

$$\frac{1-2m}{\xi} - 2\beta = 0 \tag{2.73}$$

is true with the following choice of coefficients

$$m = \frac{1}{2} \tag{2.74}$$
$$\beta = 0.$$

Looking at the zeroth order term,

$$p^2 b^2 \xi^{2p-2} + \frac{m^2 - p^2 \nu^2}{\xi^2} = -A_1^2 \tilde{h}(\xi) \tag{2.75}$$

if it is required that $m = p\nu$, the last term goes away

$$p^2 b^2 \xi^{2p-2} = -A_1^2 \tilde{h}(\xi). \tag{2.76}$$

Solving for b results in

$$b = \frac{\xi^{1-p}}{p} i A_1 \sqrt{\tilde{h}(\xi)}. \tag{2.77}$$

Note that when b is substituted into the solution form, the result in the Bessel function is

$$J_\nu\Big(\frac{\xi^{1-p}}{p} i A_1 \sqrt{\tilde{h}(\xi)} \xi^p\Big) \tag{2.78}$$

and canceling ξ^p results in

$$J_\nu\Big(\frac{1}{p} i A_1 \sqrt{\tilde{h}(\xi)} \xi\Big). \tag{2.79}$$

Thus the choice of p has no effect on the power of ξ in the Bessel function and it is dependent only on the variation of ξ in $\tilde{h}(\xi)$. Therefore, p and ν can be arbitrarily chosen so as long as they satisfy $m = p\nu$. It may appear to be desirable to choose $\nu = 1$ to have Bessel functions of integer order or $\nu = \frac{1}{2}$ since Bessel functions of order $\nu = \pm\frac{1}{2}$ can be expressed in terms of hyperbolic sinh and cosh

$$I_{\frac{1}{2}}\Big(A_1 \xi^p\Big) = \sqrt{\frac{2}{A_1 \pi \xi^p}} \sinh(A_1 \xi^p) \tag{2.80}$$

$$I_{-\frac{1}{2}}\Big(A_1 \xi^p\Big) = \sqrt{\frac{2}{A_1 \pi \xi^p}} \cosh(A_1 \xi^p) \tag{2.81}$$

The functions cosh and sinh are generally easier to work with than Bessel functions. However, when ξ is raised to a non-integer power the derivative and integral of cosh and sinh become quite complex and are not as simple as might be first expected. The choice of $\nu = 1$ or $\nu = \frac{1}{2}$ did not seem to increase ease of obtaining a solution in this work. The best results were obtained when ν resulted from the choice of p that canceled the power of ξ in the Bessel function. For example, if $\tilde{h}(\xi) = \xi^{-\frac{1}{2}}$, then

$$b = \frac{\xi^{1-p}}{p} iA_1 \xi^{-\frac{1}{4}} \tag{2.82}$$

and a choice of $p = \frac{3}{4}$ will cause ξ to cancel out which will simplify the solution. However more effort could be beneficial in determining an optimal choice for ν.

Returning to the general solution, Eqn. 2.72, and substituting in the determined coefficients results in

$$\theta_{1h} = \xi^{\frac{1}{2}} \left[c_1 J_\nu \left(\frac{1}{p} iA_1 \sqrt{\tilde{h}(\xi)} \xi \right) + c_2 J_{-\nu} \left(\frac{1}{p} iA_1 \sqrt{\tilde{h}(\xi)} \xi \right) \right] \tag{2.83}$$

or since the imaginary number, i, is present, Modified Bessel functions, I_ν, can be used and the i removed

$$\theta_{1h} = \xi^{\frac{1}{2}} \left[c_1 I_\nu \left(\frac{A_1}{p} \sqrt{\tilde{h}(\xi)} \xi \right) + c_2 I_{-\nu} \left(\frac{A_1}{p} \sqrt{\tilde{h}(\xi)} \xi \right) \right]. \tag{2.84}$$

2.3.4.2 Particular Solution

A common method for determining the particular solution is by variation of parameters

$$\theta_{1p} = -y_1(\xi) \int_0^\xi \frac{y_2(\xi')g(\xi')}{W(\xi')} d\xi' + y_2(\xi) \int_0^\xi \frac{y_1(\xi')g(\xi')}{W(\xi')} d\xi' \tag{2.85}$$

where $g(\xi')$ is the non-homogeneous term, y_1 and y_2 are linearly independent solutions to the homogeneous differential equation and W is the Wronskian of y_1 and y_2

$$W(y_1, y_2) = \begin{vmatrix} y_1 & y_2 \\ \frac{dy_1}{d\xi} & \frac{dy_2}{d\xi} \end{vmatrix} = y_1 \frac{dy_2}{d\xi} - y_2 \frac{dy_1}{d\xi}.$$

The Wronskian of Bessel functions can get quite complex. Fortunately, a relation has been derived for basic Bessel functions [18]

$$W(I_\nu\Big(\xi\Big),I_{-\nu}\Big(\xi\Big)) = -\frac{2\sin(\nu\pi)}{\xi\pi}. \tag{2.86}$$

This relation is valid for both Bessel functions and Modified Bessel functions that are not of integer order. For Bessel functions of integer order

$$W(J_\nu\Big(\xi\Big),Y_\nu\Big(\xi\Big)) = \frac{2}{\xi\pi} \tag{2.87}$$

$$W(I_\nu\Big(\xi\Big),K_\nu\Big(\xi\Big)) = \frac{1}{\xi}. \tag{2.88}$$

However, for the generalized Bessel equation the Wronskian is more complex due to the extra terms ξ^m and $e^{\beta\xi}$ and the fact that ξ is not raised to the power of one. There does not appear to be any simplifying relation for the Wronskian for this case in literature.

The previous relations for the Wronskian were developed by using the limiting form of the Bessel function when $\xi \to 0$, [19]

$$I_\nu\Big(\xi\Big) \simeq \Big(\frac{\xi}{2}\Big)^\nu \frac{1}{\Gamma(\nu+1)}. \tag{2.89}$$

The same process will now be extended for use with the generalized Bessel equation. First, note that

$$\Gamma(\nu+1) = \nu\Gamma(\nu) \tag{2.90}$$

and for generality assume b is a function of ξ

$$I_\nu\Big(b(\xi)\xi^p\Big) \simeq \Big(\frac{b(\xi)\xi^p}{2}\Big)^\nu \frac{1}{\nu\Gamma(\nu)}. \tag{2.91}$$

Evaluating the Wronskian

$$W\Big(\xi^m e^{\beta\xi} I_\nu\big(b(\xi)\xi^p\big), \xi^m e^{\beta\xi} I_{-\nu}\big(b(\xi)\xi^p\big)\Big) = \xi^m e^{\beta\xi} I_\nu\big(b(\xi)\xi^p\big)\frac{d}{d\xi}\Big[\xi^m e^{\beta\xi} I_{-\nu}\big(b(\xi)\xi^p\big)\Big] \\ - \xi^m e^{\beta\xi} I_{-\nu}\big(b(\xi)\xi^p\big)\frac{d}{d\xi}\Big[\xi^m e^{\beta\xi} I_\nu\big(b(\xi)\xi^p\big)\Big] \tag{2.92}$$

substituting in Eqn. 2.91

$$W = \Big(\frac{b(\xi)\xi^p}{2}\Big)^\nu \frac{\xi^m e^{\beta\xi}}{\nu\Gamma(\nu)}\frac{d}{d\xi}\Big[\Big(\frac{b(\xi)\xi^p}{2}\Big)^{-\nu}\frac{\xi^m e^{\beta\xi}}{-\nu\Gamma(-\nu)}\Big] \\ - \Big(\frac{b(\xi)\xi^p}{2}\Big)^{-\nu}\frac{\xi^m e^{\beta\xi}}{-\nu\Gamma(-\nu)}\frac{d}{d\xi}\Big[\Big(\frac{b(\xi)\xi^p}{2}\Big)^{\nu}\frac{\xi^m e^{\beta\xi}}{\nu\Gamma(\nu)}\Big] \tag{2.93}$$

and evaluating the derivatives results in

$$W = \Big(\frac{b(\xi)\xi^p}{2}\Big)^\nu \frac{\xi^m e^{\beta\xi}}{\nu\Gamma(\nu)}\Big[\Big(\frac{b(\xi)\xi^p}{2}\Big)^{-\nu}\frac{\xi^m e^{\beta\xi}}{-\nu\Gamma(-\nu)}\Big[\frac{m}{\xi}+\beta+\frac{d\big(b(\xi)\xi^p\big)}{d\xi}\frac{-\nu}{b(\xi)\xi^p}\Big]\Big] \\ - \Big(\frac{b(\xi)\xi^p}{2}\Big)^{-\nu}\frac{\xi^m e^{\beta\xi}}{-\nu\Gamma(-\nu)}\Big[\Big(\frac{b(\xi)\xi^p}{2}\Big)^{\nu}\frac{\xi^m e^{\beta\xi}}{\nu\Gamma(\nu)}\Big[\frac{m}{\xi}+\beta+\frac{d\big(b(\xi)\xi^p\big)}{d\xi}\frac{\nu}{b(\xi)\xi^p}\Big]\Big]. \tag{2.94}$$

Removing canceling terms reduces the Wronskian to

$$W = \frac{2}{b(\xi)\xi^p}\frac{(\xi^m e^{\beta\xi})^2}{\nu\Gamma(\nu)\Gamma(-\nu)}\frac{d\big(b(\xi)\xi^p\big)}{d\xi}. \tag{2.95}$$

Note that

$$\Gamma(\nu)\Gamma(-\nu) = -\frac{\pi}{\nu\sin(\pi\nu)} \tag{2.96}$$

and when substituted into the Wronskian leads to

$$W = \frac{2\sin(\pi\nu)}{b(\xi)\xi^p}\frac{(\xi^m e^{\beta\xi})^2}{\pi}\frac{d\big(b(\xi)\xi^p\big)}{d\xi}. \tag{2.97}$$

This relation could not be found in literature and will now formally be stated as

$$W\Big(\xi^m e^{\beta\xi} I_\nu\big(b(\xi)\xi^p\big), \xi^m e^{\beta\xi} I_{-\nu}\big(b(\xi)\xi^p\big)\Big) = -(\xi^m e^{\beta\xi})^2\frac{2\sin(\pi\nu)}{\pi b(\xi)\xi^p}\frac{d(b(\xi)\xi^p)}{d\xi}. \tag{2.98}$$

The plots in Figure 2.3 were created using the math software Maple^{TM} [20] to compare Eqn. 2.98 with the Wronskian found by using Maple's^{TM} Wronskian command. These plots show that both methods to determine the Wronskian are indistinguishable from each other, thus the newly developed relation is accurate. Plot (a) is a typical Wronskian for a solid and (b) for a fluid. Since this new relation provides a way to determine the Wronskian for the generalized Bessel equation solutions, the GB method can be used to solve non-homogeneous, ordinary differential equations with variable coefficients.

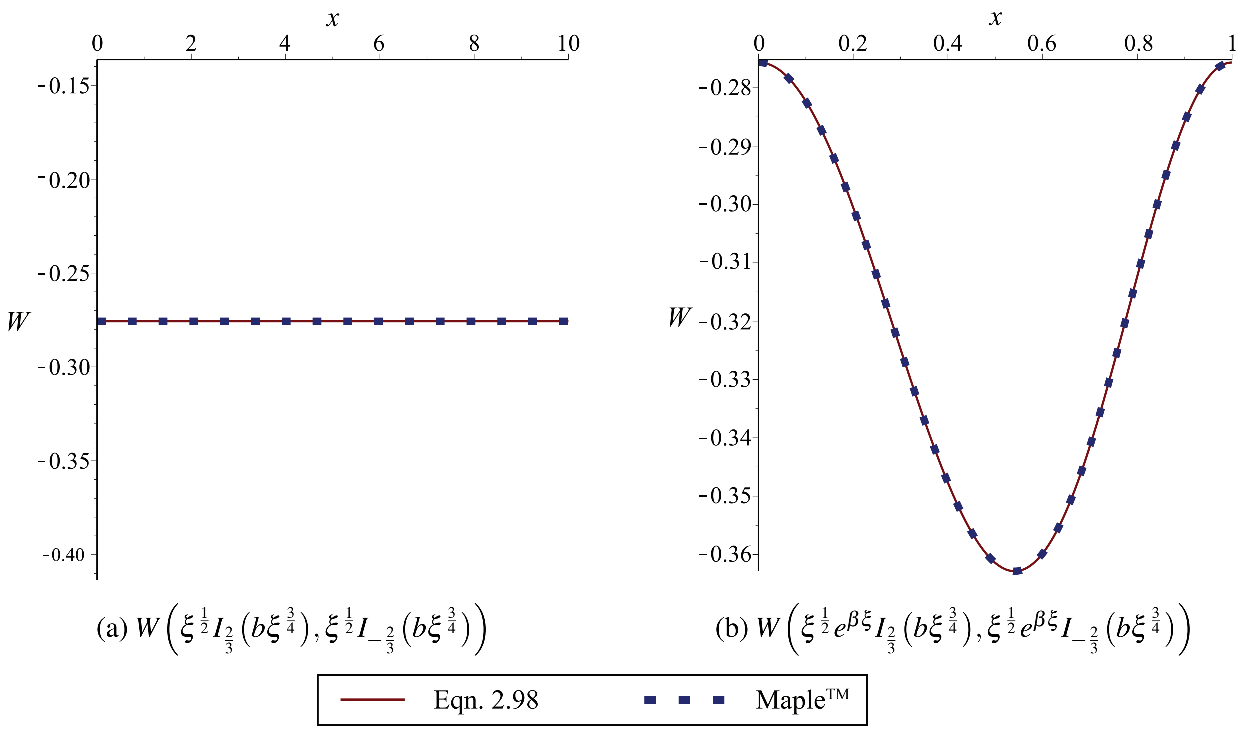

(a) $W\left(\xi^{\frac{1}{2}} I_{\frac{2}{3}}\left(b\xi^{\frac{3}{4}}\right), \xi^{\frac{1}{2}} I_{-\frac{2}{3}}\left(b\xi^{\frac{3}{4}}\right)\right)$

(b) $W\left(\xi^{\frac{1}{2}} e^{\beta\xi} I_{\frac{2}{3}}\left(b\xi^{\frac{3}{4}}\right), \xi^{\frac{1}{2}} e^{\beta\xi} I_{-\frac{2}{3}}\left(b\xi^{\frac{3}{4}}\right)\right)$

Figure 2.3: Verification of the Wronskian relation for the generalized Bessel equation solution for two cases

The particular solution can now be found by using the newly developed Wronskian relation, Eqn. 2.98, with the method of variation of parameters, Eqn. 2.85,

$$\theta_{1p} = -\xi^{\frac{1}{2}} I_\nu\left(\frac{A_1}{p}\sqrt{\tilde{h}(\xi)}\xi\right)\int_0^\xi \frac{\xi'^{\frac{1}{2}} I_{-\nu}\left(\frac{A_1}{p}\sqrt{\tilde{h}(\xi')}\xi'\right) g(\xi')}{-\frac{d(\frac{A_1}{p}\sqrt{\tilde{h}(\xi')}\xi')}{d\xi'}\frac{2\sin(\pi\nu)}{\pi\frac{A_1}{p}\sqrt{\tilde{h}(\xi')}\xi'}\xi'} d\xi'$$

$$+\xi^{\frac{1}{2}} I_{-\nu}\left(\frac{A_1}{p}\sqrt{\tilde{h}(\xi)}\xi\right)\int_0^\xi \frac{\xi'^{\frac{1}{2}} I_{\nu}\left(\frac{A_1}{p}\sqrt{\tilde{h}(\xi')}\xi'\right) g(\xi')}{-\frac{d(\frac{A_1}{p}\sqrt{\tilde{h}(\xi')}\xi')}{d\xi'}\frac{2\sin(\pi\nu)}{\pi\frac{A_1}{p}\sqrt{\tilde{h}(\xi')}\xi'}\xi'} d\xi' \qquad (2.99)$$

which simplifies to

$$\theta_{1p} = -\frac{\pi}{2\sin(\pi\nu)}\xi^{\frac{1}{2}} I_\nu\left(\frac{A_1}{p}\sqrt{\tilde{h}(\xi)}\xi\right)\int_0^\xi \frac{\xi'^{\frac{1}{2}} I_{-\nu}\left(\frac{A_1}{p}\sqrt{\tilde{h}(\xi')}\xi'\right) g(\xi')\sqrt{\tilde{h}(\xi')}}{-\frac{d(f(\xi')\xi')}{d\xi'}} d\xi' \qquad (2.100)$$

$$+\frac{\pi}{2\sin(\pi\nu)}\xi^{\frac{1}{2}} I_{-\nu}\left(\frac{A_1}{p}\sqrt{\tilde{h}(\xi)}\xi\right)\int_0^\xi \frac{\xi'^{\frac{1}{2}} I_{\nu}\left(\frac{A_1}{p}\sqrt{\tilde{h}(\xi')}\xi'\right) g(\xi')\sqrt{\tilde{h}(\xi')}}{-\frac{d(\sqrt{\tilde{h}(\xi')}\xi')}{d\xi'}} d\xi'.$$

The math software Maple^{TM} was also used for mathematical evaluation and plotting. The built in Modified Bessel functions in Maple^{TM} were found to sometimes be insufficient when solving these problems and the summation form of the Modified Bessel equation needed to be used

$$I_\nu\left(\frac{A_1}{p}\xi\right) = \left(\frac{1}{2}\frac{A_1}{p}\xi\right)^\nu \sum_{n=0}^{\infty} \frac{(\frac{1}{2}\frac{A_1}{p}\xi)^{2n}}{n!\Gamma(\nu+n+1)}. \qquad (2.101)$$

A difficulty that was encountered when evaluating these solutions was as $\frac{A_1}{p}$ gets larger, more summation terms are required for the Bessel summation. Also, as the number of summation terms increased, the numerical precision needs to be increased. As a result, larger values of $\frac{A_1}{p}$ require more time to evaluate the solutions and at a sufficiently large $\frac{A_1}{p}$, Maple^{TM} is unable to evaluate the solutions due to hardware limitations.

Applying this developed solution for laminar flow where the heat transfer coefficient varies according to

$$\tilde{h}(\xi) = \xi^{-\frac{1}{2}} \qquad (2.102)$$

and choosing

$$\nu = \frac{2}{3} \tag{2.103}$$

$$p = \frac{3}{4} \tag{2.104}$$

$$g = \tilde{q}(\xi') \tag{2.105}$$

and from Eqn. 2.100 the particular solution is

$$\begin{aligned}\theta_{1p} = &-\frac{4\pi}{3\sqrt{3}}\xi^{\frac{1}{2}} I_{\frac{2}{3}}\left(\frac{4}{3}A_1\xi^{\frac{3}{4}}\right)\int_0^{\xi} \xi'^{\frac{1}{2}} I_{-\frac{2}{3}}\left(\frac{4}{3}A_1\xi'^{\frac{3}{4}}\right)\tilde{q}(\xi')d\xi' \\ &+\frac{4\pi}{3\sqrt{3}}\xi^{\frac{1}{2}} I_{-\frac{2}{3}}\left(\frac{4}{3}A_1\xi^{\frac{3}{4}}\right)\int_0^{\xi} \xi'^{\frac{1}{2}} I_{\frac{2}{3}}\left(\frac{4}{3}A_1\xi'^{\frac{3}{4}}\right)\tilde{q}(\xi')d\xi'.\end{aligned} \tag{2.106}$$

Thus the general solution is

$$\begin{aligned}\theta_1 = &\xi^{\frac{1}{2}}\left[c_1 I_{\frac{2}{3}}\left(\frac{4}{3}A_1\xi^{\frac{3}{4}}\right) + c_2 I_{-\frac{2}{3}}\left(\frac{4}{3}A_1\xi^{\frac{3}{4}}\right)\right] \\ &-\frac{4\pi}{3\sqrt{3}}\xi^{\frac{1}{2}} I_{\frac{2}{3}}\left(\frac{4}{3}A_1\xi^{\frac{3}{4}}\right)\int_0^{\xi} \xi'^{\frac{1}{2}} I_{-\frac{2}{3}}\left(\frac{4}{3}A_1\xi'^{\frac{3}{4}}\right)\tilde{q}(\xi')d\xi' \\ &+\frac{4\pi}{3\sqrt{3}}\xi^{\frac{1}{2}} I_{-\frac{2}{3}}\left(\frac{4}{3}A_1\xi^{\frac{3}{4}}\right)\int_0^{\xi} \xi'^{\frac{1}{2}} I_{\frac{2}{3}}\left(\frac{4}{3}A_1\xi'^{\frac{3}{4}}\right)\tilde{q}(\xi')d\xi'\end{aligned} \tag{2.107}$$

In order to apply the boundary conditions and determine the constants the derivative will need to be found which is

$$\begin{aligned}\frac{d\theta_1}{d\xi} = &A_1\xi^{\frac{1}{4}}\left[c_1 I_{-\frac{1}{3}}\left(\frac{4}{3}A_1\xi^{\frac{3}{4}}\right) + c_2 I_{\frac{1}{3}}\left(\frac{4}{3}A_1\xi^{\frac{3}{4}}\right)\right] \\ &-\frac{4A_1\pi}{3\sqrt{3}}\xi^{\frac{1}{4}} I_{-\frac{1}{3}}\left(\frac{4}{3}A_1\xi^{\frac{3}{4}}\right)\int_0^{\xi} \xi'^{\frac{1}{2}} I_{-\frac{2}{3}}\left(\frac{4}{3}A_1\xi'^{\frac{3}{4}}\right)\tilde{q}(\xi')d\xi' \\ &+\frac{4A_1\pi}{3\sqrt{3}}\xi^{\frac{1}{4}} I_{\frac{1}{3}}\left(\frac{4}{3}A_1\xi^{\frac{3}{4}}\right)\int_0^{\xi} \xi'^{\frac{1}{2}} I_{\frac{2}{3}}\left(\frac{4}{3}A_1\xi'^{\frac{3}{4}}\right)\tilde{q}(\xi')d\xi'.\end{aligned} \tag{2.108}$$

Apply the boundary condition at $\xi = 0$

$$0 = \left[c_1\xi^{\frac{1}{4}} I_{-\frac{1}{3}}\left(\frac{4}{3}A_1\xi^{\frac{3}{4}}\right) + c_2\xi^{\frac{1}{4}} I_{\frac{1}{3}}\left(\frac{4}{3}A_1\xi^{\frac{3}{4}}\right)\right]\Big|_{\xi=0}. \tag{2.109}$$

Note that

$$\lim_{\xi \to 0} \xi^{\frac{1}{4}} I_{-\frac{1}{3}}\left(\frac{4}{3}A_1\xi^{\frac{3}{4}}\right) \longrightarrow \frac{2^{\frac{1}{3}}}{(\frac{4}{3}A_1)^{\frac{1}{3}}\Gamma(\frac{2}{3})} \tag{2.110}$$

$$\xi^{\frac{1}{4}} I_{\frac{1}{3}}\left(\frac{4}{3}A_1\xi^{\frac{3}{4}}\right)\Big|_{\xi=0} = 0 \tag{2.111}$$

which results in

$$c_1 = 0. \tag{2.112}$$

Applying the boundary condition at $\xi = 1$, the constant is

$$c_2 = \frac{4\pi}{3\sqrt{3}} \frac{I_{-\frac{1}{3}}\left(\frac{4}{3}A_1\right)}{I_{\frac{1}{3}}\left(\frac{4}{3}A_1\right)} \int_0^1 \xi'^{\frac{1}{2}} I_{-\frac{2}{3}}\left(\frac{4}{3}A_1\xi'^{\frac{3}{4}}\right)\tilde{q}(\xi')d\xi' - \frac{4\pi}{3\sqrt{3}} \int_0^1 \xi'^{\frac{1}{2}} I_{\frac{2}{3}}\left(\frac{4}{3}A_1\xi'^{\frac{3}{4}}\right)\tilde{q}(\xi')d\xi' \tag{2.113}$$

For turbulent flow past a flat plate

$$\tilde{h}(\xi) = \xi^{-\frac{1}{5}} \tag{2.114}$$

and choosing

$$\nu = \frac{5}{9} \tag{2.115}$$

$$p = \frac{9}{10} \tag{2.116}$$

$$g = \tilde{q}(\xi'). \tag{2.117}$$

The solution is found by the same process as previously demonstrated. The non-dimensional temperature is

$$\begin{aligned}\theta_1 =& c_2\xi^{\frac{1}{2}} I_{-\frac{5}{9}}\left(\frac{10}{9}A_1\xi^{\frac{9}{10}}\right) - \frac{5\pi}{9\sin(\frac{5}{9}\pi)}\xi^{\frac{1}{2}} I_{\frac{5}{9}}\left(B\xi^{\frac{9}{10}}\right) \int_0^{\xi} I_{-\frac{5}{9}}\left(\frac{10}{9}A_1\xi'^{\frac{9}{10}}\right) \xi'^{\frac{1}{2}}\tilde{q}(\xi')d\xi' \\ &+ \frac{5\pi}{9\sin(\frac{5}{9}\pi)}\xi^{\frac{1}{2}} I_{-\frac{5}{9}}\left(\frac{10}{9}A_1\xi^{\frac{9}{10}}\right) \int_0^{\xi} I_{\frac{5}{9}}\left(\frac{10}{9}A_1\xi'^{\frac{9}{10}}\right)\xi'^{\frac{1}{2}}\tilde{q}(\xi')d\xi'\end{aligned} \tag{2.118}$$

and the constant is

$$
\begin{aligned}
c_2 = & \frac{5\pi}{9\sin(\frac{5}{9}\pi)} \frac{I_{-\frac{4}{9}}\left(\frac{10}{9}A_1\right)}{I_{\frac{4}{9}}\left(\frac{10}{9}A_1\right)} \int_0^1 I_{-\frac{5}{9}}\left(\frac{10}{9}A_1 \xi'^{\frac{9}{10}}\right) \xi'^{\frac{1}{2}} \tilde{q}(\xi') d\xi' \\
& - \frac{5\pi}{9\sin(\frac{5}{9}\pi)} \int_0^1 I_{\frac{5}{9}}\left(\frac{10}{9}A_1 \xi'^{\frac{9}{10}}\right) \xi'^{\frac{1}{2}} \tilde{q}(\xi') d\xi'.
\end{aligned} \tag{2.119}
$$

2.4 Analysis

Using the integral equation, IE, and generalized Bessel, GB, solutions developed previously, the temperature profile of the flat plate will be compared when using $\bar{h}$ to $h(\xi)$. The problem will be considered with both a uniform heat generation, $\tilde{q} = 1$, and a center focused heat source represented by $\tilde{q} = -\xi^2 + \xi$. For the IE method an iterative solution is required and convergence was monitored by how closely the surface heat rate matches the heat generation rate in the plate

$$
A_1^2 \int_0^1 \tilde{h}(\xi)\theta_1(\xi) d\xi = \int_0^1 \tilde{q}(\xi) d\xi. \tag{2.120}
$$

In order to gain confidence in the developed solutions, they were first verified with each other. The IE method using $h(\xi)$ was compared with the GB method and the IE method using $\bar{h}$ was compared to the common method used for $\bar{h}$. The results in Figures 2.4 and 2.5 show that the solutions match well. The only discrepancy is when A_1^2 is large the IE method has trouble matching at the end of the plate. This is likely due to the fact that as A_1^2 gets larger, greater relaxation is necessary for stability of the solution. The end of the plate at $\xi = 1$ is the last location that convergence is achieved and the rate of convergence slows as full convergence is approached. In order to reach full convergence for large A_1^2 an impractical amount of time is required. Increasing relaxation near convergence can often increase convergence rate, however, in this case it was only found to lead to instability, even when only increased slightly.

Figures 2.4 and 2.5 also show that for turbulent flow, the difference between the maximum and minimum temperatures in the plate is smaller than for laminar flow. This means that there is less temperature variation in the plate which leads to a lower degree of conjugation. This conclusion can also be made from looking at the difference in θ values between the $h(\xi)$ and $\bar{h}$ cases for laminar and turbulent flows. For example, at $\xi = 1$, the temperature for $h(\xi)$ minus the tem-

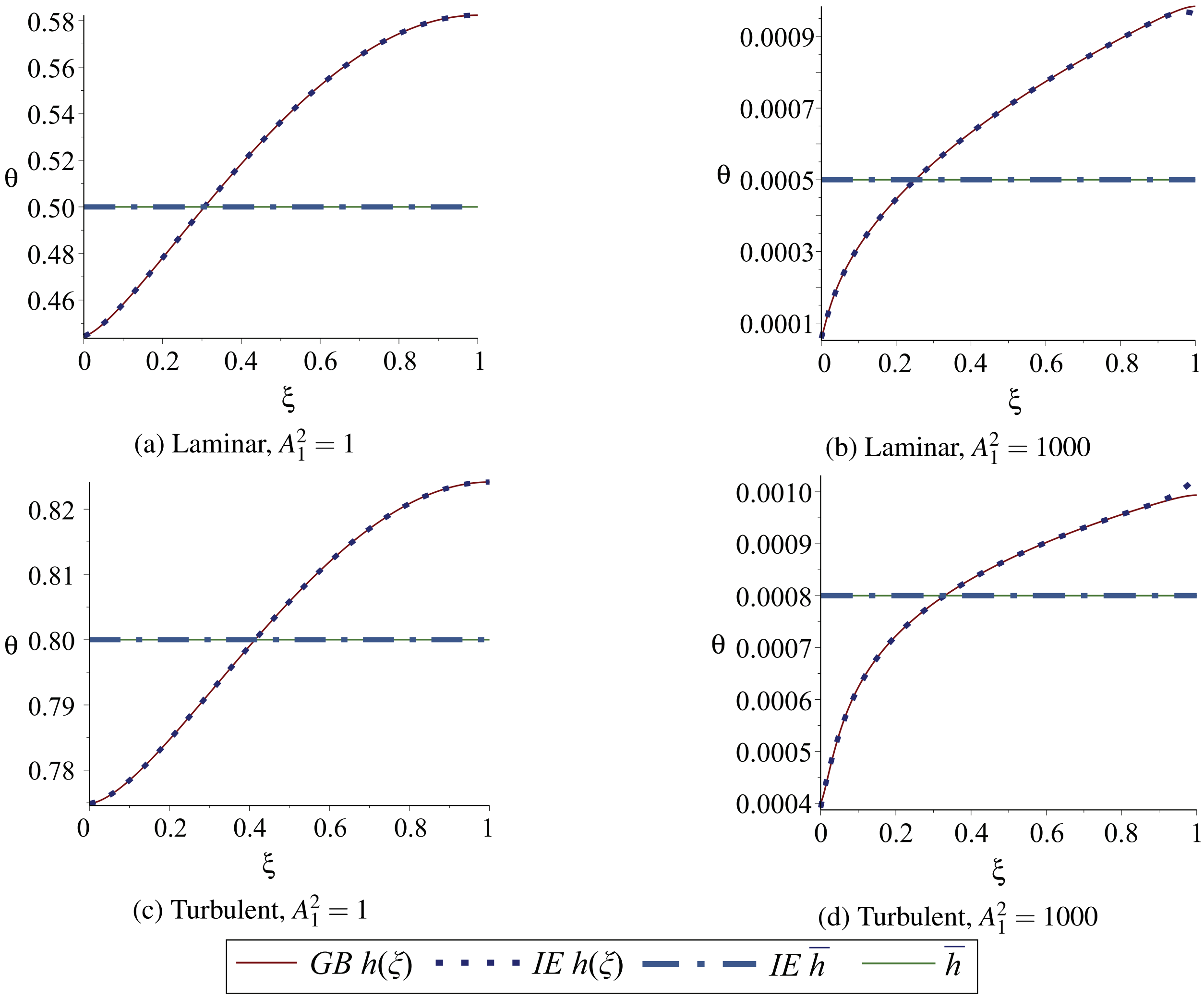

Figure 2.4: Non-dimensional temperature profiles, θ, with a uniform heat generation, $\tilde{q} = 1$, for the generalized Bessel method (GB) and the integral equation method (IE) for $h(x)$ and IE and the common method for $\bar{h}$

perature for $\bar{h}$ is less for turbulent flow than laminar. Thus, conjugate effects seem to be less for turbulent flow. This agrees with Dorfman's [12] conjugation guidelines. These same trends would be seen in the remainder of the plots in this chapter and thus plots for turbulent flow will not be shown further. Just note that heat transfer is greater for turbulent flow and thus conjugation is less.

For a uniform heat generation, $\tilde{q} = 1$, and $\bar{h}$, θ is constant across the plate. This is expected since everything that influences θ is constant. For the $h(\xi)$ case, θ is lowest at the front end of the plate, $\xi = 0$, and highest at the back end, $\xi = 1$. This is expected since $h(\xi)$ is highest at the front end which leads to a higher heat rate and thus a lower temperature. The use of $\bar{h}$ over predicts the

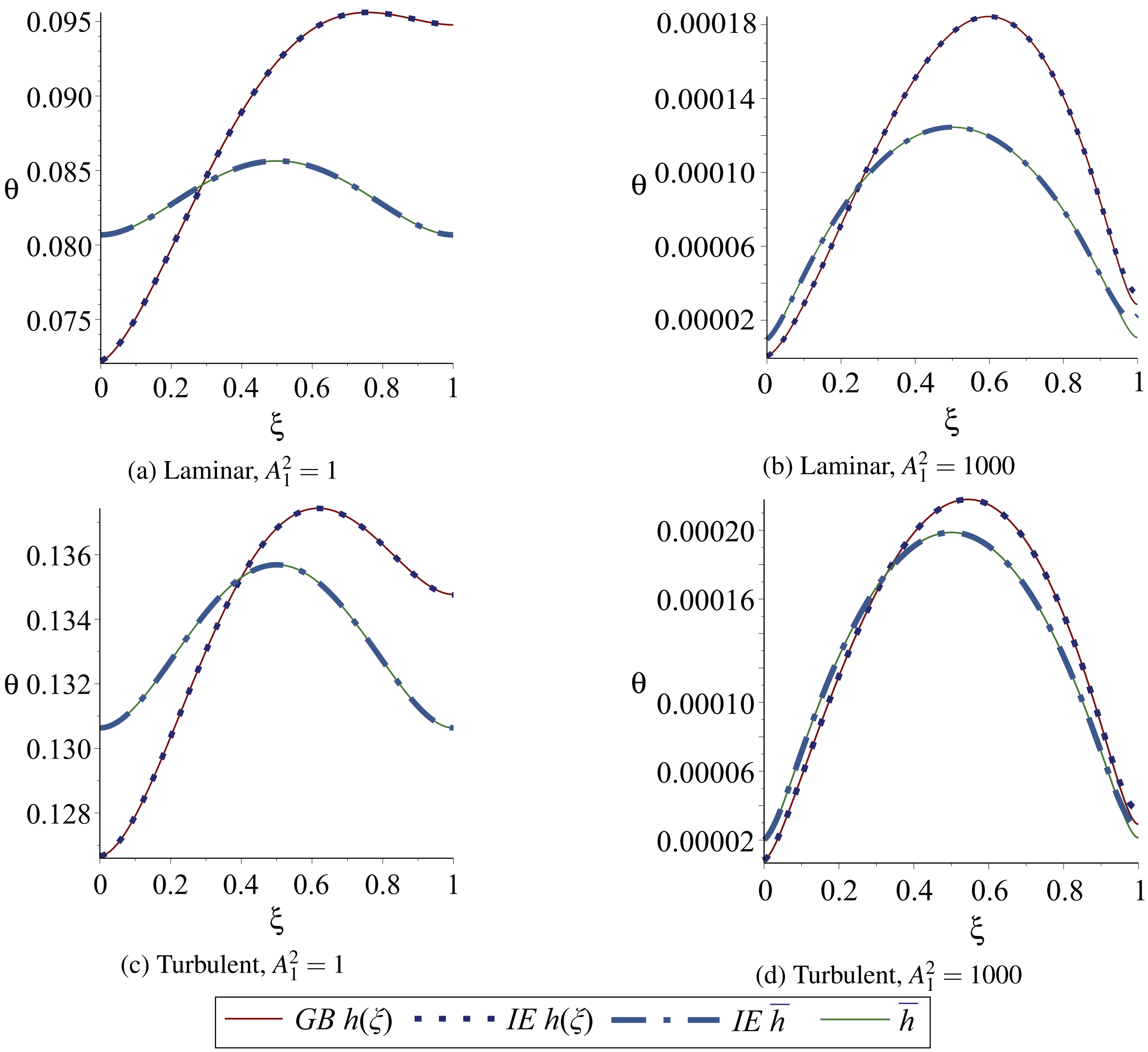

(a) Laminar, $A_1^2 = 1$ (b) Laminar, $A_1^2 = 1000$ (c) Turbulent, $A_1^2 = 1$ (d) Turbulent, $A_1^2 = 1000$

Figure 2.5: Non-dimensional temperature profiles, θ, with a heat generation of the shape, $\tilde{q} = -\xi^2 + \xi$, for the generalized Bessel method (GB) and the integral equation method (IE) for $h(x)$ and IE and the common method for $\bar{h}$

temperature at the front end and under predicts the temperature at the back end. Since the back end has the highest temperature, $\bar{h}$ under predicts the maximum temperature of the plate. This could be disastrous if used for calculating peak chip temperatures in electronics cooling.

For heat generation with a peak at the center of the plate, $\tilde{q} = -\xi^2 + \xi$ and $\bar{h}$, the maximum temperature is at the center of the plate. For the $h(\xi)$ case, θ_{max} is further along the plate but seems to approach the center as A_1^2 gets larger. The shape of θ also approaches that of $\bar{h}$ for large A_1^2.

Recall that

$$A_1^2 = \frac{h_0 d_1}{k_1}\frac{L^2}{d_1^2} = Bi\frac{L^2}{d_1^2}. \tag{2.121}$$

Since it was assumed that $Bi = 0.1$, $\frac{L^2}{d_1^2}$ will be the main contributer to a large A_1^2. As the length becomes much larger than the plate thickness, A_1^2 becomes large. At first it might seem like a longer plate should give a greater length for a temperature difference, however the effect of $h(\xi)$ dies out as ξ increases. A short plate will have a highly variable $h(\xi)$, but for a long plate $h(\xi)$ will approach $\bar{h}$. For a long plate, the highly variable region at the leading edge becomes a very small part of plate and becomes insignificant.

In Figure 2.6, θ is plotted for various A_1^2 for both $h(\xi)$ and $\bar{h}$. It can be seen that θ decreases with increasing A_1^2. Figure 2.7 is the plot of the non-dimensional temperature difference between

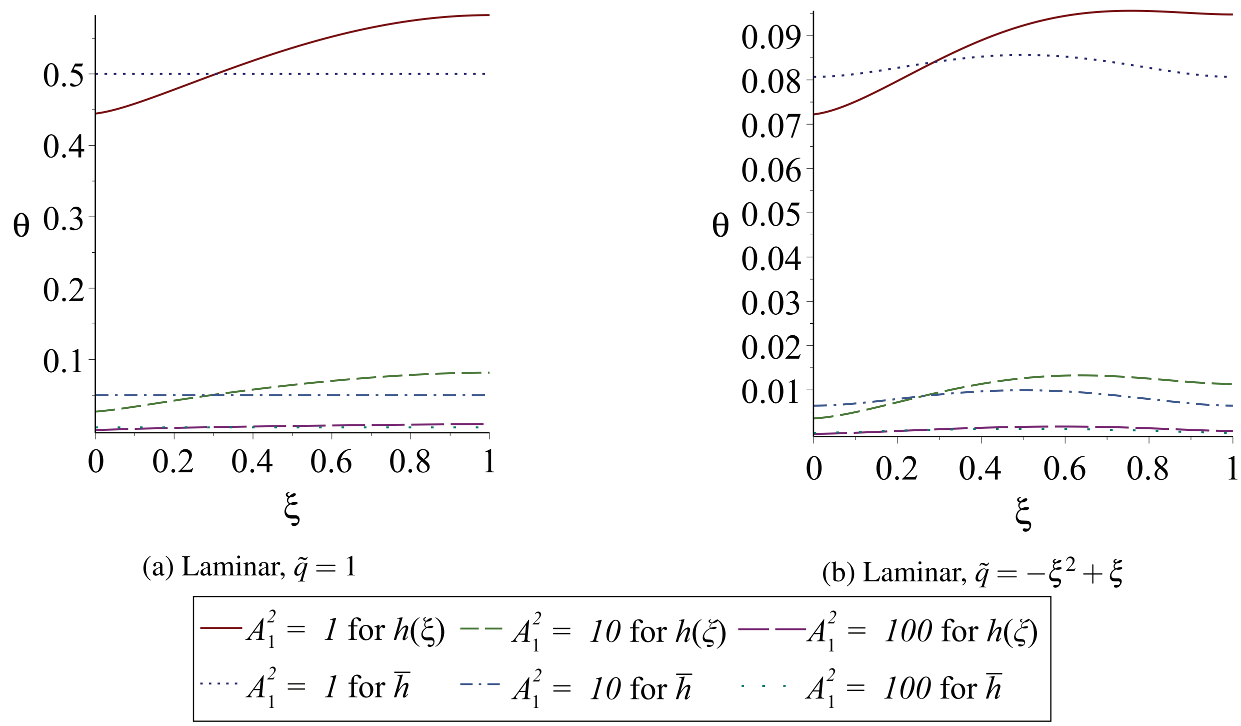

Figure 2.6: Non-dimensional temperature profiles, θ, comparing use of $h(\xi)$ and $\bar{h}$ for differing A^2

the $h(\xi)$ and $\bar{h}$ profiles, $\Delta\theta = \theta(h(\xi)) - \theta(\bar{h})$. As A_1^2 increases, $\Delta\theta$ decreases. Thus, for larger A_1^2, the lower the discrepancy between the use of $\bar{h}$ and $h(\xi)$. Note that in Figure 2.7 there is very little difference between $\Delta\theta$ for $A_1^2 = 0.1$ and $A_1^2 = 0.01$. Thus as A_1^2 gets sufficiently small, the discrepancy does not increase.

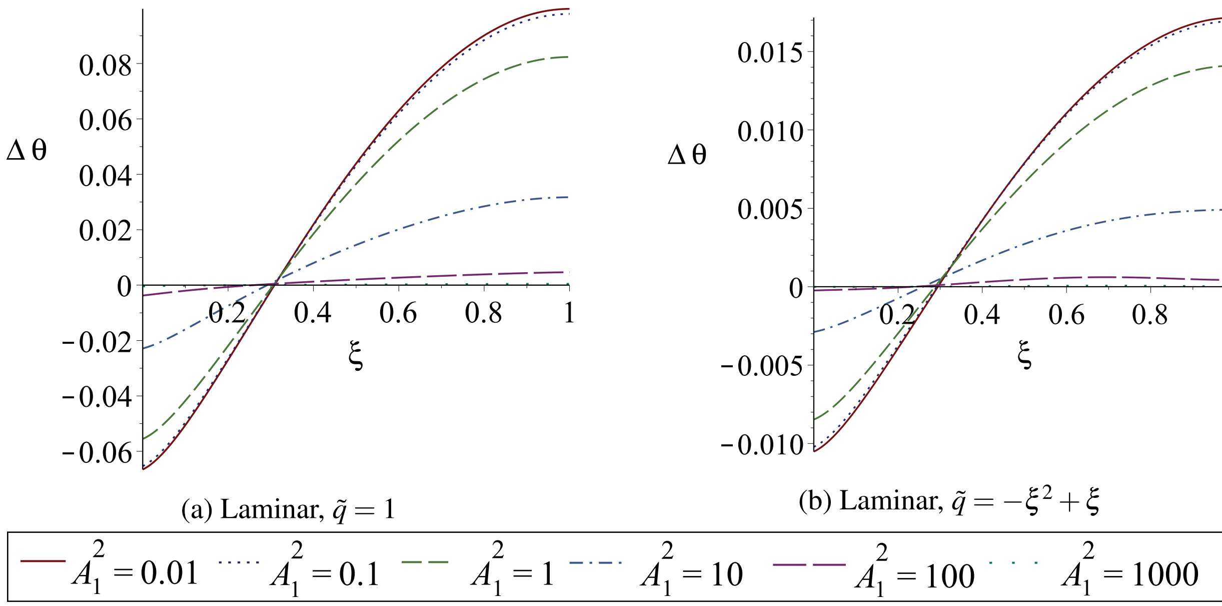

(a) Laminar, $\tilde{q} = 1$

(b) Laminar, $\tilde{q} = -\xi^2 + \xi$

Figure 2.7: Non-dimensional temperature difference, $\Delta\theta = \theta(h(\xi)) - \theta(\bar{h})$ for the flat plate with differing A_1^2

Physically, a small A_1^2 would be a short and thick plate. Whereas a large A_1^2 would be a long and thin plate. For reference, note that

$$\frac{L}{d_1} = \sqrt{10A_1^2}. \tag{2.122}$$

Thus $A_1^2 = 0.1$ leads to $\frac{L}{d_1} = 1$ and $A_1^2 = 1000$ to $\frac{L}{d_1} = 100$.

Tables 2.1-2.4 are intended to be used to obtain a quick solution for any A_1^2 values in the given range for this problem without needing to resolve. The tables can also be used to obtain a quick perspective on the discrepancy the temperature profile would have if $\bar{h}$ is used instead of $h(\xi)$. To use the tables, first calculate the A_1^2 value for the specific problem. Then, for $\tilde{q} = 1$, the maximum and minimum θ can be found from the tables for both $h(\xi)$ and $\bar{h}$. For $\tilde{q} = \xi^2 + \xi$, the maximum θ, θ_{max}, and its location can be found. Then the non-dimensionalizations can be reversed and the actual temperature profile can be found.

Table 2.1: Laminar flow past a flat plate for a uniform heat generation, $\tilde{q} = 1$

	$h(\xi)$		$\bar{h}$		$\Delta\theta = \theta(h(\xi)) - \theta(\bar{h})$	
A_1^2	$\theta(\xi = 0)$	$\theta(\xi = 1)$	$\theta(\xi = 0)$	$\theta(\xi = 1)$	$\Delta\theta(\xi = 0)$	$\Delta\theta(\xi = 1)$
.01	49.93	50.104	50	50	-0.0666	0.109
.1	4.935	5.098	5	5	-0.0653	0.0984
1	0.444	.582	0.5	0.5	-0.0555	0.0824
10	0.0271	0.0816	0.05	0.05	-0.0229	0.0316
100	0.00124	.00950	0.005	0.005	-0.00376	0.00448
1000	0.0000574	0.000984	0.0005	0.0005	-0.000443	0.000484

Table 2.2: Turbulent flow past a flat plate for a uniform heat generation, $\tilde{q} = 1$

	$h(\xi)$		$\bar{h}$		$\Delta\theta = \theta(h(\xi)) - \theta(\bar{h})$	
A_1^2	$\theta(\xi = 0)$	$\theta(\xi = 1)$	$\theta(\xi = 0)$	$\theta(\xi = 1)$	$\Delta\theta(\xi = 0)$	$\Delta\theta(\xi = 1)$
.01	79.972	80.0274	80	80	-0.028	0.0274
.1	7.972	8.027	8	8	-0.028	0.027
1	0.775	0.824	0.8	0.8	-0.025	0.024
10	0.0667	0.0914	0.08	0.08	-0.0133	0.0114
100	0.00518	0.0098	0.008	0.008	-0.00282	0.0018
1000	0.000392	0.000994	0.0008	0.0008	-0.000408	0.000194

Table 2.3: Laminar flow past a flat plate for a varying heat generation, $\tilde{q} = -\xi^2 + \xi$

	$h(\xi)$		$\bar{h}$		$\Delta\theta_{max} = \theta_{max}(h(\xi)) - \theta_{max}(\bar{h})$	
A_1^2	θ_{max}	ξ	θ_{max}	ξ	$\Delta\theta_{max}$	ξ
.01	8.348	0.796	8.336	0.5	0.0172	1
.1	0.848	0.792	0.836	0.5	0.0169	1
1	0.0956	0.757	0.0856	0.5	0.0141	1
10	0.0133	0.636	0.00992	0.5	0.00492	1
100	0.00172	0.588	0.00120	0.5	0.000606	0.692
1000	0.000184	0.598	0.000125	0.5	0.0000692	0.688

Table 2.4: Turbulent flow past a flat plate for a varying heat generation, $\tilde{q} = -\xi^2 + \xi$

	$h(\xi)$		$\bar{h}$		$\Delta\theta_{max} = \theta_{max}(h(\xi)) - \theta_{max}(\bar{h})$	
A_1^2	θ_{max}	ξ	θ_{max}	ξ	$\Delta\theta_{max}$	ξ
0.01	13.338	0.624	13.336	0.5	0.00474	1
0.1	1.338	0.629	1.336	0.5	0.00467	1
1	0.137	0.617	0.136	0.5	0.00412	1
10	0.0160	0.567	0.0152	0.5	0.00180	1
100	0.00204	0.538	0.00188	0.5	0.000229	0.725
1000	0.000218	0.543	0.000199	0.5	0.0000268	0.703

CHAPTER 3. CONJUGATE HEAT TRANSFER BETWEEN TWO SOLIDS

3.1 Problem Introduction

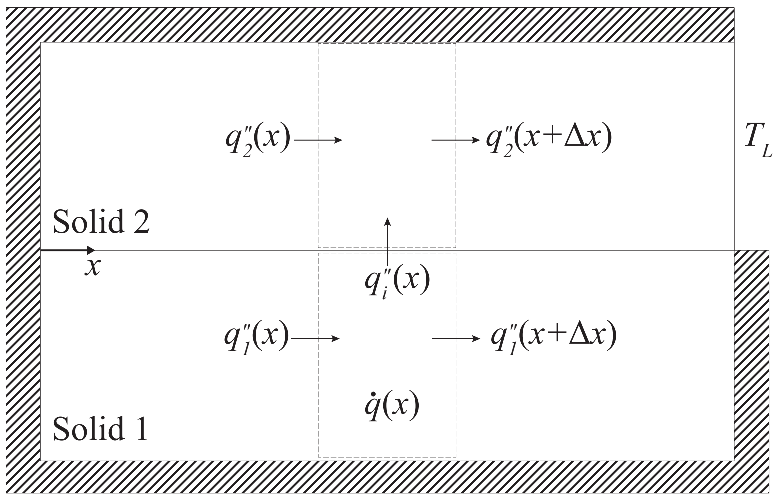

Figure 3.1: Conjugate heat transfer between two solids

This chapter considers the general problem presented in Figure 2.1, with the top subdomain as a solid, solid 2, as shown in Figure 3.1. The left boundary condition in solid 2 is adiabatic and the right boundary is a specified temperature, T_L. Essentially, heat is generated in solid 1, transfered across the interface to solid 2 and leaves the system through the right boundary. The interface heat flux will be approximated by

$$q_i''(x) = U(x)(T_1(x) - T_2(x)) \tag{3.1}$$

where $U(x)$ is the conductance heat transfer coefficient that will perform identically to the convective heat transfer coefficient, $h(x)$, but will be used for the solid-solid problem to avoid confusion since $h(x)$ is generally understood to be used between a fluid and a solid. The interface heat flux contains the temperatures from both subdomains which causes this problem to be coupled. As done in Chapter 2 with h and $\dot{q}$, let $U(x) = U_0\tilde{U}(x)$ where U_0 is the magnitude and $\tilde{U}(x)$ is a dimensionless variation of U.

The interface heat flux will vary as a surface exposed to a laminar external fluid flow, $\tilde{U}(x) = \frac{x^{-\frac{1}{2}}}{L^{-\frac{1}{2}}}$, where the heat transfer is greatest at $x = 0$ and decreases with increasing x. Thus the heat will generally flow in a clockwise direction which is the same pattern that is observed for a similar fluid-solid problem.

The boundary conditions for solid 2 were chosen with the intent to simulate a fluid-solid problem but simplified by removing the advection terms from the fluid. The heat will flow in generally the same direction as for the fluid problem, clockwise. The temperature boundary condition was chosen because it allows the heat to flow in this same pattern. Since this approach does not appear to have been performed before in literature, it was hoped that insight may be revealed into the fundamental phenomena of the coupling effects of conjugate heat transfer that may be masked by the typically dominating effects of fluid advection.

The formulation of this problem may be causing some confusion with respect to the conjugate definitions given in Chapter 2. The conjugate boundary condition defined previously required both the heat flux and the temperature to match at the interface. However this problem only has a single heat flux boundary condition at the interface similar to a convective boundary condition. Due to the assumption of one-dimension, the interface condition cannot match for both subdomains, otherwise both would have identical temperature profiles. Also, since there is no variation in the y-direction, the conjugate boundary condition equating the heat fluxes using Fourier's Law would not work since $\frac{dT}{dy} = 0$. Some may not consider this a conjugate problem due to the one-dimensional approximation. However, the subdomains are still coupled and it is hoped to find some insight into the coupling effects of conjugate heat transfer.

3.2 Analytical Solutions

The solution methods developed in Section 2.3, the integral equation, IE, and generalized Bessel, GB, methods, are used to obtain solutions to this solid-solid problem for $U(x)$. Two separate solutions are used in order to verify that the solutions are correct. The integral equation method as well as a transient solution will also be used for the $\bar{U}$ solution. The transient solution is being used because the common solution method for $\bar{h}$ developed in Section 2.3.1 was not evaluating well for this problem. Therefore a solution was found to the transient problem which will be used with a large time, t, to obtain a steady-state solution. The final transient solution will be presented below but the full worked out solution can be found in Appendix A.2.3.

The governing equation to be solved for solid 1 will be the same as found from the energy balance in Chapter 2, Eqn. 2.18, with the same boundary conditions

$$\frac{d^2\theta_1(\xi)}{d\xi^2} = \frac{q_i''(\xi)}{\dot{q}_0 d_1} - \tilde{q}(\xi) \tag{3.2}$$

$$\left.\frac{d\theta_1}{d\xi}\right|_{\xi=0} = 0 \tag{3.3}$$

$$\left.\frac{d\theta_1}{d\xi}\right|_{\xi=1} = 0. \tag{3.4}$$

Substituting in the interface heat flux, Eqn. 3.1, non-dimensionalized with the following

$$\xi = \frac{x}{L} \tag{3.5}$$

$$\theta_1 = \frac{k_1}{\dot{q}_0 L^2}(T_1 - T_L) \tag{3.6}$$

$$\theta_2 = \frac{k_1}{\dot{q}_0 L^2}(T_2 - T_L) \tag{3.7}$$

$$A_1^2 = \frac{U_0 L^2}{k_1 d_1} \tag{3.8}$$

results in

$$\frac{d^2\theta_1(\xi)}{d\xi^2} = A_1^2 \xi^{-\frac{1}{2}} \big(\theta_1(\xi) - \theta_2(\xi)\big) - \tilde{q}(\xi). \tag{3.9}$$

Solid 2 will have the same governing equation as solid 1 except all subscripts will change from 1 to 2, there is no volumetric heat generation and there is a sign change on the interface heat flux since the energy is entering rather than leaving the subdomain. Defining

$$A_2^2 = \frac{U_0 L^2}{k_2 d_2} \tag{3.10}$$

the governing equation is

$$\frac{d^2\theta_2(\xi)}{d\xi^2} = -A_2^2 \xi^{-\frac{1}{2}} \big(\theta_1(\xi) - \theta_2(\xi)\big) \tag{3.11}$$

with boundary conditions

$$\left.\frac{dT_2}{dx}\right|_{x=0} = 0 \tag{3.12}$$

$$T_2(L) = T_L \tag{3.13}$$

which non-dimensionalized are

$$\left.\frac{d\theta_2}{d\xi}\right|_{\xi=0} = 0 \tag{3.14}$$

$$\theta_2(1) = 0. \tag{3.15}$$

The IE method can be solved with arbitrary functions so $\tilde{U}(\xi)$ will be used rather than specifying the function. The solution to Eqn. 3.9 using the IE method is

$$\theta_1 = c_2 + \int_0^{\xi}\int_0^{\xi'} \left[A_1^2\tilde{U}(\xi'')\big(\theta_1(\xi'') - \theta_2(\xi'')\big) - \tilde{q}(\xi'')\right] d\xi'' d\xi' \tag{3.16}$$

where the constant is

$$c_2 = -\frac{1}{A_1^2\int_0^1 \tilde{U}(\xi')d\xi'}\int_0^1 \left[A_1^2\tilde{U}(\xi')\Big(\int_0^{\xi'}\int_0^{\xi''} \left[A_1^2\tilde{U}(\xi''')\big(\theta_1(\xi''') - \theta_2(\xi''')\big) - \tilde{q}(\xi''')\right] d\xi''' d\xi'' - \theta_2(\xi')\Big) - \tilde{q}(\xi')\right] d\xi'. \tag{3.17}$$

The solution to Eqn. 3.11 for solid 2 is

$$\theta_2 = \int_0^1\int_0^{\xi'} \left[A_2^2\tilde{U}(\xi'')\big(\theta_1(\xi'') - \theta_2(\xi'')\big)\right] d\xi'' d\xi' - \int_0^{\xi}\int_0^{\xi'} \left[A_2^2\tilde{U}(\xi'')\big(\theta_1(\xi'') - \theta_2(\xi'')\big)\right] d\xi'' d\xi'. \tag{3.18}$$

The full solutions can be found in Appendix A.2.1. This solution will be solved for both a variable and an average heat transfer coefficient.

The solution for the temperature field for solid 1 using the GB method for a variable heat transfer coefficient, $\tilde{U}(\xi) = \xi^{-\frac{1}{2}}$, is

$$\begin{aligned}\theta_1 &= c_2 \xi^{\frac{1}{2}} I_{-\frac{2}{3}}\Big(\frac{4}{3}A_1\xi^{\frac{3}{4}}\Big)\\ &- \frac{4\pi}{3\sqrt{3}}\xi^{\frac{1}{2}} I_{\frac{2}{3}}\big(\frac{4}{3}A_1\xi^{\frac{3}{4}}\big)\int_0^{\xi} I_{-\frac{2}{3}}\big(\frac{4}{3}A_1\xi'^{\frac{3}{4}}\big)\Big(A_1^2\theta_2(\xi') + \xi'^{\frac{1}{2}}\tilde{q}(\xi')\Big)d\xi'\\ &+ \frac{4\pi}{3\sqrt{3}}\xi^{\frac{1}{2}} I_{-\frac{2}{3}}\big(\frac{4}{3}A_1\xi^{\frac{3}{4}}\big)\int_0^{\xi} I_{\frac{2}{3}}\big(\frac{4}{3}A_1\xi'^{\frac{3}{4}}\big)\Big(A_1^2\theta_2(\xi') + \xi'^{\frac{1}{2}}\tilde{q}(\xi')\Big)d\xi'\end{aligned} \tag{3.19}$$

where the constant is

$$\begin{aligned}c_2 &= \frac{4\pi}{3\sqrt{3}}\frac{I_{-\frac{1}{3}}\big(\frac{4}{3}A_1\big)}{I_{\frac{1}{3}}\Big(\frac{4}{3}A_1\Big)}\int_0^1 I_{-\frac{2}{3}}\big(\frac{4}{3}A_1\xi'^{\frac{3}{4}}\big)\Big(A_1^2\theta_2(\xi') + \xi'^{\frac{1}{2}}\tilde{q}(\xi')\Big)d\xi'\\ &- \frac{4\pi}{3\sqrt{3}}\int_0^1 I_{\frac{2}{3}}\big(\frac{4}{3}A_1\xi'^{\frac{3}{4}}\big)\Big(A_1^2\theta_2(\xi') + \xi'^{\frac{1}{2}}\tilde{q}(\xi')\Big)d\xi'.\end{aligned} \tag{3.20}$$

The solution for the temperature field for solid 2 is

$$\begin{aligned}\theta_2 = c_4\xi^{\frac{1}{2}} I_{-\frac{2}{3}}\Big(\frac{4}{3}A_2\xi^{\frac{3}{4}}\Big) - \frac{4\pi A_2^2}{3\sqrt{3}}\xi^{\frac{1}{2}} I_{\frac{2}{3}}\big(\frac{4}{3}A_2\xi^{\frac{3}{4}}\big)\int_0^{\xi} I_{-\frac{2}{3}}\big(\frac{4}{3}A_2\xi'^{\frac{3}{4}}\big)\theta_1(\xi')d\xi'\\ + \frac{4\pi A_2^2}{3\sqrt{3}}\xi^{\frac{1}{2}} I_{-\frac{2}{3}}\big(\frac{4}{3}A_2\xi^{\frac{3}{4}}\big)\int_0^{\xi} I_{\frac{2}{3}}\big(\frac{4}{3}A_2\xi'^{\frac{3}{4}}\big)\theta_1(\xi')d\xi'\end{aligned} \tag{3.21}$$

where the constant is

$$c_4 = \frac{4\pi A_2^2}{3\sqrt{3}}\frac{I_{\frac{2}{3}}\big(\frac{4}{3}A_2\big)}{I_{-\frac{2}{3}}\Big(\frac{4}{3}A_2\Big)}\int_0^1 I_{-\frac{2}{3}}\big(\frac{4}{3}A_2\xi'^{\frac{3}{4}}\big)\theta_1(\xi')d\xi' - \frac{4\pi A_2^2}{3\sqrt{3}}\int_0^1 I_{\frac{2}{3}}\big(\frac{4}{3}A_2\xi'^{\frac{3}{4}}\big)\theta_1(\xi')d\xi'. \tag{3.22}$$

The full solutions can be found in Appendix A.2.2.

The transient solution for solid 1 is

$$\begin{aligned}\theta_1 &= e^{-A_1^2\tau}\Big[\theta_0 + \int_0^{\tau}\int_0^1 (A_1^2\theta_2(\xi,\tau) + \tilde{q}(\xi,\tau))d\xi e^{A_1^2\tau'}d\tau'\Big]\\ &+ 2\sum_{n=1}^{\infty}\cos(n\pi\xi)e^{-((n\pi)^2+A_1^2)\tau}\Big[\int_0^{\tau}\int_0^1 (A_1^2\theta_2(\xi,\tau)\\ &+ \tilde{q}(\xi,\tau))\cos(n\pi\xi)d\xi e^{((n\pi)^2+A_1^2)\tau'}d\tau'\Big]\end{aligned} \tag{3.23}$$

where τ is the non-dimensional time, which is assumed large, $\tau \to \infty$, for the steady-state solution.

The solution for solid 2 is

$$\theta_2 = \sum_{n=0}^{\infty} \cos(\frac{(2n+1)\pi}{2}\xi) e^{-((\frac{(2n+1)\pi}{2})^2 + A_2^2)\kappa\tau} \Big[\frac{4(-1)^n}{(2n+1)\pi}\theta_0 + 2\kappa A_2^2 \int_0^{\tau} \int_0^1 \theta_1(\xi,\tau) \cos(\frac{(2n+1)\pi}{2}\xi) d\xi e^{((\frac{(2n+1)\pi}{2})^2 + A_2^2)\kappa\tau'} d\tau' \Big]. \tag{3.24}$$

3.3 Analysis

The solutions presented above will now be analyzed. Only the temperature profile for solid 1, θ_1, will be plotted for simplicity and since it is the temperature field of most interest. Since the problem is coupled, an iterative solution is required for all cases. During solution evaluation, convergence was monitored by how closely the interface heat rate matches the heat generation rate in solid 1

$$A_1^2 \int_0^1 \tilde{h}(\xi)\theta_1(\xi) d\xi = \int_0^1 \tilde{q}(\xi) d\xi. \tag{3.25}$$

The only parameters that can vary for the solutions are A_1^2, A_2^2, and $\tilde{q}$. It was anticipated that the ratio $\frac{A_1^2}{A_2^2}$ would be consistent throughout solutions and the number of parameters could be reduced even further. However, when looking at Figure 3.2a and 3.2d it can be clearly seen that even though the ratio $\frac{A_1^2}{A_2^2} = 1$ in both cases, the results are distinctly different. When looked at more closely, the ratio is equal to $\frac{k_2 d_2}{k_1 d_1}$, which can explain the fact that A_1^2 and A_2^2 cannot be combined. The thermal conductivity, k, and the thickness, d, have competing conjugation effects. Increasing k will essentially speed the flow of energy and increase the temperature uniformity in the solid and decrease conjugation. However, increasing d will effectively slow the flow of energy by having more volume to absorb the energy, thus increasing conjugation.

Figure 3.2 shows that the IE and GB solutions match well for the $U(\xi)$ case and the IE and transient solutions match well for the $\bar{U}$ case. This gives confidence that the governing equations were solved correctly. It can also be seen from the plots, that in general the $U(\xi)$ case has a higher temperature than $\bar{U}$, thus $\bar{U}$ tends to under predict the temperature. However, for small A_2^2, it can over predict the temperature at small ξ. It can also be noted that $\bar{U}$ is always highest at $\xi = 0$ and lowest at $\xi = 1$ and generally has the same shape. Shape refers to the general slope of the profile,

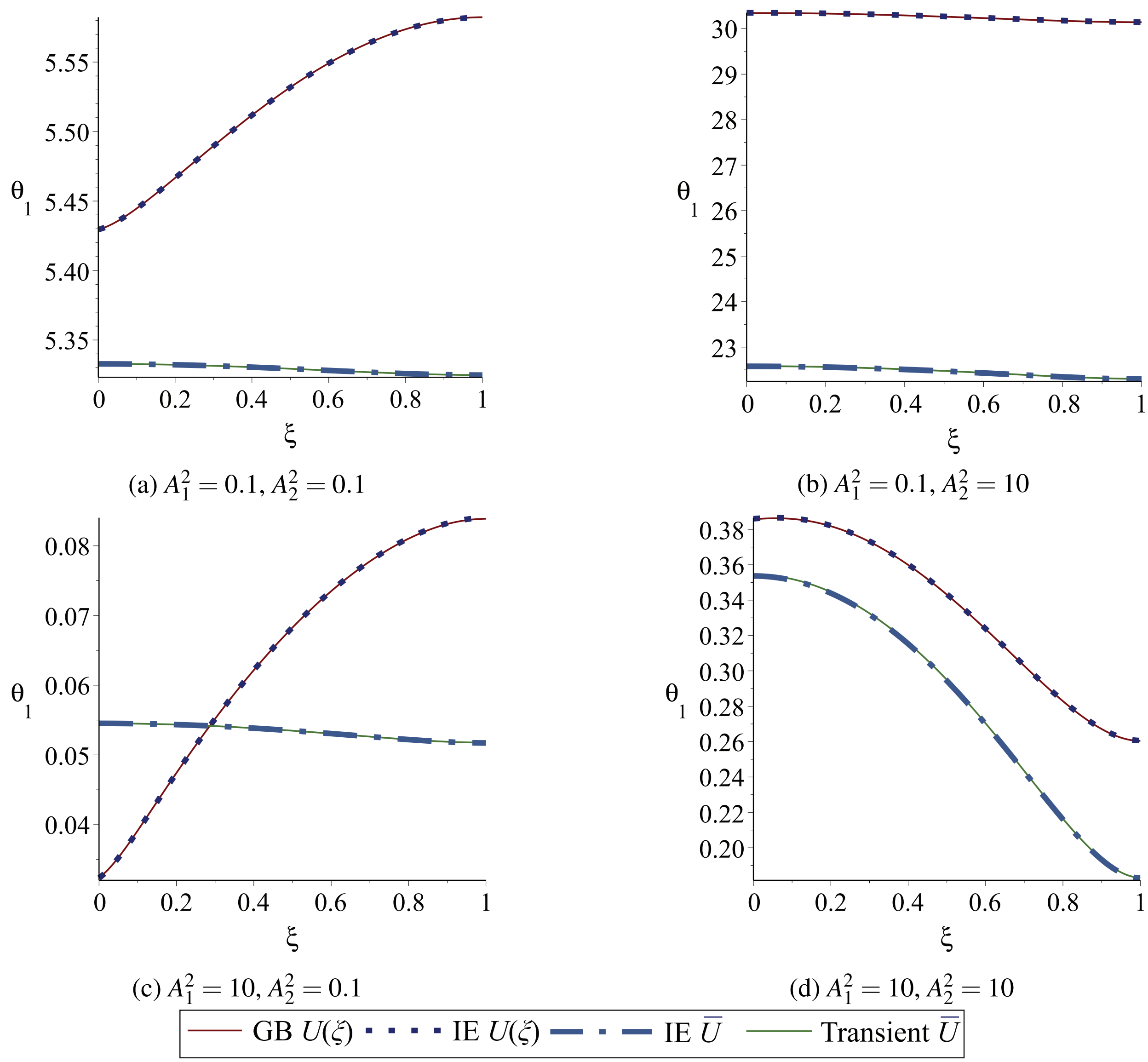

Figure 3.2: Verification of solutions for θ_1 for $U(\xi)$ and $\bar{U}$ for various A_1^2 and A_2^2

either being positive or negative. For the $U(\xi)$ case when A_2^2 is high, the shape of the temperature profile generally follows the shape for $\bar{U}$. When A_2^2 is low, the temperature profile flips and the lowest temperature is at $\xi = 0$, as can be seen in Figures 3.2a and 3.2c. When A_1^2 is high, the difference between the $U(\xi)$ and the $\bar{U}$ solutions, $\Delta\theta = \theta_1(U(\xi)) - \theta_1(\bar{U})$ is smaller and when A_1^2 is low, $\Delta\theta$ is greater. In other words, it seems that A_2^2 tends to have more effect on the shape of θ_1 and A_1^2 has a greater effect on the magnitude of $\Delta\theta$. As A_2^2 gets large the shape and magnitude of θ_1 approach that for $\bar{U}$.

Figure 3.3 is a plot of the temperature profile in solid 1 for varying A_2^2 around the shape transition value for A_2^2. The transition from being the minimum temperature at $\xi = 0$ to the maximum temperature occurs around $A_2^2 = 2.25$. The profiles have been brought together on the plot by offsetting each profile by some various value in order to compare the profiles.

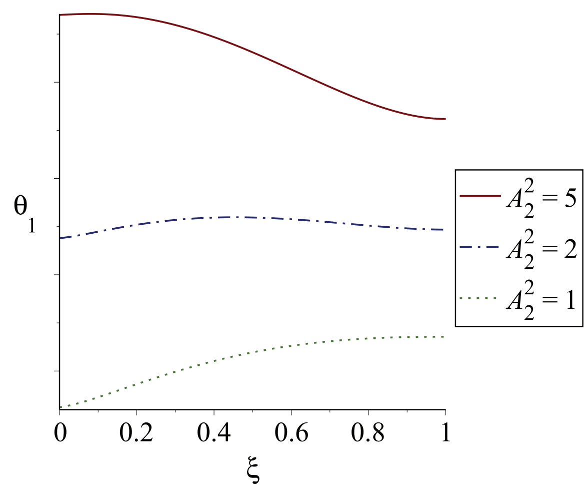

Figure 3.3: Plot of solid 1 temperature profiles that have been offset to show how the shape transitions from a positive to negative slope with increasing A_2^2

Figure 3.4 is a plot of $\Delta\theta$ for varying A^2 where $A_1^2 = A_2^2$ is true for all cases. The plot shows that even though the shape of θ_1 can be very different for different values of $A_1^2 = A_2^2$, as can be seen in Figure 3.2, $\Delta\theta$ still decreases for increasing A^2. Thus for larger A^2 values, the difference between $U(\xi)$ and $\bar{U}$ solutions becomes smaller. This implies that there is less conjugation in problems with larger A^2 values.

Looking back at Figure 3.2, increasing A_1^2 while holding A_2^2 constant, comparing the top plots to the bottom plots, decreases the temperature magnitude. On the other hand, increasing A_2^2 while holding A_1^2 constant, comparing the left plots to the right plots, increases temperature magnitude. This is because increasing A_2^2 is essentially reducing the conductivity, or slowing the flow of energy, and reducing the thickness, which decreases the amount of energy it can hold, of solid 2. This is essentially reducing the amount of energy that can leave solid 1 thus increasing the temperature of solid 1.

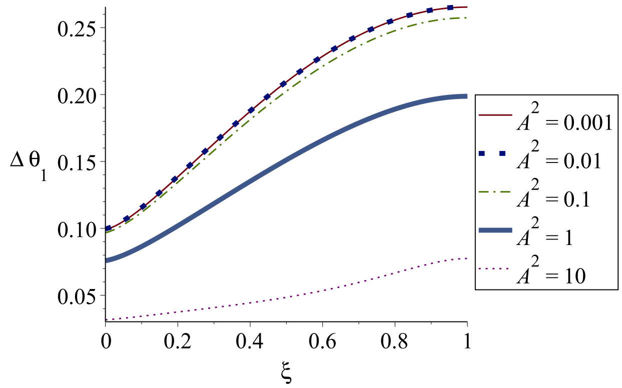

Figure 3.4: The difference in temperature profiles between use of a variable and an average heat transfer coefficient, $\Delta\theta_1 = \theta_1(h(\xi)) - \theta_1(\bar{h})$, for various $A_1^2 = A_2^2 = A^2$

Figure 3.5 shows plots for various A_1^2 for a low and a high value of A_2^2 and Figure 3.6 shows plots for various A_2^2 for a low and a high value of A_1^2. Increasing A_1^2 while holding A_2^2 constant decreases $\Delta\theta$. On the other hand, increasing A_2^2 while holding A_1^2 constant increases $\Delta\theta$.

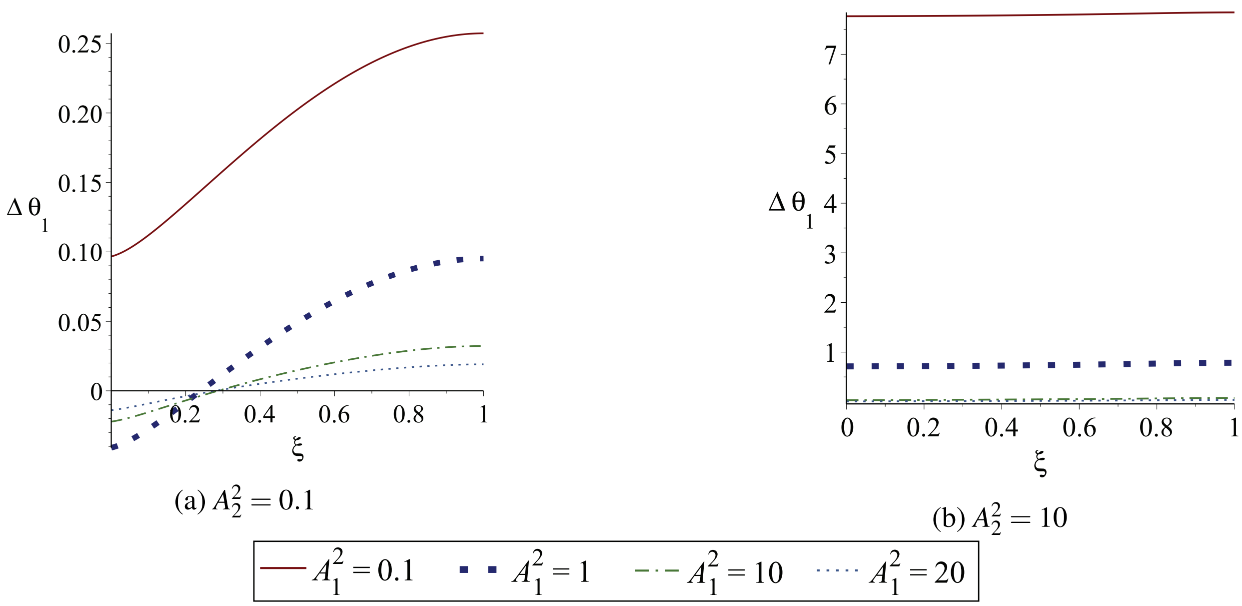

Figure 3.5: Plots of the temperature difference, $\Delta\theta_1 = \theta_1(h(\xi)) - \theta_1(\bar{h})$, in solid 1 for various A_1^2 for a small and large A_2^2

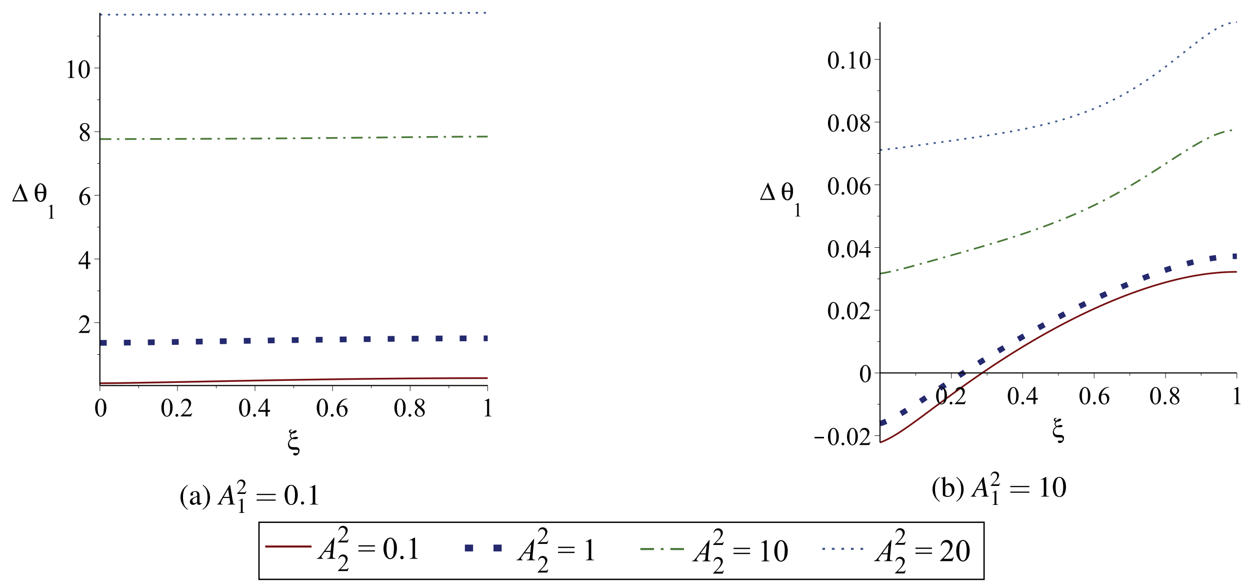

Figure 3.6: Plots of the temperature difference, $\Delta\theta_1 = \theta_1(h(\xi)) - \theta_1(\bar{h})$, in solid 1 for various A_2^2 for a small and large A_1^2

Figure 3.7 is the same plot as Figure 3.2 except for a variable heat generation, $\tilde{q} = -\xi^2 + \xi$. As before, the solutions match well and confidence can be had the equations were solved correctly. The same trends as seen in Figure 3.2 appear to be present.

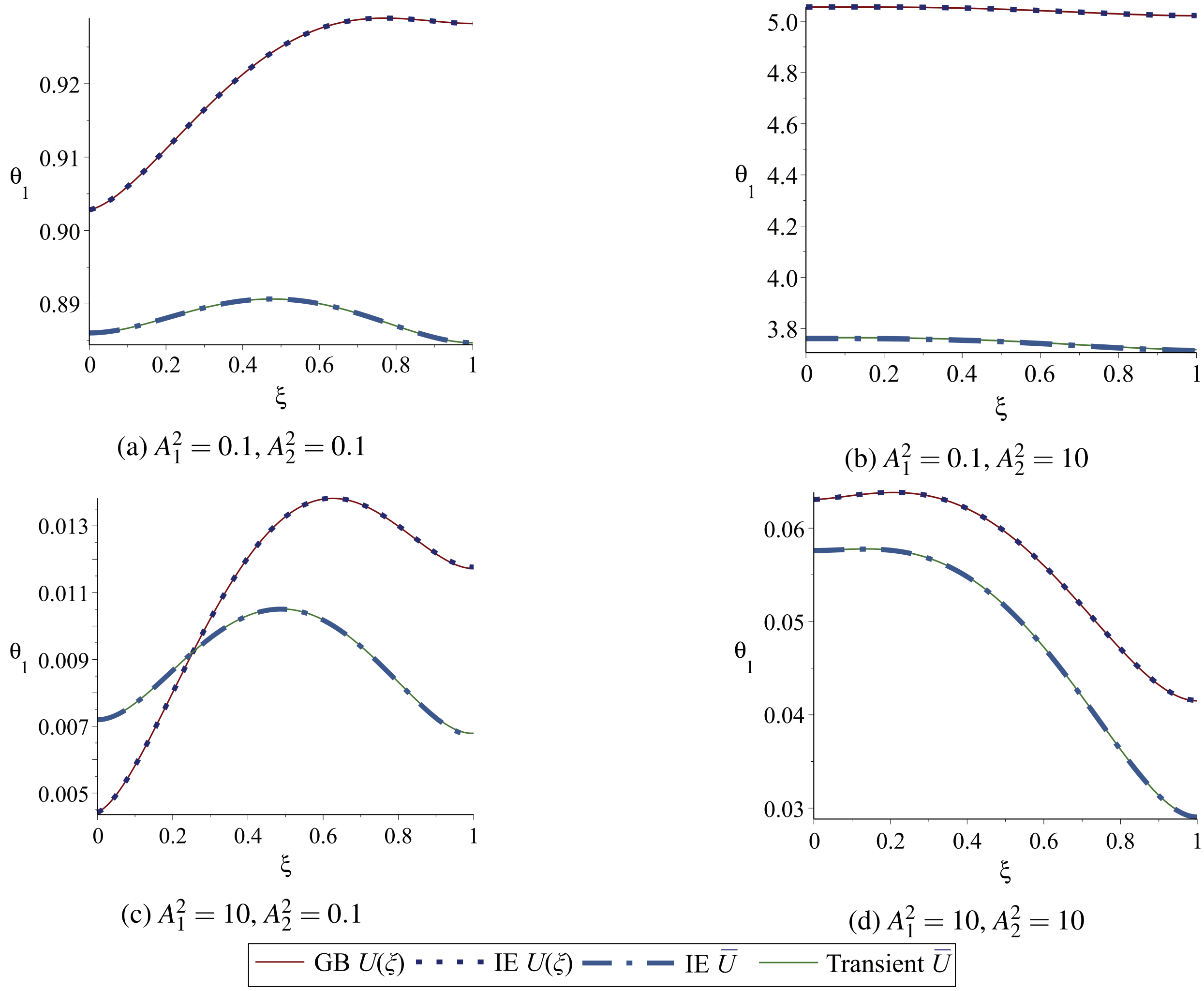

Figure 3.7: Verification of solutions for θ_1 for $h(\xi)$ and $\bar{h}$ for differing A_1^2 and A_2^2 for $\tilde{q} = -\xi^2 + \xi$

CHAPTER 4. CONJUGATE HEAT TRANSFER BETWEEN A FLUID AND A SOLID

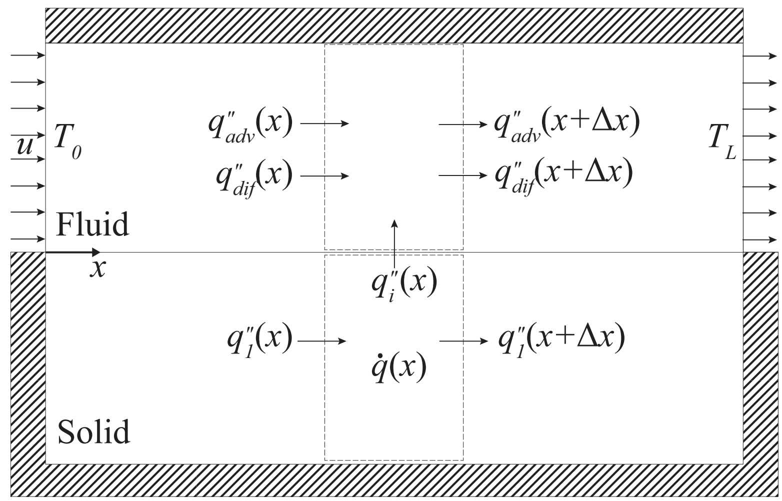

Figure 4.1: Conjugate heat transfer between a fluid and a solid for an internal flow

4.1 Problem Introduction

This chapter considers the general problem presented in Chapter 2, Figure 2.1, with the top subdomain as a fluid as shown in Figure 4.1. The left boundary condition in the fluid is an inlet with a constant temperature, T_0, and the right boundary is an outlet with a constant temperature, T_L. Essentially, heat is generated in the solid, transfered across the interface to the fluid and leaves the system through the outlet boundary. The interface heat flux will be approximated by

$$q''_i = h(x)(T_1(x) - T_2(x)) \tag{4.1}$$

where $h(x) = h_0\tilde{h}(x)$. As before, h_0 is the magnitude and $\tilde{h}(x)$ is the dimensionless variation of h.

As stated in Chapter 2 the purpose of this problem is to model an internal flow past a solid that has a sufficient thickness to result in a significant variation in the solid temperature field. This scenario can be related to physical applications such as radiofrequency cardiac ablation where blood flows through the heart and the heart tissue is being heated by an electrode. It can also relate to electronics cooling where chips are cooled by forced convection inside electronic devices.

It was desired to solve this problem including both the diffusion and advection terms in order to see how the solution changes as the fluid velocity becomes small, $u \rightarrow 0$, and diffusion begins to be the dominate mode of heat transfer. However, appropriate boundary conditions could not be found that accurately modeled the amount of energy leaving each boundary due to diffusion. If the constant temperature boundary conditions are used when diffusion is considered, the results can be as in Figure 4.2 where the fluid temperature, T_2, becomes higher than the solid temperature, T_1. This unrealistic result comes from that fact that T_L is calculated assuming all the generated energy is leaving through the exit boundary. In reality, there may be some energy leaving through the inlet boundary. Thus, the solution is only valid when advection dominates diffusion such that diffusion has no effect on the inlet temperature. Kays suggests that the effect of axial diffusion is small for $Pe = 10$ and completely negligible for $Pe = 100$. Also, axial diffusion can be important in short heated sections [21]. This suggests that solutions for small Pe and A^2 values could be inaccurate.

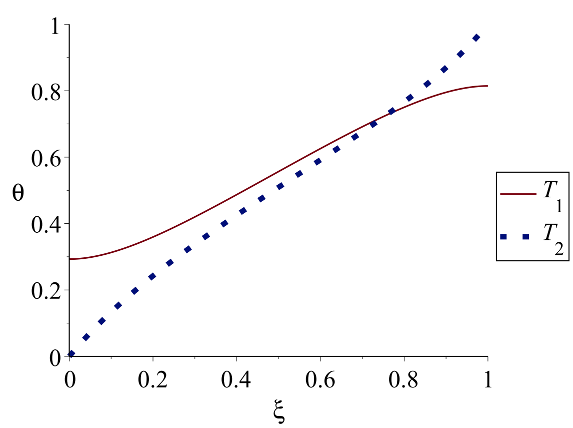

Figure 4.2: Fluid and solid temperature profiles for a case when diffusion is considered in the fluid with constant temperature boundary conditions

4.2 Energy Balance

Performing an energy balance on the fluid using the Law of Conservation of Energy

$$\dot{E}_{in} - \dot{E}_{out} + \dot{E}_{gen} = \dot{E}_{st} \tag{4.2}$$

results in

$$\begin{aligned} &q''_{adv}(x,t)wd_2 + q''_{dif}(x,t)wd_2 - q''_{adv}(x+\Delta x,t)wd_2 - q''_{dif}(x+\Delta x,t)wd_2 \\ &+ h(x+\frac{\Delta x}{2})\Big(T_1(x+\frac{\Delta x}{2},t) - T_2(x+\frac{\Delta x}{2},t)\Big)w\Delta x = \rho_2 c_{p2} w d_2 \Delta x \frac{\partial T_2(x,t)}{\partial t} \end{aligned} \tag{4.3}$$

where q''_{dif} is the heat flux due to diffusion and q''_{adv} is the heat flux due to advection. Canceling w and taking the limit as Δx approaches zero

$$\begin{aligned} &\lim_{\Delta x \to 0} \frac{-(q''_{adv}(x+\Delta x,t) - q''_{adv}(x,t)}{\Delta x} d_2 + \frac{-(q''_{dif}(x+\Delta x,t) - q''_{dif}(x,t)}{\Delta x} d_2 \\ &+ h(x+\frac{\Delta x}{2})\Big(T_1(x+\frac{\Delta x}{2},t) - T_2(x+\frac{\Delta x}{2},t)\Big) = \rho_2 c_{p2} d_2 \Delta x \frac{\partial T_2(x,t)}{\partial t} \end{aligned} \tag{4.4}$$

results in

$$-d_2 \frac{\partial q''_{adv}(x,t)}{\partial x} - d_2 \frac{\partial q''_{dif}(x,t)}{\partial x} + h(x)\Big(T_1(x,t) - T_2(x,t)\Big) = \rho_2 c_{p2} d_2 \frac{\partial T_2(x,t)}{\partial t}. \tag{4.5}$$

The heat fluxes will be represented as

$$q''_{dif} = -k_2 \frac{dT_2(x,t)}{dx} \tag{4.6}$$

$$q''_{adv} = \frac{\dot{m} c_{p2} T_2(x,t)}{A_c} \tag{4.7}$$

where A_c is the fluid cross-sectional area

$$-\frac{d_2 \dot{m} c_{p2}}{A_c} \frac{\partial T_2(x,t)}{\partial x} + d_2 k_2 \frac{\partial^2 T_2(x,t)}{\partial x^2} + h(x)\Big(T_1(x,t) - T_2(x,t)\Big) = \rho_2 c_{p2} d_2 \frac{\partial T_2(x,t)}{\partial t}. \tag{4.8}$$

Rearranging and recalling that $\dot{m} = \rho_2 u A_c$ and $\alpha_2 = \frac{k_2}{\rho_2 c_{p2}}$ results in

$$\frac{\partial^2 T_2(x,t)}{\partial x^2} - \frac{u}{\alpha_2}\frac{\partial T_2(x,t)}{\partial x} = \frac{1}{\alpha_2}\frac{\partial T_2(x,t)}{\partial t} - \frac{h(x)}{k_2 d_2}\Big(T_1(x,t) - T_2(x,t)\Big) \tag{4.9}$$

$$T_2(0,t) = T_0 \tag{4.10}$$

$$T_2(L,t) = T_L \tag{4.11}$$

$$T_2(x,0) = T_0. \tag{4.12}$$

Non-dimensionalize with the following

$$\xi = \frac{x}{L} \tag{4.13}$$

$$\theta_1 = \frac{k_1}{\dot{q}_0 L^2}(T_2) \tag{4.14}$$

$$\theta_2 = \frac{k_1}{\dot{q}_0 L^2}(T_2) \tag{4.15}$$

$$\tau = \frac{\alpha_1 t}{L^2} \tag{4.16}$$

$$A_2^2 = \frac{h_0 L^2}{k_2 d_2} \tag{4.17}$$

$$P_e = \frac{uL}{\alpha_2} \tag{4.18}$$

$$\kappa = \frac{\alpha_2}{\alpha_1} \tag{4.19}$$

where *Pe* is the Pectlet number. The governing equation and boundary conditions become

$$\frac{\partial^2 \theta_2(\xi)}{\partial \xi^2} - P_e\frac{\partial \theta_2(\xi)}{\partial \xi} = \frac{1}{\kappa}\frac{\partial \theta_2(\xi,\tau)}{\partial \tau} - A_2^2\tilde{h}(\xi)(\theta_1(\xi) - \theta_2(\xi)) \tag{4.20}$$

$$\theta_2(0,\tau) = \theta_0 \tag{4.21}$$

$$\theta_2(1,\tau) = \theta_L \tag{4.22}$$

$$\theta_2(\xi,0) = \theta_0. \tag{4.23}$$

Note that for small $\frac{A_2^2}{A_1^2 P_e}$, the second term becomes negligible and $\theta_L = \theta_0$ which means θ_2 is essentially a constant. Removing the transient term results in

$$\frac{\partial^2\theta_2(\xi)}{\partial\xi^2} - P_e\frac{\partial\theta_2(\xi)}{\partial\xi} = \frac{1}{\kappa}\frac{\partial\theta_2(\xi,\tau)}{\partial\tau} - A_2^2\tilde{h}(\xi)(\theta_1(\xi)-\theta_2(\xi)). \tag{4.24}$$

Assuming all the energy in the system leaves through the outlet boundary, the outlet temperature can be determined by equating the heat generation in the solid to the heat flux leaving the outlet

$$\theta_L = \theta_0 + \frac{A_2^2}{A_1^2 P_e}\int_0^1 \tilde{q}(\xi)d\xi. \tag{4.25}$$

4.3 Analytical Solutions

The solutions for the solid will be the same as those found for solid 1 in the solid-solid problem in Chapter 3. The generalized Bessel method can be used to find a solution for the fluid governing equation. However, evaluating the resulting solution can be difficult. The non-dimensional temperature for the fluid is

$$\begin{aligned}\theta_2 = {} & \xi^{\frac{1}{2}} e^{\frac{P_e}{2}\xi}\left[c_1 I_{\frac{2}{3}}\left(B_2(\xi)\xi^{\frac{3}{4}}\right) + c_2 I_{-\frac{2}{3}}\left(B_2(\xi)\xi^{\frac{3}{4}}\right)\right] \\ & - \frac{A_2^2\pi}{\sqrt{3}}\xi^{\frac{1}{2}} e^{\frac{P_e}{2}\xi} I_{\frac{2}{3}}\left(B_2(\xi)\xi^{\frac{3}{4}}\right)\int_0^\xi e^{-\frac{P_e}{2}\xi'} I_{-\frac{2}{3}}\left(B_2(\xi){\xi'}^{\frac{3}{4}}\right)\theta_1(\xi)\frac{(P_e^2{\xi'}^{\frac{1}{2}} + 4A_2^2)}{(P_e^2{\xi'}^{\frac{1}{2}} + 3A_2^2)}d\xi' \\ & + \frac{A_2^2\pi}{\sqrt{3}}\xi^{\frac{1}{2}} e^{\frac{P_e}{2}\xi} I_{-\frac{2}{3}}\left(B_2(\xi)\xi^{\frac{3}{4}}\right)\int_0^\xi e^{-\frac{P_e}{2}\xi'} I_{\frac{2}{3}}\left(B_2(\xi){\xi'}^{\frac{3}{4}}\right)\theta_1(\xi)\frac{(P_e^2{\xi'}^{\frac{1}{2}} + 4A_2^2)}{(P_e^2{\xi'}^{\frac{1}{2}} + 3A_2^2)}d\xi'\end{aligned} \tag{4.26}$$

with constants

$$\begin{aligned}c_1 = {} & \frac{\theta_L}{e^{\frac{P_e}{2}} I_{\frac{2}{3}}\left(B_2(\xi)\right)} - c_2\frac{I_{-\frac{2}{3}}\left(B_2(\xi)\right)}{I_{\frac{2}{3}}\left(B_2(\xi)\right)} + \frac{A_2^2\pi}{\sqrt{3}}\int_0^1 e^{-\frac{P_e}{2}\xi'} I_{-\frac{2}{3}}\left(B_2(\xi){\xi'}^{\frac{3}{4}}\right)\theta_1(\xi)\frac{(P_e^2{\xi'}^{\frac{1}{2}} + 4A_2^2)}{(P_e^2{\xi'}^{\frac{1}{2}} + 3A_2^2)}d\xi' \\ & - \frac{A_2^2\pi}{\sqrt{3}}\frac{I_{-\frac{2}{3}}\left(B_2(\xi)\right)}{I_{\frac{2}{3}}\left(B_2(\xi)\right)}\int_0^1 e^{-\frac{P_e}{2}\xi'} I_{\frac{2}{3}}\left(B_2(\xi){\xi'}^{\frac{3}{4}}\right)\theta_1(\xi)\frac{(P_e^2{\xi'}^{\frac{1}{2}} + 4A_2^2)}{(P_e^2{\xi'}^{\frac{1}{2}} + 3A_2^2)}d\xi'\end{aligned} \tag{4.27}$$

and

$$c_2 = \frac{2^{\frac{5}{3}} A_2^{\frac{2}{3}} \pi}{3^{\frac{7}{6}} \Gamma(\frac{2}{3})} \theta_0 \tag{4.28}$$

where

$$B_2(\xi) = \frac{4}{3}\sqrt{(\frac{P_e}{2})^2 \xi^{\frac{1}{2}} + A_2^2}. \tag{4.29}$$

All terms are now multiplied by an additional function of ξ, $e^{\frac{P_e}{2}\xi}$. Also, inside the Bessel function, $\frac{4}{3}\sqrt{(\frac{P_e}{2})^2 \xi^{\frac{1}{2}} + A_2^2}$, does not simply as did for the solid and thus there are multiple terms that contain ξ. These make the integrals more difficult to evaluate and temperature profiles could not be found.

Only one solution was able to be evaluated consistently enough to plot any results. This solution used the technique from the integral equation method to lump the term with h into the source term. This allows an integral transformation, $\psi(\xi) = \frac{d\theta_2(\xi)}{d\xi}$, to be used to convert the second order governing equation to first order

$$\frac{d\psi(\xi)}{d\xi} - P_e \psi(\xi) = -A_2^2 \tilde{h}(\xi)\big(\theta_1(\xi) - \theta_2(\xi)\big). \tag{4.30}$$

An integrating factor was used to solve, resulting in

$$\theta_2(\xi) = \theta_0 + \frac{(e^{P_e\xi} - 1)}{(e^{P_e} - 1)} \left[\frac{A_2^2 \int_0^1 \tilde{q}(\xi) d\xi}{A_1^2 P_e} + \int_0^1 e^{P_e\xi} \int_0^{\xi} \left[e^{-P_e\xi'} A_2^2 \tilde{h}(\xi')\big(\theta_1(\xi') - \theta_2(\xi')\big)\right] d\xi' d\xi \right]$$
$$- \int_0^{\xi} e^{P_e\xi} \int_0^{\xi} \left[e^{-P_e\xi'} A_2^2 \tilde{h}(\xi')\big(\theta_1(\xi') - \theta_2(\xi')\big)\right] d\xi' d\xi. \tag{4.31}$$

The full solution can be found in Appendix A.3.1

It will be required that $Pe > 50$ to make sure that diffusion does not affect the inlet temperature and lead to misleading results. Even though solutions to the problem were obtained, they could only be evaluated for a very limited range of parameter values. Due to the difficulty in obtaining evaluable solutions, the results were not verified with other solution methods as has been done in the other chapters.

4.4 Analysis

Only a few temperature profiles for the fluid-solid problem were able to be obtained. The plots in Figure 4.3 are for the non-dimensional temperature profile for the solid, θ_1, for various values of A_1^2, A_2^2 and Pe for $h(\xi)$ and $\bar{h}$. It can be seen that for small A_2^2, changing Pe seems to have little effect on the temperature profile. For large A_2^2, increasing Pe reduces the temperature with the greatest effect at $\xi = 1$. The only case where the average heat transfer coefficient over predicts the temperature is for a small A_1^2 and a large A_2^2. As observed with the other problems in this work, increasing A_1^2 decreases the temperature magnitude. In general, larger A^2 values and smaller Pe, increase the variation in the temperature profile in the average heat transfer coefficient case.

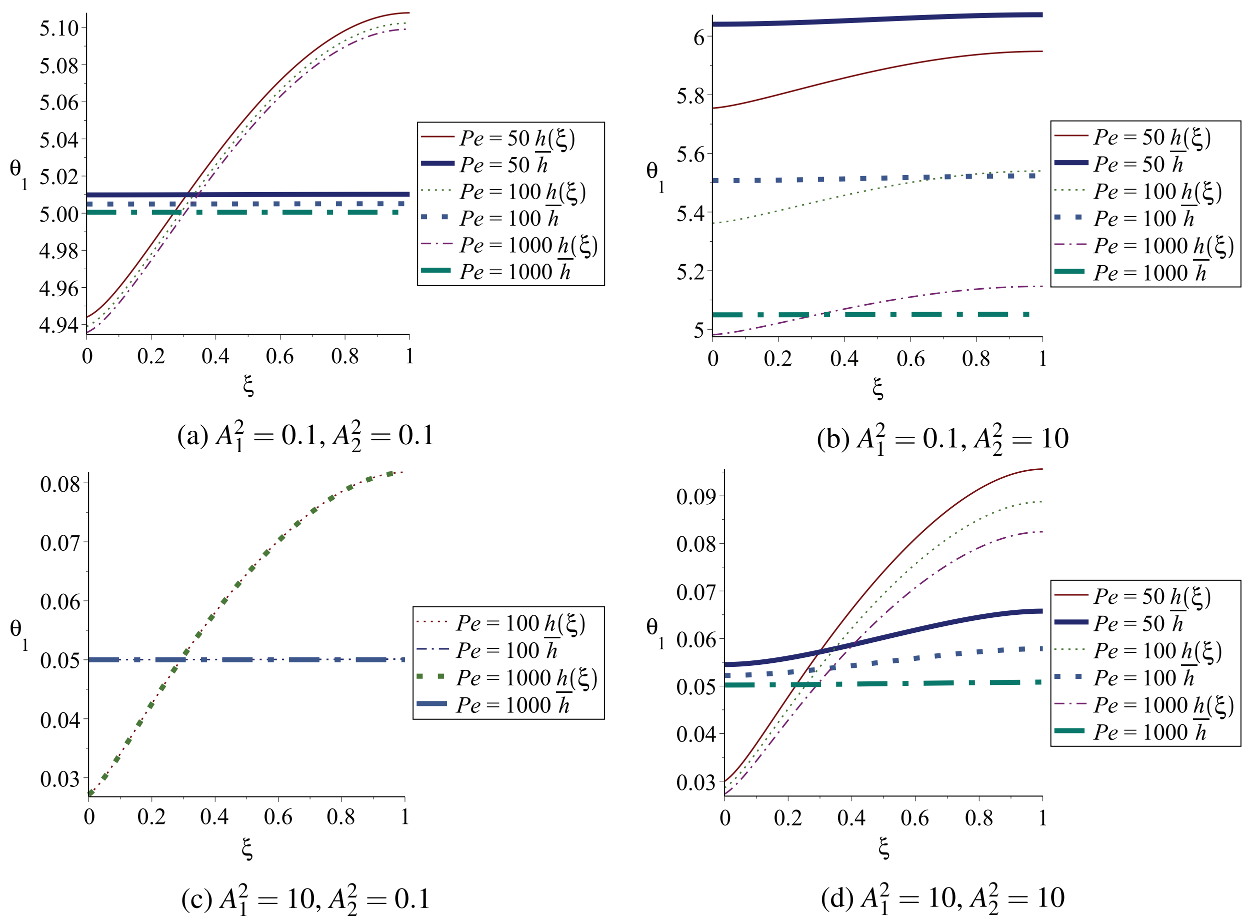

(a) $A_1^2 = 0.1, A_2^2 = 0.1$

(b) $A_1^2 = 0.1, A_2^2 = 10$

(c) $A_1^2 = 10, A_2^2 = 0.1$

(d) $A_1^2 = 10, A_2^2 = 10$

Figure 4.3: Plots for the non-dimensional temperature profile for the solid, θ_1, with various A_1^2, A_2^2 and Pe for $h(\xi)$ and $\bar{h}$

CHAPTER 5. CONCLUSION

5.1 Summary

The purpose of this work was to attempted to provide a more clear explanation of conjugate heat transfer than is currently in literature. Conjugate heat transfer was defined as the modeling of thermal interactions between coupled unique subdomains with varying and unknown interface boundary conditions. The term unique refers to differences between the subdomains' differential equations, material properties or boundary conditions. A conjugate approach is the proper way to solve heat transfer problems. Approximations such as using a heat transfer coefficient make solving heat transfer problems easier but results in a less accurate solution of the temperature field.

A common misconception about conjugate heat transfer is that it only considers heat transfer between a fluid and a solid. As shown in Chapter 3, any coupled problem can be considered conjugate even if it is between two solids.

The Brun number, a non-dimensional number previously developed in literature to judge the conjugation of a specific problem, was discussed and shown that it is essentially a Biot number as suggested by Dorfman [12]. The Brun number does not work in all situations and thus there is no universal parameter for all cases to predict whether a problem needs to be solved with a conjugate approach.

This work attempted to determine the discrepancy in the temperature field that arises between using a local, or variable, heat transfer coefficient and an average heat transfer coefficient. Simple one-dimensional conjugate problems were presented and solved analytically. The problems contained a variable coefficient in the governing equation for which the common methods to solve the differential equation are no longer valid. Two methods, the integral equation and generalized Bessel methods were developed and presented to handle the variable coefficient. The generalized Bessel method had previously only been used with homogeneous governing equations [16]. This work extended the use of the generalized Bessel method to non-homogeneous problems by developing a general relation for the Wronskian of the general solution to the generalized Bessel equation. The relation is

$$W\left(x^m e^{\beta x} I_\nu\left(b(x)x^p\right), x^m e^{\beta x} I_{-\nu}\left(b(x)x^p\right)\right) = -(x^m e^{\beta x})^2 \frac{2\sin(\pi\nu)}{\pi b(x)x^p}\frac{d(b(x)x^p)}{dx}. \tag{5.1}$$

This relation allows the generalized Bessel equation to be used for non-homogeneous problems which enables variable heat transfer coefficients to be used in analysis of differential equations.

The solution methods developed may not be useful for conjugate problems due to the difficulty evaluating the resulting solutions. However, they can be beneficial to solve decoupled problems by increasing solution accuracy by allowing to use variable convective heat transfer coefficient instead of needing to use an average convective heat transfer coefficient. Although, improved and more robust solution evaluation techniques could allow these solutions to be used more widely.

A flat plate problem was solved in Chapter 2 using the developed solution methods. The results agree with Dorfman [12] that there is less conjugation for turbulent flow. The parameter of interest that was varied throughout the solutions is

$$A_1^2 = \frac{h_0 d_1}{k_1}\frac{L^2}{d_1^2} = Bi\frac{L^2}{d_1^2}. \tag{5.2}$$

Thus, for these one-dimensional problems, the value for A_1^2 is dominated by the aspect ratio $\frac{L^2}{d_1^2}$. A large A_1^2 represents a long and thin plate whereas a small A_1^2 results from a short and thick plate. It was found that larger A_1^2 leads to less problem conjugation. Therefore, conjugation is less in a long, thin plate. Also, use of an average heat transfer coefficient over a variable heat transfer coefficient tends to generally under predict the plate temperature.

Tables were developed that allow the temperature profile for the flat plate problem to be quickly found for various A_1^2 by simply calculating A_1^2 for the specific problem. The discrepancy between the average and variable heat transfer coefficient solution can also be found.

Chapter 3 analyzed a conjugate problem between two one-dimensional solids. The same trends found from the flat plate problem were observed. In addition is was found that A_2^2 tends to have more effect on the shape of the temperature profile of solid 1 and A_1^2 has a greater effect on the magnitude of the difference in temperature profiles between the use of an average and variable heat transfer coefficient. The slope of the temperature profile for the average heat transfer coefficient case is always negative. However, the variable heat transfer coefficient case has a positive slope for small A_2^2 and transitions to a negative slope for larger A_2^2. Thus, using an average heat transfer coefficient can give opposite conclusions in some cases. In general increasing the A^2 values reduced conjugation. However, increasing A_2^2 while holding A_1^2 constant increases conjugation.

5.2 Future Work

This work compared the temperature fields obtained when using a variable heat transfer coefficient and an average heat transfer coefficient to see the affect averaging the heat transfer coefficient has on the temperature field. It would be useful to compare a variable heat transfer coefficient to a fully conjugate solution. This would required two-dimensional analysis and would give improved understanding of the error that arises from using and average heat transfer coefficient.

Dorfman [12] suggests that conjugate effects can be more significant for transient problems. It would be useful to analyze transient problems and see how the error of using $\bar{h}$ changes with time. This would be especially useful for radiofrequency cardiac ablation where the heating time could be reduced if the time-dependent temperature field were better understood.

REFERENCES

[1] Wood, A. J., and Morady, F., 1999. "Radio-frequency ablation as treatment for cardiac arrhythmias." *New England Journal of Medicine,* **340**(7), pp. 534–544. 1

[2] Fedorov, A. G., and Viskanta, R., 2000. "Three-dimensional conjugate heat transfer in the microchannel heat sink for electronic packaging." *International Journal of Heat and Mass Transfer,* **43**(3), pp. 399 – 415. 1

[3] Hsieh, C., and Shang, H., 1988. "Solution of boundary value heat conduction problems with variable convective coefficients by a boundary condition dissection method." *Nuclear Engineering and Design,* **110**(1), pp. 17–31. 1, 91

[4] Cole, K., 1996. "Heat transfer from a flush-mounted heat source-limiting cases and the conjugate peclet number." *ASME, NEW YORK, NY,(USA).,* **59**, pp. 145–157. 3, 11

[5] Perelman, T. L., 1961. "On conjugated problems of heat transfer." *International Journal of Heat and Mass Transfer,* **3**(4), pp. 293–303. 3

[6] Dorfman, A., and Renner, Z., 2009. "Conjugate problems in convective heat transfer: Review." *Mathematical Problems in Engineering,* **2009**. 3

[7] "conjugate", 2015. Dictionary.com unabridged, Dec. 4

[8] Sidebotham, G., 2015. *Heat Transfer Modeling*. Springer. 5

[9] Bergman, T. L., L. A. S. I. F. P., and DeWitt, D. P., 2011. *Fundamentals of heat and mass transfer*. John Wiley and Sons. 8

[10] Luikov, A. V., 1974. "Conjugate convective heat transfer problems." *International Journal of Heat and Mass Transfer,* **17**(2), pp. 257–265. 10

[11] Li, Y., and Ortega, A. "Forced convection from a rectangular heat source in uniform shear flow: The conjugate peclet number in the thin plate limit." In *Thermal and Thermomechanical Phenomena in Electronic Systems, 1998. ITHERM'98. The Sixth Intersociety Conference on*, IEEE, pp. 284–294. 11

[12] Dorfman, A. S., 2009. *Conjugate Problems in Convective Heat Transfer*. Taylor and Francis. 11, 12, 13, 36, 60, 61, 62

[13] Petrikevich, B. B., Panin, S. D., and Astrakhov, A. V., 2000. "Use of integral boundary-layer theory for solving conjugate problems of heat transfer in channels of high-power plants." *Journal of Engineering Physics and Thermophysics,* **73**(1), pp. 131–137. 12

[14] Modest, M. F., 2013. *Radiative heat transfer*. Academic press. 23

[15] Moore, T. J., and Jones, M. R., 2015. "Solving nonlinear heat transfer problems using variation of parameters." *International Journal of Thermal Sciences,* **93**, pp. 29–35. 23

[16] Kraus, A. D., Aziz, A., and Welty, J., 2002. *Extended surface heat transfer*. John Wiley and Sons. 25, 60

[17] Hahn, D. W., and Ozisik, M. N., 2012. *Heat conduction*. John Wiley and Sons. 26

[18] DLMF NIST Digital Library of Mathematical Functions http://dlmf.nist.gov/, Release 1.0.9 of 2014-08-29. 29

[19] Prosperetti, A., 2013. "Advanced mathematics for applications." *SIAM Review Vol. 55, Issue 2 (June 2013),* **55**(2), p. 403. 29

[20] Maple 16.00. Maplesoft, a division of Waterloo Maple Inc., W. O. 31

[21] Kays, W. M., Crawford, M. E., and Weigand, B., 2012. *Convective heat and mass transfer*. Tata McGraw-Hill Education. 54

APPENDIX A. ANALYTICAL SOLUTIONS

This appendix contains development of solutions used throughout each chapter.

A.1 The Common Solution Method for a Constant Coefficient is Not Valid for a Variable Coefficient

Return to the governing equation, Eqn. 2.26, but for mathematical simplicity let $\tilde{h}(\xi)$ be squared,

$$\frac{d^2\theta_1(\xi)}{d\xi^2} - A_1^2\tilde{h}(\xi)^2\theta_1(\xi) = -\tilde{q}(\xi) \tag{A.1}$$

and try to solve using the commonly used general solution for an average heat transfer coefficient, $\bar{h}$, but with a variable coefficient, $h(\xi)$. The homogeneous equation would first be solved

$$\frac{d^2\theta_1(\xi)}{d\xi^2} - A_1^2\tilde{h}(\xi)\theta_1(\xi) = 0. \tag{A.2}$$

At first glance this differential equation looks familiar and the general solution from any introductory differential equation textbook would be used

$$\theta_1(x) = c_1\cosh(A_1\tilde{h}(\xi)\xi) + c_2\sinh(A_1\tilde{h}(\xi)\xi). \tag{A.3}$$

This solution to the differential equation can be checked by substituting it back into the differential equation, Eqn. A.2,

$$\begin{aligned} 0 = {} & c_1\frac{d^2\cosh(A_1\tilde{h}(\xi)\xi)}{d\xi^2} + c_2\frac{d^2\sinh(A_1\tilde{h}(\xi)\xi)}{d\xi^2} \\ & - c_1A_1^2\tilde{h}(\xi)\cosh(A_1\tilde{h}(\xi)\xi) - c_2A_1^2\tilde{h}(\xi)\sinh(A_1\tilde{h}(\xi)\xi). \end{aligned} \tag{A.4}$$

Evaluating the derivatives once gives

$$0 = c_1 \frac{d}{d\xi}[\frac{d(A_1\tilde{h}(\xi)\xi)}{d\xi}\sinh(A_1\tilde{h}(\xi)\xi)] + c_2\frac{d}{d\xi}[\frac{d(A_1\tilde{h}(\xi)\xi)}{d\xi}\cosh(A_1\tilde{h}(\xi)\xi)]$$
$$-c_1A_1^2\tilde{h}(\xi)\cosh(A_1\tilde{h}(\xi)\xi) - c_2A_1^2\tilde{h}(\xi)\sinh(A_1\tilde{h}(\xi)\xi) \quad \text{(A.5)}$$

and evaluating the derivatives again

$$0 = c_1\frac{d^2(A_1\tilde{h}(\xi)\xi)}{d\xi^2}\sinh(A_1\tilde{h}(\xi)\xi) + c_1\Big(\frac{d(A_1\tilde{h}(\xi)\xi)}{d\xi}\Big)^2\cosh(A_1\tilde{h}(\xi)\xi)$$
$$+c_2\frac{d^2(A_1\tilde{h}(\xi)\xi)}{d\xi^2}\cosh(A_1\tilde{h}(\xi)\xi) + c_2\Big(\frac{d(A_1\tilde{h}(\xi)\xi)}{d\xi}\Big)^2\sinh(A_1\tilde{h}(\xi)\xi)$$
$$-c_1A_1^2\tilde{h}(\xi)\cosh(A_1\tilde{h}(\xi)\xi) - c_2A_1^2\tilde{h}(\xi)\sinh(A_1\tilde{h}(\xi)\xi). \quad \text{(A.6)}$$

Performing the product rule on the derivatives

$$0 = c_1[\frac{d^2(\tilde{h}(\xi))}{d\xi^2}\xi + 2\frac{d(\tilde{h}(\xi))}{d\xi}]A_1\sinh(A_1\tilde{h}(\xi)\xi)$$
$$+c_1[\Big(\frac{d(\tilde{h}(\xi))}{d\xi}\xi\Big)^2 + 2\frac{d(\tilde{h}(\xi))}{d\xi}\tilde{h}(\xi)\xi + \tilde{h}(\xi)^2]A_1^2\cosh(A_1\tilde{h}(\xi)\xi)$$
$$+c_2[\frac{d^2(\tilde{h}(\xi))}{d\xi^2}\xi + 2\frac{d(\tilde{h}(\xi))}{d\xi}]A_1\cosh(A_1\tilde{h}(\xi)\xi)$$
$$+c_2[\Big(\frac{d(\tilde{h}(\xi))}{d\xi}\xi\Big)^2 + 2\frac{d(\tilde{h}(\xi))}{d\xi}\tilde{h}(\xi)\xi + \tilde{h}(\xi)^2]A_1^2\sinh(A_1\tilde{h}(\xi)\xi)$$
$$-c_1A_1^2\tilde{h}(\xi)^2\cosh(A_1\tilde{h}(\xi)\xi) - c_2A_1^2\tilde{h}(\xi)^2\sinh(A_1\tilde{h}(\xi)\xi) \quad \text{(A.7)}$$

and removing canceling terms and rearranging results in

$$0 = [\frac{d^2(\tilde{h}(\xi))}{d\xi^2}\xi + 2\frac{d(\tilde{h}(\xi))}{d\xi}][c_2\cosh(A_1\tilde{h}(\xi)\xi) + c_1\sinh(A_1\tilde{h}(\xi)\xi)]$$
$$+[\Big(\frac{d(\tilde{h}(\xi))}{d\xi}\xi\Big)^2 + 2\frac{d(\tilde{h}(\xi))}{d\xi}\tilde{h}(\xi)\xi][c_2A_1\sinh(A_1\tilde{h}(\xi)\xi) + c_1A_1\cosh(A_1\tilde{h}(\xi)\xi)] \quad \text{(A.8)}$$

The above equation is not true for an arbitrary $\tilde{h}(\xi)$ and it is unclear if there is any $\tilde{h}(\xi)$ that could satisfy the equation. If $\tilde{h}$ is constant all the derivatives are equal to zero and Eqn A.8 is a true statement.

The general solutions that are commonly used for differential equations with constant coefficients no longer apply when the coefficients are variable.

A.2 One-Dimensional Conjugate Heat Transfer Between Two Solids

A.2.1 Integral Equation Method Solution

A.2.1.1 Solution for Solid 1

The governing equation to be solved is

$$\frac{d^2\theta_1(\xi)}{d\xi^2} = A_1^2\tilde{U}(\xi)\big(\theta_1(\xi)-\theta_2(\xi)\big)-\tilde{q}(\xi) \tag{A.9}$$

with boundary conditions

$$\left.\frac{d\theta_1}{d\xi}\right|_{\xi=0} = 0 \tag{A.10}$$

$$\left.\frac{d\theta_1}{d\xi}\right|_{\xi=1} = 0. \tag{A.11}$$

Integrate once

$$\frac{d\theta_1}{d\xi} = c_1 + \int_0^{\xi}\Big[A_1^2\tilde{U}(\xi')\big(\theta_1(\xi')-\theta_2(\xi')\big)-\tilde{q}(\xi')\Big]d\xi' \tag{A.12}$$

and again

$$\theta_1 = c_2 + c_1\xi + \int_0^{\xi}\int_0^{\xi'}\Big[A_1^2\tilde{U}(\xi'')\big(\theta_1(\xi'')-\theta_2(\xi'')\big)-\tilde{q}(\xi'')\Big]d\xi''d\xi'. \tag{A.13}$$

Apply the first boundary condition, Eqn. A.10

$$c_1 = 0. \tag{A.14}$$

Apply the second boundary condition, Eqn. A.11

$$0 = \int_0^{1}\Big[A_1^2\tilde{U}(\xi')\big(\theta_1(\xi')-\theta_2(\xi')\big)-\tilde{q}(\xi')\Big]d\xi'. \tag{A.15}$$

Substituting in θ_1

$$0 = \int_0^1 \left[A_1^2 \tilde{U}(\xi') \Big(c_2 + \int_0^{\xi'} \int_0^{\xi''} \big[A_1^2 \tilde{U}(\xi''') \big(\theta_1(\xi''') - \theta_2(\xi''') \big) - \tilde{q}(\xi''') \big] d\xi''' d\xi'' - \theta_2(\xi') \Big) - \tilde{q}(\xi') \right] d\xi' \tag{A.16}$$

and solving for c_2 results in

$$c_2 = - \frac{1}{A_1^2 \int_0^1 \tilde{U}(\xi') d\xi'} \int_0^1 \left[A_1^2 \tilde{U}(\xi') \Big(\int_0^{\xi'} \int_0^{\xi''} \big[A_1^2 \tilde{U}(\xi''') \big(\theta_1(\xi''') - \theta_2(\xi''') \big) - \tilde{q}(\xi''') \big] d\xi''' d\xi'' \right.$$
$$\left. - \theta_2(\xi') \Big) - \tilde{q}(\xi') \right] d\xi'. \tag{A.17}$$

The temperature profile is

$$\theta_1 = c_2 + \int_0^{\xi} \int_0^{\xi'} \left[A_1^2 \tilde{U}(\xi'') \big(\theta_1(\xi'') - \theta_2(\xi'') \big) - \tilde{q}(\xi'') \right] d\xi'' d\xi' \tag{A.18}$$

A.2.1.2 Solution for Solid 2

The governing equation to be solved is

$$\frac{d^2 \theta_2(\xi)}{d\xi^2} = -A_2^2 \tilde{U}(\xi) \big(\theta_1(\xi) - \theta_2(\xi) \big) \tag{A.19}$$

with boundary conditions

$$\left. \frac{d\theta_2}{d\xi} \right|_{\xi=0} = 0 \tag{A.20}$$

$$\theta_2(1) = 0. \tag{A.21}$$

Integrating once

$$\frac{d\theta_2}{d\xi} = c_3 - \int_0^{\xi} \left[A_2^2 \tilde{U}(\xi') \big(\theta_1(\xi') - \theta_2(\xi') \big) \right] d\xi' \tag{A.22}$$

and again results in

$$\theta_2 = c_4 + c_3 \xi - \int_0^{\xi} \int_0^{\xi'} \left[A_2^2 \tilde{U}(\xi'') \big(\theta_1(\xi'') - \theta_2(\xi'') \big) \right] d\xi'' d\xi' \tag{A.23}$$

Apply the first boundary condition at $\xi = 0$

$$c_3 = 0 \tag{A.24}$$

Apply the second boundary condition at $\xi = 1$

$$c_4 = \int_0^1 \int_0^{\xi'} \Big[A_2^2 \tilde{U}(\xi'') \big(\theta_1(\xi'') - \theta_2(\xi'') \big) \Big] d\xi'' d\xi' \tag{A.25}$$

and the temperature profile becomes

$$\begin{aligned} \theta_2 = & \int_0^1 \int_0^{\xi'} \Big[A_2^2 \tilde{U}(\xi'') \big(\theta_1(\xi'') - \theta_2(\xi'') \big) \Big] d\xi'' d\xi' \\ & - \int_0^{\xi} \int_0^{\xi'} \Big[A_2^2 \tilde{U}(\xi'') \big(\theta_1(\xi'') - \theta_2(\xi'') \big) \Big] d\xi'' d\xi'. \end{aligned} \tag{A.26}$$

A.2.2 Generalized Bessel Method Solution

A.2.2.1 Solution for Solid 1

The governing equation to be solved is

$$\frac{d^2\theta_1(\xi)}{d\xi^2} - A_1^2 \tilde{U}(\xi)\theta_1(\xi) = -A_1^2 \tilde{U}(\xi)\theta_2(\xi) - \tilde{q}(\xi) \tag{A.27}$$

Let

$$\tilde{U}(\xi) = \xi^{-\frac{1}{2}} \tag{A.28}$$

$$\frac{d^2\theta_1(\xi)}{d\xi^2} - A_1^2 \xi^{-\frac{1}{2}} \theta_1(\xi) = -A_1^2 \xi^{-\frac{1}{2}} \theta_2(\xi) - \tilde{q}(\xi) \tag{A.29}$$

with boundary conditions

$$\left. \frac{d\theta_1}{d\xi} \right|_{\xi=0} = 0 \tag{A.30}$$

$$\left. \frac{d\theta_1}{d\xi} \right|_{\xi=1} = 0. \tag{A.31}$$

The solution to the differential equation is the sum of the homogeneous and particular solutions

$$\theta_1 = \theta_{1h} + \theta_{1p}. \tag{A.32}$$

The homogeneous equation is

$$\frac{d^2\theta_{1h}(\xi)}{d\xi^2} - A_1^2\xi^{-\frac{1}{2}}\theta_{1h}(\xi) = 0. \tag{A.33}$$

Using the generalized Bessel equation

$$\frac{d^2R}{d\xi^2} + \left[\frac{1-2m}{\xi} - 2\alpha\right]\frac{dR}{d\xi} + \left[p^2a^2\xi^{2p-2} + \alpha^2 + \frac{\alpha(2m-1)}{\xi} + \frac{m^2-p^2\nu^2}{\xi^2}\right]R = 0 \tag{A.34}$$

with solution

$$R = \xi^m e^{\alpha\xi}\left[c_1J_\nu(a\xi^p) + c_2Y_\nu(a\xi^p)\right] \tag{A.35}$$

or if ν is not an integer

$$R = \xi^m e^{\alpha\xi}\left[c_1J_\nu(a\xi^p) + c_2J_{-\nu}(a\xi^p)\right]. \tag{A.36}$$

The coefficients for the given differential equation are

$$m = \frac{1}{2} \tag{A.37}$$

$$\alpha = 0 \tag{A.38}$$

$$p = \frac{3}{4} \tag{A.39}$$

$$\nu = \frac{2}{3} \tag{A.40}$$

$$a = \frac{4}{3}iA_1 \tag{A.41}$$

thus the general solution is

$$\theta_{1h} = \xi^{\frac{1}{2}}\left[c_1J_{\frac{2}{3}}\left(\frac{4}{3}iA_1\xi^{\frac{3}{4}}\right) + c_2J_{-\frac{2}{3}}\left(\frac{4}{3}iA_1\xi^{\frac{3}{4}}\right)\right] \tag{A.42}$$

or

$$\theta_{1h} = \xi^{\frac{1}{2}}\left[c_1 I_{\frac{2}{3}}\left(\frac{4}{3}A_1\xi^{\frac{3}{4}}\right) + c_2 I_{-\frac{2}{3}}\left(\frac{4}{3}A_1\xi^{\frac{3}{4}}\right)\right]. \tag{A.43}$$

The Wronskian is

$$W(\xi^{\frac{1}{2}}I_{\frac{2}{3}}(\frac{4}{3}A_1\xi^{\frac{3}{4}}), \xi^{\frac{1}{2}}I_{-\frac{2}{3}}(\frac{4}{3}A_1\xi^{\frac{3}{4}})) = \begin{vmatrix} \xi^{\frac{1}{2}}I_{\frac{2}{3}}\left(\frac{4}{3}A_1\xi^{\frac{3}{4}}\right) & \xi^{\frac{1}{2}}I_{-\frac{2}{3}}\left(\frac{4}{3}A_1\xi^{\frac{3}{4}}\right) \\ \frac{3}{4}\frac{4}{3}A_1\xi^{\frac{1}{4}}I_{-\frac{1}{3}}\left(\frac{4}{3}A_1\xi^{\frac{3}{4}}\right) & \frac{3}{4}\frac{4}{3}A_1\xi^{\frac{1}{4}}I_{\frac{1}{3}}\left(\frac{4}{3}A_1\xi^{\frac{3}{4}}\right) \end{vmatrix}$$

$$= -\frac{3\sqrt{3}}{4\pi} \tag{A.44}$$

Use the method of variation of parameters to obtain the particular solution

$$\begin{aligned} \theta_{1p} = &-\xi^{\frac{1}{2}}I_{\frac{2}{3}}\left(\frac{4}{3}A_1\xi^{\frac{3}{4}}\right)\int_0^{\xi}\xi'^{\frac{1}{2}}I_{-\frac{2}{3}}\left(\frac{4}{3}A_1\xi'^{\frac{3}{4}}\right)\frac{\left(-A_1^2\xi'^{-\frac{1}{2}}\theta_2(\xi')-\tilde{q}(\xi')\right)}{-\frac{3\sqrt{3}}{4\pi}}d\xi' \\ &+\xi^{\frac{1}{2}}I_{-\frac{2}{3}}\left(\frac{4}{3}A_1\xi^{\frac{3}{4}}\right)\int_0^{\xi}\xi'^{\frac{1}{2}}I_{\frac{2}{3}}\left(\frac{4}{3}A_1\xi'^{\frac{3}{4}}\right)\frac{\left(-A_1^2\xi'^{-\frac{1}{2}}\theta_2(\xi')-\tilde{q}(\xi')\right)}{-\frac{3\sqrt{3}}{4\pi}}d\xi'. \end{aligned} \tag{A.45}$$

Rearranging

$$\begin{aligned} \theta_{1p} = &-\frac{4\pi}{3\sqrt{3}}\xi^{\frac{1}{2}}I_{\frac{2}{3}}(\frac{4}{3}A_1\xi^{\frac{3}{4}})\int_0^{\xi}I_{-\frac{2}{3}}(\frac{4}{3}A_1\xi'^{\frac{3}{4}})\left(A_1^2\theta_2(\xi')+\xi'^{\frac{1}{2}}\tilde{q}(\xi')\right)d\xi' \\ &+\frac{4\pi}{3\sqrt{3}}\xi^{\frac{1}{2}}I_{-\frac{2}{3}}(\frac{4}{3}A_1\xi^{\frac{3}{4}})\int_0^{\xi}I_{\frac{2}{3}}(\frac{4}{3}A_1\xi'^{\frac{3}{4}})\left(A_1^2\theta_2(\xi')+\xi'^{\frac{1}{2}}\tilde{q}(\xi')\right)d\xi' \end{aligned} \tag{A.46}$$

and substituting back into the solution results in

$$\begin{aligned} \theta_1 = &\,\xi^{\frac{1}{2}}\left[c_1 I_{\frac{2}{3}}\left(\frac{4}{3}A_1\xi^{\frac{3}{4}}\right) + c_2 I_{-\frac{2}{3}}\left(\frac{4}{3}A_1\xi^{\frac{3}{4}}\right)\right] \\ &-\frac{4\pi}{3\sqrt{3}}\xi^{\frac{1}{2}}I_{\frac{2}{3}}(\frac{4}{3}A_1\xi^{\frac{3}{4}})\int_0^{\xi}I_{-\frac{2}{3}}(\frac{4}{3}A_1\xi'^{\frac{3}{4}})\left(A_1^2\theta_2(\xi')+\xi'^{\frac{1}{2}}\tilde{q}(\xi')\right)d\xi' \\ &+\frac{4\pi}{3\sqrt{3}}\xi^{\frac{1}{2}}I_{-\frac{2}{3}}(\frac{4}{3}A_1\xi^{\frac{3}{4}})\int_0^{\xi}I_{\frac{2}{3}}(\frac{4}{3}A_1\xi'^{\frac{3}{4}})\left(A_1^2\theta_2(\xi')+\xi'^{\frac{1}{2}}\tilde{q}(\xi')\right)d\xi'. \end{aligned} \tag{A.47}$$

Differentiate

$$\begin{aligned}\frac{d\theta_1}{d\xi} &= A_1\xi^{\frac{1}{4}}\left[c_1 I_{-\frac{1}{3}}\left(\frac{4}{3}A_1\xi^{\frac{3}{4}}\right) + c_2 I_{\frac{1}{3}}\left(\frac{4}{3}A_1\xi^{\frac{3}{4}}\right)\right] \\ &- \frac{4\pi}{3\sqrt{3}}A_1\xi^{\frac{1}{4}} I_{-\frac{1}{3}}\left(\frac{4}{3}A_1\xi^{\frac{3}{4}}\right)\int_0^{\xi} I_{-\frac{2}{3}}\left(\frac{4}{3}A_1\xi'^{\frac{3}{4}}\right)\left(A_1^2\theta_2(\xi') + \xi'^{\frac{1}{2}}\tilde{q}(\xi')\right)d\xi' \\ &- \frac{4\pi}{3\sqrt{3}}\xi^{\frac{1}{2}} I_{\frac{2}{3}}\left(\frac{4}{3}A_1\xi^{\frac{3}{4}}\right) I_{-\frac{2}{3}}\left(\frac{4}{3}A_1\xi^{\frac{3}{4}}\right)\left(A_1^2\theta_2(\xi) + \xi^{\frac{1}{2}}\tilde{q}(\xi')\right) \\ &+ \frac{4\pi}{3\sqrt{3}}A_1\xi^{\frac{1}{4}} I_{\frac{1}{3}}\left(\frac{4}{3}A_1\xi^{\frac{3}{4}}\right)\int_0^{\xi} I_{\frac{2}{3}}\left(\frac{4}{3}A_1\xi'^{\frac{3}{4}}\right)\left(A_1^2\theta_2(\xi') + \xi'^{\frac{1}{2}}\tilde{q}(\xi')\right)d\xi' \\ &+ \frac{4\pi}{3\sqrt{3}}\xi^{\frac{1}{2}} I_{-\frac{2}{3}}\left(\frac{4}{3}A_1\xi^{\frac{3}{4}}\right) I_{\frac{2}{3}}\left(\frac{4}{3}A_1\xi^{\frac{3}{4}}\right)\left(A_1^2\theta_2(\xi) + \xi^{\frac{1}{2}}\tilde{q}(\xi')\right)\end{aligned} \tag{A.48}$$

The 3rd and last term cancel

$$\begin{aligned}\frac{d\theta_1}{d\xi} &= A_1\xi^{\frac{1}{4}}\left[c_1 I_{-\frac{1}{3}}\left(\frac{4}{3}A_1\xi^{\frac{3}{4}}\right) + c_2 I_{\frac{1}{3}}\left(\frac{4}{3}A_1\xi^{\frac{3}{4}}\right)\right] \\ &- \frac{4\pi}{3\sqrt{3}}A_1\xi^{\frac{1}{4}} I_{-\frac{1}{3}}\left(\frac{4}{3}A_1\xi^{\frac{3}{4}}\right)\int_0^{\xi} I_{-\frac{2}{3}}\left(\frac{4}{3}A_1\xi'^{\frac{3}{4}}\right)\left(A_1^2\theta_2(\xi') + \xi'^{\frac{1}{2}}\tilde{q}(\xi')\right)d\xi' \\ &+ \frac{4\pi}{3\sqrt{3}}A_1\xi^{\frac{1}{4}} I_{\frac{1}{3}}\left(\frac{4}{3}A_1\xi^{\frac{3}{4}}\right)\int_0^{\xi} I_{\frac{2}{3}}\left(\frac{4}{3}A_1\xi'^{\frac{3}{4}}\right)\left(A_1^2\theta_2(\xi') + \xi'^{\frac{1}{2}}\tilde{q}(\xi')\right)d\xi'\end{aligned} \tag{A.49}$$

Apply first boundary condition at $\xi = 0$

$$0 = \left[c_1\xi^{\frac{1}{4}} I_{-\frac{1}{3}}\left(\xi^{\frac{3}{4}}\right) + c_2\xi^{\frac{1}{4}} I_{\frac{1}{3}}\left(\xi^{\frac{3}{4}}\right)\right]\Big|_{\xi=0} \tag{A.50}$$

$$\lim_{\xi\to 0}\xi^{\frac{1}{4}} I_{-\frac{1}{3}}\left(\xi^{\frac{3}{4}}\right) \longrightarrow \frac{2^{\frac{1}{3}}}{(\frac{4}{3}A_1)^{\frac{1}{3}}\Gamma(\frac{2}{3})} \tag{A.51}$$

$$\xi^{\frac{1}{4}} I_{\frac{1}{3}}\left(\xi^{\frac{3}{4}}\right)\Big|_{\xi=0} = 0 \tag{A.52}$$

$$c_1 = 0 \tag{A.53}$$

Apply second boundary condition at $\xi = 1$

$$0 = c_2 A_1 I_{\frac{1}{3}}\left(\frac{4}{3}A_1\right) - \frac{4\pi}{3\sqrt{3}} A_1 I_{-\frac{1}{3}}\left(\frac{4}{3}A_1\right) \int_0^1 I_{-\frac{2}{3}}\left(\frac{4}{3}A_1 \xi'^{\frac{3}{4}}\right)\left(A_1^2 \theta_2(\xi') + \xi'^{\frac{1}{2}} \tilde{q}(\xi')\right) d\xi' + \frac{4\pi}{3\sqrt{3}} A_1 I_{\frac{1}{3}}\left(\frac{4}{3}A_1\right) \int_0^1 I_{\frac{2}{3}}\left(\frac{4}{3}A_1 \xi'^{\frac{3}{4}}\right)\left(\left(A_1^2 \theta_2(\xi') + \xi'^{\frac{1}{2}} \tilde{q}(\xi')\right) d\xi' \tag{A.54}$$

$$c_2 = \frac{4\pi}{3\sqrt{3}} \frac{I_{-\frac{1}{3}}\left(\frac{4}{3}A_1\right)}{I_{\frac{1}{3}}\left(\frac{4}{3}A_1\right)} \int_0^1 I_{-\frac{2}{3}}\left(\frac{4}{3}A_1 \xi'^{\frac{3}{4}}\right)\left(A_1^2 \theta_2(\xi') + \xi'^{\frac{1}{2}} \tilde{q}(\xi')\right) d\xi' - \frac{4\pi}{3\sqrt{3}} \int_0^1 I_{\frac{2}{3}}\left(\frac{4}{3}A_1 \xi'^{\frac{3}{4}}\right)\left(A_1^2 \theta_2(\xi') + \xi'^{\frac{1}{2}} \tilde{q}(\xi')\right) d\xi' \tag{A.55}$$

The temperature profile is

$$\theta_1 = c_2 \xi^{\frac{1}{2}} I_{-\frac{2}{3}}\left(\frac{4}{3}A_1 \xi^{\frac{3}{4}}\right) - \frac{4\pi}{3\sqrt{3}} \xi^{\frac{1}{2}} I_{\frac{2}{3}}\left(\frac{4}{3}A_1 \xi^{\frac{3}{4}}\right) \int_0^{\xi} I_{-\frac{2}{3}}\left(\frac{4}{3}A_1 \xi'^{\frac{3}{4}}\right)\left(A_1^2 \theta_2(\xi') + \xi'^{\frac{1}{2}} \tilde{q}(\xi')\right) d\xi' + \frac{4\pi}{3\sqrt{3}} \xi^{\frac{1}{2}} I_{-\frac{2}{3}}\left(\frac{4}{3}A_1 \xi^{\frac{3}{4}}\right) \int_0^{\xi} I_{\frac{2}{3}}\left(\frac{4}{3}A_1 \xi'^{\frac{3}{4}}\right)\left(A_1^2 \theta_2(\xi') + \xi'^{\frac{1}{2}} \tilde{q}(\xi')\right) d\xi'. \tag{A.56}$$

A.2.2.2 Solution for Solid 2

The governing equation to be solved is

$$\frac{d^2 \theta_2(\xi)}{d\xi^2} - A_2^2 \xi^{-\frac{1}{2}} \theta_2(\xi) = -A_2^2 \xi^{-\frac{1}{2}} \theta_1(\xi) \tag{A.57}$$

with boundary conditions

$$\frac{\partial \theta_2}{\partial \xi}\Big|_{\xi=0} = 0 \tag{A.58}$$

$$\theta_2(1) = 0 \tag{A.59}$$

The solution to the differential equation is the sum of the homogeneous and particular solutions

$$\theta_2 = \theta_{2h} + \theta_{2p}. \tag{A.60}$$

The homogeneous solution and Wronskian are the same as for solid 1

$$\theta_{2h} = \xi^{\frac{1}{2}}\left[c_3 I_{\frac{2}{3}}\left(\frac{4}{3}A_2\xi^{\frac{3}{4}}\right) + c_4 I_{-\frac{2}{3}}\left(\frac{4}{3}A_2\xi^{\frac{3}{4}}\right)\right] \tag{A.61}$$

$$W = -\frac{3\sqrt{3}}{4\pi}. \tag{A.62}$$

The particular solution will also be the same as solid 1 except $\tilde{q}(\xi) = 0$

$$\begin{aligned}\theta_{2p} = &-\frac{4\pi}{3\sqrt{3}}\xi^{\frac{1}{2}} I_{\frac{2}{3}}\big(\frac{4}{3}A_2\xi^{\frac{3}{4}}\big)\int_0^{\xi} I_{-\frac{2}{3}}\big(\frac{4}{3}A_2\xi'^{\frac{3}{4}}\big)\Big(A_2^2\theta_1(\xi')\Big)d\xi' \\ &+\frac{4\pi}{3\sqrt{3}}\xi^{\frac{1}{2}} I_{-\frac{2}{3}}\big(\frac{4}{3}A_2\xi^{\frac{3}{4}}\big)\int_0^{\xi} I_{\frac{2}{3}}\big(\frac{4}{3}A_2\xi'^{\frac{3}{4}}\big)\Big(A_2^2\theta_1(\xi')\Big)d\xi'.\end{aligned} \tag{A.63}$$

$$\begin{aligned}\theta_2 = \xi^{\frac{1}{2}}\left[c_3 I_{\frac{2}{3}}\left(\frac{4}{3}A_2\xi^{\frac{3}{4}}\right) + c_4 I_{-\frac{2}{3}}\left(\frac{4}{3}A_2\xi^{\frac{3}{4}}\right)\right] - \frac{4\pi}{3\sqrt{3}}A_2^2\xi^{\frac{1}{2}} I_{\frac{2}{3}}\big(\frac{4}{3}A_2\xi^{\frac{3}{4}}\big)\int_0^{\xi} I_{-\frac{2}{3}}\big(\frac{4}{3}A_2\xi'^{\frac{3}{4}}\big)\theta_1(\xi')d\xi' \\ + \frac{4\pi}{3\sqrt{3}}A_2^2\xi^{\frac{1}{2}} I_{-\frac{2}{3}}\big(\frac{4}{3}A_2\xi^{\frac{3}{4}}\big)\int_0^{\xi} I_{\frac{2}{3}}\big(\frac{4}{3}A_2\xi'^{\frac{3}{4}}\big)\theta_1(\xi')d\xi'\end{aligned} \tag{A.64}$$

Apply the first boundary condition at $\xi = 0$

$$0 = A_2\xi^{\frac{1}{4}}\left[c_3 I_{-\frac{1}{3}}\left(\frac{4}{3}A_2\xi^{\frac{3}{4}}\right) + c_4 I_{\frac{1}{3}}\left(\frac{4}{3}A_2\xi^{\frac{3}{4}}\right)\right]_{\xi=0} \tag{A.65}$$

noting that

$$\lim_{\xi\to 0} A_2\xi^{\frac{1}{4}} c_4 I_{\frac{1}{3}}\left(\frac{4}{3}A_2\xi^{\frac{3}{4}}\right) \longrightarrow 0 \tag{A.66}$$

and

$$\lim_{\xi\to 0} A_2\xi^{\frac{1}{4}} c_3 I_{-\frac{1}{3}}\left(\frac{4}{3}A_2\xi^{\frac{3}{4}}\right) \longrightarrow \frac{3}{4}\frac{2^{\frac{1}{3}}(\frac{4}{3}A_2)^{\frac{2}{3}}}{\Gamma(\frac{2}{3})} \tag{A.67}$$

which results in

$$c_3 = 0. \tag{A.68}$$

Apply the second boundary condition at $\xi = 1$

$$\begin{aligned} 0 = c_4 I_{-\frac{2}{3}}\left(\frac{4}{3}A_2\right) - \frac{4\pi}{3\sqrt{3}} A_2^2 I_{\frac{2}{3}}\left(\frac{4}{3}A_2\right) \int_0^1 I_{-\frac{2}{3}}\left(\frac{4}{3}A_2 \xi'^{\frac{3}{4}}\right) \theta_1(\xi') d\xi' \\ + \frac{4\pi}{3\sqrt{3}} A_2^2 I_{-\frac{2}{3}}\left(\frac{4}{3}A_2\right) \int_0^1 I_{\frac{2}{3}}\left(\frac{4}{3}A_2 \xi'^{\frac{3}{4}}\right) \theta_1(\xi') d\xi'. \end{aligned} \tag{A.69}$$

Solving for the constant

$$c_4 = \frac{4\pi A_2^2}{3\sqrt{3}} \frac{I_{\frac{2}{3}}\left(\frac{4}{3}A_2\right)}{I_{-\frac{2}{3}}\left(\frac{4}{3}A_2\right)} \int_0^1 I_{-\frac{2}{3}}\left(\frac{4}{3}A_2 \xi'^{\frac{3}{4}}\right) \theta_1(\xi') d\xi' - \frac{4\pi A_2^2}{3\sqrt{3}} \int_0^1 I_{\frac{2}{3}}\left(\frac{4}{3}A_2 \xi'^{\frac{3}{4}}\right) \theta_1(\xi') d\xi' \tag{A.70}$$

the temperature profile is

$$\begin{aligned} \theta_2 = c_4 \xi^{\frac{1}{2}} I_{-\frac{2}{3}}\left(\frac{4}{3}A_2 \xi^{\frac{3}{4}}\right) - \frac{4\pi A_2^2}{3\sqrt{3}} \xi^{\frac{1}{2}} I_{\frac{2}{3}}\left(\frac{4}{3}A_2 \xi^{\frac{3}{4}}\right) \int_0^{\xi} I_{-\frac{2}{3}}\left(\frac{4}{3}A_2 \xi'^{\frac{3}{4}}\right) \theta_1(\xi') d\xi' \\ + \frac{4\pi A_2^2}{3\sqrt{3}} \xi^{\frac{1}{2}} I_{-\frac{2}{3}}\left(\frac{4}{3}A_2 \xi^{\frac{3}{4}}\right) \int_0^{\xi} I_{\frac{2}{3}}\left(\frac{4}{3}A_2 \xi'^{\frac{3}{4}}\right) \theta_1(\xi') d\xi'. \end{aligned} \tag{A.71}$$

A.2.3 Transient Solution for an Average Heat Transfer Coefficient

A.2.3.1 Solution for Solid 1

The governing equation to be solved is

$$\frac{\partial^2 \theta_1(\xi,\tau)}{\partial \xi^2} - A_1^2 \theta_1(\xi,\tau) = \frac{\partial \theta_1(\xi,\tau)}{\partial \tau} - A_1^2 \theta_2(\xi,\tau) - \tilde{q}(\xi,\tau). \tag{A.72}$$

Let $g(\xi,\tau) = -A_1^2 \theta_2(\xi,\tau) - \tilde{q}(\xi,\tau)$ and the equation becomes

$$\frac{\partial^2 \theta_1(\xi,\tau)}{\partial \xi^2} - A_1^2 \theta_1(\xi,\tau) = \frac{\partial \theta_1(\xi,\tau)}{\partial \tau} + g(\xi,\tau) \tag{A.73}$$

with boundary conditions

$$\left.\frac{d\theta_1}{d\xi}\right|_{\xi=0} = 0 \tag{A.74}$$

$$\left.\frac{d\theta_1}{d\xi}\right|_{\xi=1} = 0 \tag{A.75}$$

$$\theta_1(\xi, 0) = \theta_0. \tag{A.76}$$

First, look at the homogeneous case

$$\frac{\partial^2 \theta_{1h}(\xi,\tau)}{\partial \xi^2} - A_1^2 \theta_{1h}(\xi,\tau) = \frac{\partial \theta_{1h}(\xi,\tau)}{\partial \tau} \tag{A.77}$$

Using separation of variables and assuming a solution of the form $\theta_{1h}(\xi,\tau) = \phi(\xi)a(\tau)$

$$\frac{\partial^2 \phi(\xi)}{\partial \xi^2} a(\tau) - A_1^2 \phi(\xi) a(\tau) = \frac{\partial a(\tau)}{\partial \tau} \phi(\xi) \tag{A.78}$$

and defining a separation constant, $-\lambda^2$

$$\frac{1}{\phi(\xi)} \frac{\partial^2 \phi(\xi)}{\partial \xi^2} - A_1^2 = \frac{1}{a(\tau)} \frac{\partial a(\tau)}{\partial \tau} = -\lambda^2 \tag{A.79}$$

results in

$$\frac{d^2 \phi(\xi)}{d\xi^2} + (\lambda^2 - A_1^2)\phi(\xi) = 0. \tag{A.80}$$

The general solution is

$$\phi(\xi) = c_2 \cos(\sqrt{\lambda^2 - A_1^2}\xi) + c_3 \sin(\sqrt{\lambda^2 - A_1^2}\xi). \tag{A.81}$$

Differentiate

$$\frac{d\phi(\xi)}{d\xi} = -c_2\sqrt{\lambda^2 - A_1^2}\sin(\sqrt{\lambda^2 - A_1^2}\xi) + c_3\sqrt{\lambda^2 - A_1^2}\cos(\sqrt{\lambda^2 - A_1^2}\xi) \tag{A.82}$$

Apply the boundary condition at $\xi = 0$

$$c_3 = 0. \tag{A.83}$$

Apply the boundary condition at $\xi = 1$,

$$0 = -c_2\sqrt{\lambda^2 - A_1^2}\sin(\sqrt{\lambda^2 - A_1^2}) \tag{A.84}$$

$c_2 = 0$ gives the trivial solution and thus $\sin(\sqrt{\lambda^2 - A_1^2}) = 0$ must be true, which means

$$\sqrt{\lambda^2 - A_1^2} = n\pi \tag{A.85}$$

and the separation constant is

$$\lambda = \sqrt{(n\pi)^2 + A_1^2}. \tag{A.86}$$

The spatial eigenfunction is

$$\phi_n(\xi) = \cos(n\pi\xi) \tag{A.87}$$

and the transient temperature profile is

$$\theta_1 = \sum_{n=0}^{\infty} \phi_n(\xi) a_n(\tau) \tag{A.88}$$

Eigenfunction expansion of $g(\xi, \tau)$

$$g(\xi, \tau) = \sum_{n=0}^{\infty} G_n(\tau)\phi_n(\xi) \tag{A.89}$$

Integrate both side of the equation

$$\int_0^1 g(\xi, \tau)\cos(m\pi\xi)d\xi = \sum_{n=0}^{\infty} G_n(\tau)\int_0^1 \cos(n\pi\xi)\cos(m\pi\xi)d\xi. \tag{A.90}$$

Note that

$$\int_0^1 \cos(n\pi\xi)\cos(m\pi\xi)d\xi = \begin{cases} \frac{1}{2} & \text{if } n = m \\ 1 & \text{if } n = m = 0 \\ 0 & \text{if } n \neq m \end{cases} \tag{A.91}$$

and solve for the expansion coefficient

$$G_n(\tau) = 2\int_0^1 g(\xi, \tau)\cos(n\pi\xi)d\xi. \tag{A.92}$$

Note that for $n = 0$

$$G_0(\tau) = \int_0^1 g(\xi, \tau)d\xi. \tag{A.93}$$

Substitute into governing equation

$$\sum_{n=0}^{\infty}\frac{d^2\phi_n(\xi)}{d\xi^2}a_n(\tau)-A_1^2\sum_{n=0}^{\infty}\phi_n(\xi)a_n(\tau)=\sum_{n=0}^{\infty}\phi_n(\xi)\frac{da_n(\tau)}{d\tau}+\sum_{n=0}^{\infty}G_n(\tau)\phi_n(\xi) \tag{A.94}$$

and note that $\frac{d^2\phi_n(\xi)}{d\xi^2}=-(\lambda^2-A_1^2)\phi(\xi)$,

$$-\sum_{n=0}^{\infty}(\lambda^2-A_1^2)\phi_n(\xi)a_n(\tau)-A_1^2\sum_{n=0}^{\infty}\phi_n(\xi)a_n(\tau)=\sum_{n=0}^{\infty}\phi_n(\xi)\frac{da_n(\tau)}{d\tau}+\sum_{n=0}^{\infty}G_n(\tau)\phi_n(\xi) \tag{A.95}$$

$$\sum_{n=0}^{\infty}\Big[\frac{da_n(\tau)}{d\tau}+\lambda^2a_n(\tau)\Big]\phi_n(\xi)=-\sum_{n=0}^{\infty}G_n(\tau)\phi_n(\xi) \tag{A.96}$$

$$\frac{da_n(\tau)}{d\tau}+\lambda^2a_n(\tau)=-G_n(\tau) \tag{A.97}$$

Solve using the integrating factor $e^{\lambda^2\tau}$

$$e^{\lambda^2\tau}\big[\frac{da_n(\tau)}{d\tau}+\lambda^2a_n(\tau)\big]=-G_n(\tau)e^{\lambda^2\tau} \tag{A.98}$$

$$\frac{d}{d\tau}\big[e^{\lambda^2\tau}a_n(\tau)\big]=-G_n(\tau)e^{\lambda^2\tau} \tag{A.99}$$

Integrate both sides

$$e^{\lambda^2\tau}a_n(\tau)+C_n=-\int_0^{\tau}G_n(\tau')e^{\lambda^2\tau'}d\tau' \tag{A.100}$$

$$a_n(\tau)=e^{-\lambda^2\tau}[-C_n-\int_0^{\tau}G_n(\tau')e^{\lambda^2\tau'}d\tau'] \tag{A.101}$$

Sub into Eqn. A.88 and apply the initial condition

$$\theta_0=\sum_{n=0}^{\infty}\Big[-C_n\Big]\cos(n\pi\xi) \tag{A.102}$$

Integrate both side of the equation

$$\int_0^1\theta_0\cos(m\pi\xi)d\xi=-\sum_{n=0}^{\infty}C_n\int_0^1\cos(n\pi\xi)\cos(m\pi\xi)d\xi \tag{A.103}$$

and again note that

$$\int_0^1 \cos(n\pi\xi)\cos(m\pi\xi)d\xi = \begin{cases} \frac{1}{2} & \text{if } n = m \\ 1 & \text{if } n = m = 0 \\ 0 & \text{if } n \neq m \end{cases} \cdot \tag{A.104}$$

$$C_n = -2\theta_0 \int_0^1 \cos(n\pi\xi)d\xi \tag{A.105}$$

$$C_n = 0 \tag{A.106}$$

Except for $C_0 = -\theta_0$. The temperature profile is now

$$\theta_1 = \sum_{n=0}^{\infty} \cos(n\pi\xi)e^{-((n\pi)^2+A_1^2)\tau}\Big[-C_n - \int_0^{\tau} G_n(\tau')e^{((n\pi)^2+A_1^2)\tau'}d\tau'\Big] \tag{A.107}$$

pulling out the summation at $n = 0$

$$\theta_1 = e^{-A_1^2\tau}\Big[-C_0 - \int_0^{\tau} G_0(\tau')e^{A_1^2\tau'}d\tau'\Big] - \sum_{n=1}^{\infty}\cos(n\pi\xi)e^{-((n\pi)^2+A_1^2)\tau}\Big[\int_0^{\tau} G_n(\tau')e^{((n\pi)^2+A_1^2)\tau'}d\tau'\Big] \tag{A.108}$$

and substitute in all coefficients

$$\begin{aligned} \theta_1 = e^{-A_1^2\tau}\Big[\theta_0 + \int_0^{\tau}\int_0^1 (A_1^2\theta_2(\xi,\tau) + \tilde{q}(\xi,\tau))d\xi e^{A_1^2\tau'}d\tau'\Big] \\ + 2\sum_{n=1}^{\infty}\cos(n\pi\xi)e^{-((n\pi)^2+A_1^2)\tau}\Big[\int_0^{\tau}\int_0^1 (A_1^2\theta_2(\xi,\tau) \\ + \tilde{q}(\xi,\tau))\cos(n\pi\xi)d\xi e^{((n\pi)^2+A_1^2)\tau'}d\tau'\Big] \end{aligned} \tag{A.109}$$

A.2.3.2 Solution for Solid 2

The governing equation to be solved is

$$\frac{\partial^2\theta_2(\xi,\tau)}{\partial\xi^2} - A_2^2\theta_2(\xi,\tau) = \frac{1}{\kappa}\frac{\partial\theta_2(\xi,\tau)}{\partial\tau} - A_2^2\theta_1(\xi,\tau) \tag{A.110}$$

Let $g(\xi,\tau) = -A_2^2\theta_1(\xi,\tau)$

$$\frac{\partial^2\theta_{2A}(\xi,\tau)}{\partial\xi^2} - A_2^2\theta_{2A}(\xi,\tau) = \frac{1}{\kappa}\frac{\partial\theta_{2A}(\xi,\tau)}{\partial\tau} + g(\xi,\tau) \tag{A.111}$$

The boundary conditions are

$$\left.\frac{\partial\theta_2}{\partial\xi}\right|_{\xi=0} = 0 \tag{A.112}$$

$$\theta_2(1,\tau) = 0 \tag{A.113}$$

$$\theta_2(\xi,0) = \theta_0 \tag{A.114}$$

First, look at the homogeneous case to find the eigenfunctions that satisfy the homogeneous boundary conditions.

$$\frac{\partial^2\theta_{2h}(\xi,\tau)}{\partial\xi^2} - A_2^2\theta_{2h}(\xi,\tau) = \frac{1}{\kappa}\frac{\partial\theta_{2h}(\xi,\tau)}{\partial\tau} \tag{A.115}$$

with boundary conditions

$$\left.\frac{\partial\theta_{2Ah}}{\partial\xi}\right|_{\xi=0} = 0 \tag{A.116}$$

$$\theta_{2Ah}(1,\tau) = 0 \tag{A.117}$$

$$\theta_{2Ah}(\xi,0) = \theta_0 - \theta_{2B}(\xi) \tag{A.118}$$

Using separation of variables

$$\frac{\partial^2\phi(\xi)}{\partial\xi^2}a(\tau) - A_2^2\phi(\xi)a(\tau) = \frac{\partial a(\tau)}{\partial\tau}\phi(\xi) \tag{A.119}$$

$$\frac{1}{\phi(\xi)}\frac{\partial^2\phi(\xi)}{\partial\xi^2} - A_2^2 = \frac{1}{a(\tau)}\frac{\partial a(\tau)}{\partial\tau} = -\lambda^2 \tag{A.120}$$

$$\frac{d^2\phi(\xi)}{d\xi^2} + (\lambda^2 - A_2^2)\phi(\xi) = 0 \tag{A.121}$$

$$\phi(\xi) = c_2\cos(\sqrt{\lambda^2 - A_2^2}\xi) + c_3\sin(\sqrt{\lambda^2 - A_2^2}\xi) \tag{A.122}$$

$$\frac{d\phi(\xi)}{d\xi} = -c_2\sqrt{\lambda^2 - A_2^2}\sin(\sqrt{\lambda^2 - A_2^2}\xi) + c_3\sqrt{\lambda^2 - A_2^2}\cos(\sqrt{\lambda^2 - A_2^2}\xi) \tag{A.123}$$

Apply the boundary condition at $\xi = 0$

$$c_3 = 0 \tag{A.124}$$

Apply the boundary condition at $\xi = 1$

$$0 = c_2 \cos(\sqrt{\lambda^2 - A_2^2}) \tag{A.125}$$

$c_2 = 0$ gives the trivial solution and thus $\cos(\sqrt{\lambda^2 - A_2^2}) = 0$.

$$\sqrt{\lambda^2 - A_2^2} = \frac{(2n+1)\pi}{2} \tag{A.126}$$

$$\lambda = \sqrt{(\frac{(2n+1)\pi}{2})^2 + A_2^2} \tag{A.127}$$

$$\phi_n(\xi) = \cos(\frac{(2n+1)\pi}{2}\xi) \tag{A.128}$$

$$\theta_{2A} = \sum_{n=0}^{\infty} \phi_n(\xi) a_n(\tau) \tag{A.129}$$

Eigenfunction expansion of $g(\xi,\tau)$

$$g(\xi,\tau) = \sum_{n=0}^{\infty} G_n(\tau)\phi_n(\xi) \tag{A.130}$$

Integrate both side

$$\int_0^1 g(\xi,\tau)\cos(\frac{(2m+1)\pi}{2}\xi)d\xi = \sum_{n=0}^{\infty} G_n(\tau)\int_0^1 \cos(\frac{(2n+1)\pi}{2}\xi)\cos(\frac{(2m+1)\pi}{2}\xi)d\xi \tag{A.131}$$

noting that

$$\int_0^1 \cos(\frac{(2n+1)\pi}{2}\xi)\cos(\frac{(2m+1)\pi}{2}\xi)d\xi = \begin{cases} \frac{1}{2} & \text{if } n = m \\ 0 & \text{if } n \neq m \end{cases} \tag{A.132}$$

$$\int_0^1 g(\xi,\tau)\cos(\frac{(2n+1)\pi}{2}\xi)d\xi = G_n(\tau)\frac{1}{2} \tag{A.133}$$

$$G_n(\tau) = 2\int_0^1 g(\xi,\tau)\cos(\frac{(2n+1)\pi}{2}\xi)d\xi \tag{A.134}$$

substitute into the governing equation

$$\sum_{n=0}^{\infty}\frac{d^2\phi_n(\xi)}{d\xi^2}a_n(\tau) - A_1^2\sum_{n=0}^{\infty}\phi_n(\xi)a_n(\tau) = \frac{1}{\kappa}\sum_{n=0}^{\infty}\phi_n(\xi)\frac{da_n(\tau)}{d\tau} + \sum_{n=0}^{\infty}G_n(\tau)\phi_n(\xi) \tag{A.135}$$

Note $\frac{d^2\phi_n(\xi)}{d\xi^2} = -(\lambda^2 - A_1^2)\phi(\xi)$

$$-\sum_{n=0}^{\infty}(\lambda^2 - A_1^2)\phi_n(\xi)a_n(\tau) - A_1^2\sum_{n=0}^{\infty}\phi_n(\xi)a_n(\tau) = \frac{1}{\kappa}\sum_{n=0}^{\infty}\phi_n(\xi)\frac{da_n(\tau)}{d\tau} + \sum_{n=0}^{\infty}G_n(\tau)\phi_n(\xi) \tag{A.136}$$

$$\sum_{n=0}^{\infty}\Big[\frac{1}{\kappa}\frac{da_n(\tau)}{d\tau} + \lambda^2 a_n(\tau)\Big]\phi_n(\xi) = -\sum_{n=0}^{\infty}G_n(\tau)\phi_n(\xi) \tag{A.137}$$

$$\frac{1}{\kappa}\frac{da_n(\tau)}{d\tau} + \lambda^2 a_n(\tau) = -G_n(\tau) \tag{A.138}$$

$$\frac{da_n(\tau)}{d\tau} + \kappa\lambda^2 a_n(\tau) = -\kappa G_n(\tau) \tag{A.139}$$

Solve using the integrating factor $e^{\kappa\lambda^2\tau}$

$$e^{\kappa\lambda^2\tau}\big[\frac{da_n(\tau)}{d\tau} + \kappa\lambda^2 a_n(\tau)\big] = -\kappa G_n(\tau)e^{\kappa\lambda^2\tau} \tag{A.140}$$

$$\frac{d}{d\tau}\big[e^{\kappa\lambda^2\tau}a_n(\tau)\big] = -\kappa G_n(\tau)e^{\kappa\lambda^2\tau} \tag{A.141}$$

Integrate both sides

$$e^{\kappa\lambda^2\tau}a_n(\tau) + C_n = -\kappa\int_0^{\tau}G_n(\tau')e^{\kappa\lambda^2\tau'}d\tau' \tag{A.142}$$

$$a_n(\tau) = e^{-\kappa\lambda^2\tau}[-C_n - \kappa\int_0^{\tau}G_n(\tau')e^{\kappa\lambda^2\tau'}d\tau'] \tag{A.143}$$

Substitute into Eqn. A.129 and apply initial condition

$$\theta_0 - \theta_{2B}(\xi) = \sum_{n=0}^{\infty}\Big[-C_n\Big]\cos(\frac{(2n+1)\pi}{2}\xi) \tag{A.144}$$

$$\int_0^1 \left[\theta_0 - \theta_{2B}(\xi)\right] \cos(\frac{(2m+1)\pi}{2}\xi) d\xi = -\sum_{n=0}^{\infty} C_n \int_0^1 \cos(\frac{(2n+1)\pi}{2}\xi) \cos(\frac{(2m+1)\pi}{2}\xi) d\xi \tag{A.145}$$

$$\int_0^1 \cos(\frac{(2n+1)\pi}{2}\xi) \cos(\frac{(2m+1)\pi}{2}\xi) d\xi = \begin{cases} \frac{1}{2} & \text{if } n = m \\ 0 & \text{if } n \neq m \end{cases} \tag{A.146}$$

$$C_n = -2\int_0^1 [\theta_0 - \theta_{2B}(\xi)] \cos(\frac{(2n+1)\pi}{2}\xi) d\xi \tag{A.147}$$

Integrating and some arranging results in

$$C_n = -\frac{4(-1)^n}{(2n+1)\pi}[\theta_0 - \theta_L \frac{(2n+1)^2\pi^2}{4A_2^2 + (2n+1)^2\pi^2}] \tag{A.148}$$

$$\theta_{2A} = \sum_{n=1}^{\infty} \cos(\frac{(2n+1)\pi}{2}\xi) e^{-((\frac{(2n+1)\pi}{2})^2 + A_2^2)\kappa\tau} \left[-C_n - \kappa \int_0^{\tau} G_n(\tau') e^{((\frac{(2n+1)\pi}{2})^2 + A_2^2)\kappa\tau'} d\tau' \right] \tag{A.149}$$

Substitute in the coefficients

$$\begin{aligned} \theta_{2A} = \sum_{n=0}^{\infty} \cos(\frac{(2n+1)\pi}{2}\xi) e^{-((\frac{(2n+1)\pi}{2})^2 + A_2^2)\kappa\tau} \Big[\frac{4(-1)^n}{(2n+1)\pi}[\theta_0 - \theta_L \frac{(2n+1)^2\pi^2}{4A_2^2 + (2n+1)^2\pi^2}] \\ - 2\kappa \int_0^{\tau} \int_0^1 g(\xi,\tau) \cos(\frac{(2n+1)\pi}{2}\xi) d\xi e^{((\frac{(2n+1)\pi}{2})^2 + A_2^2)\kappa\tau'} d\tau' \Big] \end{aligned} \tag{A.150}$$

The temperature profile is

$$\begin{aligned} \theta_2 = \sum_{n=0}^{\infty} \cos(\frac{(2n+1)\pi}{2}\xi) e^{-((\frac{(2n+1)\pi}{2})^2 + A_2^2)\kappa\tau} \Big[\frac{4(-1)^n}{(2n+1)\pi}\theta_0 \\ + 2\kappa A_2^2 \int_0^{\tau} \int_0^1 \theta_1(\xi,\tau) \cos(\frac{(2n+1)\pi}{2}\xi) d\xi e^{((\frac{(2n+1)\pi}{2})^2 + A_2^2)\kappa\tau'} d\tau' \Big]. \end{aligned} \tag{A.151}$$

A.3 One-Dimensional Conjugate Heat Transfer Between a Fluid and a Solid

A.3.1 Integral Equation Method Solution

The governing equation to be solved is

$$\frac{\partial^2 \theta_2(\xi)}{\partial \xi^2} - P_e \frac{\partial \theta_2(\xi)}{\partial \xi} = -A_2^2 \tilde{h}(\xi)(\theta_1(\xi) - \theta_2(\xi)) \tag{A.152}$$

with boundary conditions

$$\theta_2(0) = \theta_0 \tag{A.153}$$

$$\theta_2(1) = \theta_L \tag{A.154}$$

where

$$\theta_L = \theta_0 + \frac{A_2^2}{A_1^2 P_e} \int_0^1 \tilde{q}(\xi) d\xi. \tag{A.155}$$

Substituting in $\psi(\xi) = \frac{d\theta_2(\xi)}{d\xi}$, the equation becomes

$$\frac{d\psi(\xi)}{d\xi} - P_e \psi(\xi) = -A_2^2 \tilde{h}(\xi)\big(\theta_1(\xi) - \theta_2(\xi)\big). \tag{A.156}$$

The differential equation can be solved using an integrating factor $e^{\int_0^\xi -P_e d\xi} = e^{-P_e \xi}$. Multiply both side of the equation by $e^{-P_e \xi}$

$$e^{-P_e \xi} \frac{d\psi(\xi)}{d\xi} - e^{-P_e \xi} P_e \psi(\xi) = -e^{-P_e \xi} A_2^2 \tilde{h}(\xi)\big(\theta_1(\xi) - \theta_2(\xi)\big). \tag{A.157}$$

Note the left side of the equation can be rewritten

$$\frac{d}{d\xi}(e^{-P_e \xi} \psi(\xi)) = -e^{-P_e \xi} A_2^2 \tilde{h}(\xi)\big(\theta_1(\xi) - \theta_2(\xi)\big). \tag{A.158}$$

Integrating both side of the equation,

$$\int_0^\xi \frac{d}{d\xi'}(e^{-P_e \xi'} \psi(\xi')) d\xi' = -\int_0^\xi \Big[e^{-P_e \xi'} A_2^2 \tilde{h}(\xi')\big(\theta_1(\xi') - \theta_2(\xi')\big)\Big] d\xi' \tag{A.159}$$

evaluating the left side

$$e^{-P_e \xi} \psi(\xi) - c_1 = -\int_0^\xi \Big[e^{-P_e \xi'} A_2^2 \tilde{h}(\xi')\big(\theta_1(\xi') - \theta_2(\xi')\big)\Big] d\xi' \tag{A.160}$$

and solving for $\psi(\xi)$ results in

$$\psi(\xi) = e^{P_e \xi} \left[c_1 - \int_0^\xi \Big[e^{-P_e \xi'} A_2^2 \tilde{h}(\xi')\big(\theta_1(\xi') - \theta_2(\xi')\big)\Big] d\xi'\right]. \tag{A.161}$$

Reverse substitute $\psi(\xi) = \frac{d\theta_2(\xi)}{d\xi}$ into the equation

$$\frac{d\theta_2(\xi)}{d\xi} = e^{P_e\xi}\left[c_1 - \int_0^{\xi}\left[e^{-P_e\xi'}A_2^2\tilde{h}(\xi')\big(\theta_1(\xi') - \theta_2(\xi')\big)\right]d\xi'\right] \tag{A.162}$$

and integrate

$$\theta_2(\xi) = c_2 + c_1\frac{1}{P_e}[e^{P_e\xi} - 1] - \int_0^{\xi}\left[e^{P_e\xi}\int_0^{\xi}\left[e^{-P_e\xi'}A_2^2\tilde{h}(\xi')\big(\theta_1(\xi') - \theta_2(\xi')\big)\right]d\xi'\right]d\xi \tag{A.163}$$

Let $F(\xi) = e^{P_e\xi}\int_0^{\xi}\left[e^{-P_e\xi'}A_2^2\tilde{h}(\xi')\big(\theta_1(\xi') - \theta_2(\xi')\big)\right]d\xi'$

$$\theta_2(\xi) = c_2 + c_1\frac{1}{P_e}[e^{P_e\xi} - 1] - \int_0^{\xi}F(\xi)d\xi \tag{A.164}$$

Apply the boundary condition at $\xi = 0$,

$$c_2 = \theta_0 \tag{A.165}$$

and the boundary condition at $\xi = 1$,

$$c_1 = \frac{1}{\frac{1}{P_e}[e^{P_e} - 1]}\left[\theta_L - \theta_0 + \int_0^1 F(\xi)d\xi\right]. \tag{A.166}$$

The temperature profile becomes

$$\theta_2(\xi) = \theta_0 + \frac{[e^{P_e\xi} - 1]}{[e^{P_e} - 1]}\left[\theta_L - \theta_0 + \int_0^1 F(\xi)d\xi\right] - \int_0^{\xi}F(\xi)d\xi \tag{A.167}$$

and substituting in θ_L and $F(\xi)$ results in

$$\begin{aligned}\theta_2(\xi) = \theta_0 + \frac{(e^{P_e\xi} - 1)}{(e^{P_eL} - 1)}&\left[\frac{A_2^2\int_0^1\tilde{q}(\xi)d\xi}{A_1^2P_e}\right.\\ &\left.+\int_0^1 e^{P_e\xi}\int_0^{\xi}\left[e^{-P_e\xi'}A_2^2\tilde{h}(\xi')\big(\theta_1(\xi') - \theta_2(\xi')\big)\right]d\xi'd\xi\right]\\ &-\int_0^{\xi}e^{P_e\xi}\int_0^{\xi}\left[e^{-P_e\xi'}A_2^2\tilde{h}(\xi')\big(\theta_1(\xi') - \theta_2(\xi')\big)\right]d\xi'd\xi\end{aligned} \tag{A.168}$$

A.3.2 Generalized Bessel Method Solution

The governing equation to be solved is

$$\frac{d^2\theta_2(\xi)}{d\xi^2} - P_e\frac{\partial\theta_2(\xi)}{\partial\xi} - A_2^2\xi^{-\frac{1}{2}}\theta_2(\xi) = -A_2^2\xi^{-\frac{1}{2}}\theta_1(\xi) \tag{A.169}$$

with boundary conditions

$$\theta_2(0) = \theta_0 \tag{A.170}$$

$$\theta_2(1) = \theta_L \tag{A.171}$$

where

$$\theta_L = \theta_0 + \frac{A_2^2\int_0^1 \tilde{q}(\xi)d\xi}{A_1^2 P_e}. \tag{A.172}$$

The solution to the differential equation is the sum of the homogeneous and particular solutions

$$\theta_2 = \theta_{2h} + \theta_{2p}. \tag{A.173}$$

The homogeneous equation is

$$\frac{d^2\theta_2(\xi)}{d\xi^2} - P_e\frac{\partial\theta_2(\xi)}{\partial\xi} - A_2^2\xi^{-\frac{1}{2}}\theta_2(\xi) = 0 \tag{A.174}$$

Using the generalized Bessel equation

$$\frac{d^2R}{d\xi^2} + \left[\frac{1-2m}{\xi} - 2\alpha\right]\frac{dR}{d\xi} + \left[p^2a^2\xi^{2p-2} + \alpha^2 + \frac{\alpha(2m-1)}{\xi} + \frac{m^2-p^2\nu^2}{\xi^2}\right]R = 0 \tag{A.175}$$

with solution

$$R = \xi^m e^{\alpha\xi}\left[c_1 J_\nu(a\xi^p) + c_2 Y_\nu(a\xi^p)\right] \tag{A.176}$$

or if ν is not an integer

$$R = \xi^m e^{\alpha\xi}\left[c_1 J_\nu(a\xi^p) + c_2 J_{-\nu}(a\xi^p)\right] \tag{A.177}$$

where the coefficients are

$$m = \frac{1}{2} \tag{A.178}$$
$$\alpha = \frac{P_e}{2} \tag{A.179}$$
$$p = \frac{3}{4} \tag{A.180}$$
$$\nu = \frac{2}{3} \tag{A.181}$$
$$a = \frac{4}{3} i \sqrt{(\frac{P_e}{2})^2 \xi^{\frac{1}{2}} + A_2^2}. \tag{A.182}$$

The general solution is

$$\theta_{1h} = \xi^{\frac{1}{2}} e^{\frac{P_e}{2}\xi} \left[c_1 J_{\frac{2}{3}} \left(\frac{4}{3} i \sqrt{(\frac{P_e}{2})^2 \xi^{\frac{1}{2}} + A_2^2} \xi^{\frac{3}{4}} \right) + c_2 J_{-\frac{2}{3}} \left(\frac{4}{3} i \sqrt{(\frac{P_e}{2})^2 \xi^{\frac{1}{2}} + A_2^2} \xi^{\frac{3}{4}} \right) \right] \tag{A.183}$$

or

$$\theta_{1h} = \xi^{\frac{1}{2}} e^{\frac{P_e}{2}\xi} \left[c_1 I_{\frac{2}{3}} \left(\frac{4}{3} \sqrt{(\frac{P_e}{2})^2 \xi^{\frac{1}{2}} + A_2^2} \xi^{\frac{3}{4}} \right) + c_2 I_{-\frac{2}{3}} \left(\frac{4}{3} \sqrt{(\frac{P_e}{2})^2 \xi^{\frac{1}{2}} + A_2^2} \xi^{\frac{3}{4}} \right) \right]. \tag{A.184}$$

Let

$$B_2(\xi) = \frac{4}{3} \sqrt{(\frac{P_e}{2})^2 \xi^{\frac{1}{2}} + A_2^2} \tag{A.185}$$

$$\theta_{1h} = \xi^{\frac{1}{2}} e^{\frac{P_e}{2}\xi} \left[c_1 I_{\frac{2}{3}} \left(B_2(\xi) \xi^{\frac{3}{4}} \right) + c_2 I_{-\frac{2}{3}} \left(B_2(\xi) \xi^{\frac{3}{4}} \right) \right] \tag{A.186}$$

The Wronskian is

$$W = -\frac{\sqrt{3} e^{P_e \xi}}{\pi} \frac{(P_e^2 \xi^{\frac{1}{2}} + 3A_2^2)}{(P_e^2 \xi^{\frac{1}{2}} + 4A_2^2)}. \tag{A.187}$$

Using the method of variation of parameters, the particular solution is

$$\begin{aligned} \theta_{2p} = & -\frac{A_2^2 \pi}{\sqrt{3}} \xi^{\frac{1}{2}} e^{\frac{P_e}{2}\xi} I_{\frac{2}{3}} \left(B_2(\xi) \xi^{\frac{3}{4}} \right) \int_0^{\xi} e^{-\frac{P_e}{2}\xi'} I_{-\frac{2}{3}} \left(B_2(\xi) \xi'^{\frac{3}{4}} \right) \theta_1(\xi) \frac{(P_e^2 \xi'^{\frac{1}{2}} + 4A_2^2)}{(P_e^2 \xi'^{\frac{1}{2}} + 3A_2^2)} d\xi' \\ & + \frac{A_2^2 \pi}{\sqrt{3}} \xi^{\frac{1}{2}} e^{\frac{P_e}{2}\xi} I_{-\frac{2}{3}} \left(B_2(\xi) \xi^{\frac{3}{4}} \right) \int_0^{\xi} e^{-\frac{P_e}{2}\xi'} I_{\frac{2}{3}} \left(B_2(\xi) \xi'^{\frac{3}{4}} \right) \theta_1(\xi) \frac{(P_e^2 \xi'^{\frac{1}{2}} + 4A_2^2)}{(P_e^2 \xi'^{\frac{1}{2}} + 3A_2^2)} d\xi' \end{aligned} \tag{A.188}$$

and thus the temperature profile is

$$\theta_2 = \xi^{\frac{1}{2}} e^{\frac{P_e}{2}\xi}\left[c_1 I_{\frac{2}{3}}\left(B_2(\xi)\xi^{\frac{3}{4}}\right) + c_2 I_{-\frac{2}{3}}\left(B_2(\xi)\xi^{\frac{3}{4}}\right)\right] \tag{A.189}$$
$$- \frac{A_2^2\pi}{\sqrt{3}}\xi^{\frac{1}{2}} e^{\frac{P_e}{2}\xi} I_{\frac{2}{3}}\left(B_2(\xi)\xi^{\frac{3}{4}}\right)\int_0^{\xi} e^{-\frac{P_e}{2}\xi'} I_{-\frac{2}{3}}\left(B_2(\xi)\xi'^{\frac{3}{4}}\right)\theta_1(\xi)\frac{(P_e^2\xi'^{\frac{1}{2}}+4A_2^2)}{(P_e^2\xi'^{\frac{1}{2}}+3A_2^2)}d\xi'$$
$$+ \frac{A_2^2\pi}{\sqrt{3}}\xi^{\frac{1}{2}} e^{\frac{P_e}{2}\xi} I_{-\frac{2}{3}}\left(B_2(\xi)\xi^{\frac{3}{4}}\right)\int_0^{\xi} e^{-\frac{P_e}{2}\xi'} I_{\frac{2}{3}}\left(B_2(\xi)\xi'^{\frac{3}{4}}\right)\theta_1(\xi)\frac{(P_e^2\xi'^{\frac{1}{2}}+4A_2^2)}{(P_e^2\xi'^{\frac{1}{2}}+3A_2^2)}d\xi'$$

Apply the boundary condition at $\xi = 0$

$$\theta_0 = \xi^{\frac{1}{2}} e^{\frac{P_e}{2}\xi} c_2 I_{-\frac{2}{3}}\left(B_2(\xi)\xi^{\frac{3}{4}}\right) \tag{A.190}$$

noting that

$$\lim_{\xi\to 0}\xi^{\frac{1}{2}} e^{\frac{P_e}{2}\xi} I_{\frac{2}{3}}\left(B_2(\xi)\xi^{\frac{3}{4}}\right) \longrightarrow 0 \tag{A.191}$$

$$\lim_{\xi\to 0}\xi^{\frac{1}{2}} e^{\frac{P_e}{2}\xi} I_{-\frac{2}{3}}\left(B_2(\xi)\xi^{\frac{3}{4}}\right) \longrightarrow \frac{3^{\frac{7}{6}}\Gamma(\frac{2}{3})}{2^{\frac{5}{3}}A_2^{\frac{2}{3}}\pi} \tag{A.192}$$

and thus

$$c_2 = \frac{2^{\frac{5}{3}}A_2^{\frac{2}{3}}\pi}{3^{\frac{7}{6}}\Gamma(\frac{2}{3})}\theta_0. \tag{A.193}$$

Apply the boundary condition at $\xi = 1$

$$\theta_L = e^{\frac{P_e}{2}}\left[c_1 I_{\frac{2}{3}}\left(B_2(\xi)\right) + c_2 I_{-\frac{2}{3}}\left(B_2(\xi)\right)\right] \tag{A.194}$$
$$- \frac{A_2^2\pi}{\sqrt{3}} e^{\frac{P_e}{2}} I_{\frac{2}{3}}\left(B_2(\xi)\right)\int_0^{1} e^{-\frac{P_e}{2}\xi'} I_{-\frac{2}{3}}\left(B_2(\xi)\xi'^{\frac{3}{4}}\right)\theta_1(\xi)\frac{(P_e^2\xi'^{\frac{1}{2}}+4A_2^2)}{(P_e^2\xi'^{\frac{1}{2}}+3A_2^2)}d\xi'$$
$$+ \frac{A_2^2\pi}{\sqrt{3}} e^{\frac{P_e}{2}} I_{-\frac{2}{3}}\left(B_2(\xi)\right)\int_0^{1} e^{-\frac{P_e}{2}\xi'} I_{\frac{2}{3}}\left(B_2(\xi)\xi'^{\frac{3}{4}}\right)\theta_1(\xi)\frac{(P_e^2\xi'^{\frac{1}{2}}+4A_2^2)}{(P_e^2\xi'^{\frac{1}{2}}+3A_2^2)}d\xi'$$

and solve for c_1

$$c_1 = \frac{\theta_L}{e^{\frac{P_e}{2}} I_{\frac{2}{3}}\Big(B_2(\xi)\Big)} - c_2 \frac{I_{-\frac{2}{3}}\Big(B_2(\xi)\Big)}{I_{\frac{2}{3}}\Big(B_2(\xi)\Big)} + \frac{A_2^2 \pi}{\sqrt{3}} \int_0^1 e^{-\frac{P_e}{2}\xi'} I_{-\frac{2}{3}}\Big(B_2(\xi){\xi'}^{\frac{3}{4}}\Big) \theta_1(\xi) \frac{(P_e^2 {\xi'}^{\frac{1}{2}} + 4A_2^2)}{(P_e^2 {\xi'}^{\frac{1}{2}} + 3A_2^2)} d\xi' \tag{A.195}$$

$$- \frac{A_2^2 \pi}{\sqrt{3}} \frac{I_{-\frac{2}{3}}\Big(B_2(\xi)\Big)}{I_{\frac{2}{3}}\Big(B_2(\xi)\Big)} \int_0^1 e^{-\frac{P_e}{2}\xi'} I_{\frac{2}{3}}\Big(B_2(\xi){\xi'}^{\frac{3}{4}}\Big) \theta_1(\xi) \frac{(P_e^2 {\xi'}^{\frac{1}{2}} + 4A_2^2)}{(P_e^2 {\xi'}^{\frac{1}{2}} + 3A_2^2)} d\xi'$$

the temperature profile is

$$\begin{aligned}
\theta_2 = {} & \xi^{\frac{1}{2}} e^{\frac{P_e}{2}\xi} \left[c_1 I_{\frac{2}{3}}\Big(B_2(\xi)\xi^{\frac{3}{4}}\Big) + c_2 I_{-\frac{2}{3}}\Big(B_2(\xi)\xi^{\frac{3}{4}}\Big) \right] \\
& - \frac{A_2^2 \pi}{\sqrt{3}} \xi^{\frac{1}{2}} e^{\frac{P_e}{2}\xi} I_{\frac{2}{3}}\Big(B_2(\xi)\xi^{\frac{3}{4}}\Big) \int_0^{\xi} e^{-\frac{P_e}{2}\xi'} I_{-\frac{2}{3}}\Big(B_2(\xi){\xi'}^{\frac{3}{4}}\Big) \theta_1(\xi) \frac{(P_e^2 {\xi'}^{\frac{1}{2}} + 4A_2^2)}{(P_e^2 {\xi'}^{\frac{1}{2}} + 3A_2^2)} d\xi' \\
& + \frac{A_2^2 \pi}{\sqrt{3}} \xi^{\frac{1}{2}} e^{\frac{P_e}{2}\xi} I_{-\frac{2}{3}}\Big(B_2(\xi)\xi^{\frac{3}{4}}\Big) \int_0^{\xi} e^{-\frac{P_e}{2}\xi'} I_{\frac{2}{3}}\Big(B_2(\xi){\xi'}^{\frac{3}{4}}\Big) \theta_1(\xi) \frac{(P_e^2 {\xi'}^{\frac{1}{2}} + 4A_2^2)}{(P_e^2 {\xi'}^{\frac{1}{2}} + 3A_2^2)} d\xi'
\end{aligned} \tag{A.196}$$

APPENDIX B. 2-D PROBLEMS

B.1 Variable Coefficients in the Convective Boundary Condition

In two-dimensional problems the variable heat transfer coefficient appears in the boundary conditions rather than the governing equation as has been considered previously in the one-dimensional problems. The trouble encountered when solving these problems is when making use of the orthogonality of the eigenfunctions to find the Fourier coefficients when using separation of variables. For example, consider the solution of some partial differential equation to be of the form

$$T_1(x,y) = \sum_{n=1}^{\infty} B_n \phi_n(x) a_n(y) \tag{B.1}$$

with the eigenfunction

$$\phi_n(x) = \cos(n\pi x). \tag{B.2}$$

Assume the interface between two regions is represented by the convective boundary condition

$$\left.\frac{dT_1(x,y)}{dy}\right|_{y=0} + \frac{h(x)}{k} T_1(x,0) = \frac{h(x)}{k} T_2(x,0). \tag{B.3}$$

When applying the convective boundary condition, after all the other boundary conditions have been applied, the result is

$$\frac{h(x)}{k} T_2(x,0)) = \sum_{n=1}^{\infty} B_n \left(\frac{da_n(y)}{dy}\right)_{y=0} \phi_n + \frac{h(x)}{k} \sum_{n=1}^{\infty} B_n a_n(0) \phi_n \tag{B.4}$$

$$\frac{h(x)}{k} T_2(x,0)) = \sum_{n=1}^{\infty} B_n \left[\left(\frac{da_n(y)}{dy}\right)_{y=0} + \frac{h(x)}{k} a_n(0)\right] \cos(n\pi x) \tag{B.5}$$

Multiply all terms by $\cos(m\pi x)$ and integrate both side of the equation

$$\int_0^1 \frac{h(x)}{k} T_2(x,0)\cos(m\pi x)dx = \int_0^1 \sum_{n=1}^{\infty} B_n\Big[\Big(\frac{da_n(y)}{dy}\Big)_{y=0} + \frac{h(x)}{k} a_n(0)\Big]\cos(n\pi x)\cos(m\pi x)dx. \tag{B.6}$$

Moving the integral inside the summation and distributing to both terms

$$\begin{aligned}\int_0^1 \frac{h(x)}{k} T_2(x,0)\cos(m\pi x)dx = \sum_{n=1}^{\infty} B_n\Big[\Big(\frac{da_n(y)}{dy}\Big)_{y=0} \int_0^1 \cos(n\pi x)\cos(m\pi x)dx \\ + a_n(0)\int_0^1 \frac{h(x)}{k}\cos(n\pi x)\cos(m\pi x)dx\Big].\end{aligned} \tag{B.7}$$

Since cos is an orthogonal function the following is true

$$\int_0^1 \cos(\lambda_n x)\cos(\lambda_m x)dx = \begin{cases} \frac{1}{2} & \text{if } n = m \\ 0 & \text{if } n \neq m \end{cases} \tag{B.8}$$

and the equation becomes

$$\int_0^1 \frac{h(x)}{k} T_2(x,0)\cos(m\pi x)dx = \frac{B_n}{2}\frac{dY_n(y)}{dy}\Big|_{y=0} + \sum_{n=1}^{\infty} B_n a_n(0)\int_0^1 \frac{h(x)}{k}\cos(n\pi x)\cos(m\pi x)dx. \tag{B.9}$$

The $h(x)$ in the last term destroys the orthogonality of cos and B_n cannot be solved. The boundary condition bisection method used by [3] could possibly be a solution. The method takes advantage of the fact that a convective boundary condition can be dissected as a linear combination of a heat flux and temperature. In other words, the convective boundary condition can be replaced with either a flux or a temperature boundary condition that is equal to some arbitrary function that will be solved by substituting the solution into the original convective boundary condition. This method was not attempted during this work.

B.2 Orthogonality of the Generalized Bessel Solution

The Bessel function is orthogonal with the weight function $w(x) = x$. This results in the following relation being true

$$\int_0^1 xJ_\nu\left(\lambda_n x\right)J_\nu\left(\lambda_m x\right)dx = \begin{cases} \int_0^1 J_\nu\left(\lambda_n x\right)^2 dx & \text{if } n = m \\ 0 & \text{if } n \neq m \end{cases} \tag{B.10}$$

When separation of variables is used to solve the partial differential equation of a fully developed, two-dimensional fluid with neglected axial conduction, it is common to obtain an equation of the form

$$\frac{d\phi}{dy} + \lambda^2 f(y)\phi = 0 \tag{B.11}$$

where $f(y)$ is the fluid velocity profile. The generalized Bessel equation can be used to solve for the eigenfunctions, ϕ_n. For the case of a Couette flow bounded by a conjugate boundary on the bottom and an insulated boundary on top, more detail on the solution and process can be found in Appendix A, the eigenvalues, λ_n, are found from an equation of the form

$$0 = J_{-\frac{2}{3}}\left(\lambda_n\right) \tag{B.12}$$

The resulting eigenvalues are listed in Table B.1.

Table B.1: Eigenvalues for $0 = J_{-\frac{2}{3}}\left(\lambda_n\right)$

λ_0	λ_1	λ_2	λ_3	λ_4
1.243046	4.429121	7.579458	10.724747	13.868375

If the same weight function that is used for the regular Bessel functions orthogonality, $w(y) = y$, is used for the generalized Bessel solution, $y^{1/2}J_{-\frac{2}{3}}\left(\lambda_n y^{\frac{3}{2}}\right)$, then

$$\int_0^1 y^2 J_{-\frac{2}{3}}\left(\lambda_n y^{\frac{3}{2}}\right)J_{-\frac{2}{3}}\left(\lambda_m y^{\frac{3}{2}}\right)dy = \begin{cases} \int_0^1 J_{-\frac{2}{3}}\left(\lambda_n y\right)^2 dy & \text{if } n = m \\ 0 & \text{if } n \neq m \end{cases} \tag{B.13}$$

Table B.2 shows the results if the eigenvalues in Table B.1 are used in Eqn. B.13. The results behave as expected for orthogonal functions since λ_n is effectively zero everywhere except on the diagonal where $m = n$.

Table B.2: Values for $\int_0^1 y^2 J_{-\frac{2}{3}}\left(\lambda_n y^{\frac{3}{2}}\right) J_{-\frac{2}{3}}\left(\lambda_m y^{\frac{3}{2}}\right) dy$ using eigenvalues from Table B.1

	λ_0^2	λ_1^2	λ_2^2	λ_3^2	λ_4^2
λ_0^2	0.1637	-1.5162×10^{-8}	3.4191×10^{-9}	-2.8862×10^{-9}	2.1604×10^{-9}
λ_1^2	-1.5162×10^{-8}	0.0477	8.5324×10^{-9}	-2.0097×10^{-9}	8.2067×10^{-10}
λ_2^2	3.4191×10^{-9}	8.5324×10^{-9}	0.02795	-4.3781×10^{-9}	2.8667×10^{-9}
λ_3^2	-2.8862×10^{-9}	-2.0097×10^{-9}	-4.3781×10^{-9}	0.0198	-1.5391×10^{-9}
λ_4^2	2.1604×10^{-9}	8.2067×10^{-10}	2.8667×10^{-9}	$0-1.5391 \times 10^{-9}$	0.0153

It is unclear whether the weight function of $w(y) = y$ is applicable to all generalized Bessel solutions or just works for the above case by chance. Further analysis is needed to investigate.